

Characterization of *Saccharomyces uvarum* CN1 for Its Use in Aromatic White Wine Production  
and Mitigation of Negative Aromas from Rot-Affected Fruit

Daniel Phillipow, B.Sc.

Centre for Biological Sciences

Submitted in partial fulfillment  
of the requirements for the degree of

Master of Science

Faculty of Mathematics and Science, Brock University, St. Catharines, Ontario

©Daniel A. Phillipow, 2025

## Abstract

Sour rot and *Botrytis cinerea* infections pose significant challenges to grape growers and wineries by negatively impacting wine quality. Infected fruit is associated with elevated concentrations of compounds, primarily acetic acid, that compromise sensory properties. To ensure quality, wineries commonly set acetic acid thresholds (0.20–0.24 g/L), rejecting fruit that exceeds these limits and causing economic losses and production delays.

A locally isolated yeast, *Saccharomyces uvarum* CN1, shows potential for acetic acid reduction. Previous work demonstrated CN1's ability to metabolize acetic acid and enhance volatile aroma compounds (VOCs) in red wines; however, its impact on aromatic white wines remains unexplored. This study investigated Riesling fermentations at three rot levels (0%, 20%, and 40% w/w) inoculated with CN1 or commercial *S. cerevisiae* EC1118. CN1-fermented wines exhibited substantial reductions in acetic acid compared to juice values (13-fold at 0% rot, 6-fold at 20%, and 5-fold at 40% ) yielding final concentrations of 0.05–0.02 g/L. GC–MS analysis showed CN1 wines contained significantly higher levels of VOCs such as ethyl isobutyrate, 2-phenylethanol, and hexanol, and significantly lower concentrations of acetate esters and medium-chain fatty acids than EC1118 wines.

Sensory analysis revealed that EC1118 wines were associated with higher tropical aroma and flavour at 0% and 40% rot, while CN1 wines were rated higher in musty aroma (40% rot) and rubber flavour (20% rot). Although some differences in sensory profile may require further optimization, with targeted use, CN1 has potential as part of a strategy for recovering fruit that might otherwise be rejected.

## Acknowledgements

I would like to begin by sincerely thanking my supervisor, Dr. Debbie Inglis, for her unwavering support, incredible patience, and guidance throughout my time in this program. Your mentorship has shaped not only this thesis, but my growth as an individual, and I'm truly grateful for your trust and direction every step of the way.

Thank you as well to Dr. Jennifer Kelly for your support, helpful feedback, and enthusiasm throughout the course of this work. I've greatly appreciated your insight and much needed kindness these past two years. A heartfelt thank you to Shufen and Lisa from the Analytical Lab for their endless patience and support. Your technical expertise and willingness to help, no matter how small the question, made a huge difference and did not go unnoticed. To Fei, thank you for answering my mountain of questions and for always taking the time to walk me through protocols, even on the busiest days. To my fellow lab group (Nadine, Fred, Reid, and Holly) thank you for the camaraderie, shared problem-solving, and much-needed humor. I couldn't have asked for a better group of people to share this journey with.

To my partner, Emily, thank you for being my steady support system and source of encouragement through it all, especially over the last few years. And finally, to my dog Howard, thank you for giving me my free after-school therapy session and somehow always knowing when I needed a break.

This wild journey would not have been the same, or possible, without each one of you.

## Contents

Abstract.....	ii
Acknowledgements .....	iii
List of Tables.....	vi
List of Figures .....	vii
<b>Chapter 1: Introduction and Literature Review .....</b>	<b>1</b>
1.1.1 Introduction .....	1
1.1.2 Study Rationale and Scope.....	2
<b>1.2 Importance and Production of Aromatic White Wines .....</b>	<b>3</b>
1.2.1 Characteristics of Aromatic White Wines.....	3
1.2.2 Winemaking Techniques for Aromatic White Wines .....	6
1.2.3 Riesling: A Benchmark Aromatic Variety .....	8
1.2.4 Challenges in Riesling Production.....	10
<b>1.3 Conventional Winemaking and Yeast Selection .....</b>	<b>12</b>
1.3.1 Role of Yeast in Alcoholic Fermentation.....	12
1.3.2 Characteristics and Dominance of <i>Saccharomyces cerevisiae</i> strains .....	13
1.3.3 Yeast Selection for Sensory Profile Optimization .....	15
1.3.4 Fermentation Metabolites and Redox Balance .....	16
<b>1.4 <i>Saccharomyces uvarum</i>.....</b>	<b>18</b>
1.4.1 Taxonomy and Identification .....	18
1.4.2 Key Physiological and Fermentative Traits.....	20
1.4.3 Application in Winemaking and Potential for use in Aromatic White Wines.....	22
<b>1.5 Grape Rot in Wine Production .....</b>	<b>24</b>
1.5.1 Sour Rot: Origin and Influence on Must Chemistry.....	24
1.5.2 <i>Botrytis cinerea</i> .....	27
1.5.3 Influence of Rot on Fermentation and Wine Quality.....	28
1.5.4 Mitigation Strategies for Rot-Compromised Fruit.....	31
<b>1.6 Preliminary Research on <i>S. uvarum</i> CN1 .....</b>	<b>33</b>
1.6.1 Background on CN1 .....	33
1.6.2 Fermentations and Pilot Trials .....	34

1.6.3 Potential in Aromatic White Wines and Remediation of Rot-Affected Fruit.....	35
1.7 Summary .....	36
1.8 Thesis Objectives and Hypotheses.....	37
1.9 Literature Cited.....	40
<b>Chapter 2 – Materials &amp; Methods .....</b>	<b>47</b>
2.1 Grape Harvest, Sorting, and Processing .....	47
2.2 Winemaking .....	48
2.2.1 Additional Fermentations Not Included in Final Dataset.....	50
2.3 Microbial Implantations and Yeast Identification .....	51
2.4 Grape, Must, and Fermentation Analysis .....	53
2.5 Volatile Organic Compounds and Volatile Fatty Acid Analysis.....	54
2.6 Sensory Evaluation.....	57
2.7 Statistical Analysis .....	61
2.8 Statement of Ethics .....	62
<b>Chapter 3: Results .....</b>	<b>62</b>
3.1 Microbial Implantations and Yeast Identification .....	62
3.2 Fermentation Kinetics and Metabolites .....	71
3.3 Volatile Organic Compounds and Volatile Fatty Acids .....	79
3.4 Sensory Evaluation.....	84
<b>Chapter 4: Discussion &amp; Conclusion.....</b>	<b>90</b>
4.1: Discussion.....	90
4.2 Conclusions and Future Research.....	97
Literature Cited .....	99
Appendix.....	104

## List of Tables

Table 2.1: Categories, CAS Numbers, odour descriptors and sensory threshold ( $\mu\text{g/L}$ ) of all VOCs and VFAs measured in wines made from increasing rot levels. ....	55
Table 2.2: Complete list of reference standards and describing terms used for descriptive analysis of Riesling wines made from partially rot-affected grapes. ....	59
Table 3.1: Sequence homology of isolates from the <i>Saccharomyces uvarum</i> CN1 and <i>S. cerevisiae</i> EC1118 2023 Riesling fermentations. ....	67
Table 3.2: Sequence homology of isolates from the <i>Saccharomyces uvarum</i> CN1 and <i>S. cerevisiae</i> EC1118 second and third trial 2023 Riesling fermentations. ....	70
Table 3.3: Chemical composition of Riesling control must (0% Rot) and must from rot affected grapes (20% Rot and 40% Rot). ....	72
Table 3.4: Chemical composition of Riesling control wine (0% Rot) and wine made from rot-affected fruit (20% Rot, and 40% Rot). ....	74
Table A1.1: Number of nucleotide differences observed in $\beta$ -tubulin and GDH1 igs sequences from CN1 and EC1118 fermentation set 1 isolates relative to their strain-specific positive controls. ....	111
Table A1.2: Volatile aroma compounds, retention times, target and confirming ions, standard curves, % recovery, calibration ranges, and % coefficient of variation (CV). ....	136
Table A1.3: Mean concentrations ( $\mu\text{g/L} \pm$ standard error) of higher alcohols, acetate esters, ethyl esters, and fatty acids in Riesling wines fermented with <i>Saccharomyces cerevisiae</i> EC1118 or <i>Saccharomyces uvarum</i> CN1 at three levels of rot inclusion (0%, 20%, 40% by weight).....	138

## List of Figures

Figure 1.1: Overview of <i>Saccharomyces</i> metabolic activities influencing aromatic white wine aroma. ....	6
Figure 1.2: Representative Riesling grape clusters showing healthy fruit (left) and sour rot-affected fruit (right). ....	11
Figure 2.1: Schematic overview of the oenological treatments conducted with increasing rot percentages (0%, 20%, and 40%) inoculated using either <i>S. cerevisiae</i> EC1118 (control) or <i>S. uvarum</i> CN1. ....	48
Figure 3.1: Proportional distribution of yeast species recovered from implantation plating across six wine fermentation treatments for fermentation set 1. ....	64
Figure 3.2: Proportional distribution of yeast species recovered from implantation plating across six additional wine fermentation treatments from set 2 and 3. ....	69
Figure 3.3: Figure 3.3: Acetic acid (g/L) in initial must and finished wines made from juice of increasing rot levels vinified with either EC1118 (a) or CN1 (b). ....	76
Figure 3.4: Temperature (°C) during fermentation. ....	77
Figure 3.5: Soluble solid levels during fermentation. ....	78
Figure 3.6: Acetic acid (g/L) in finished wines made from juice of increasing rot levels (second trial; 0% and 15% rot) and juice spiked with 0.35g/L acetic acid (third trial). ....	79
Figure 3.7: Concentration of selected higher alcohols (2-methyl-1-propanol, hexanol, and 2-phenylethanol) in wines fermented with <i>S. cerevisiae</i> EC1118 and <i>S. uvarum</i> CN1 across increasing levels of rot infection (0%, 20%, and 40%). ....	80
Figure 3.8: Concentration of selected acetate esters and ethyl in Riesling wines fermented with <i>S. cerevisiae</i> EC1118 and <i>S. uvarum</i> CN1 across increasing levels of rot infection (0%, 20%, and 40%). ....	82
Figure 3.9: Concentration of selected ethyl esters in Riesling wines fermented with <i>S. cerevisiae</i> EC1118 and <i>S. uvarum</i> CN1 across increasing levels of rot infection (0%, 20%, and 40%). ....	83
Figure 3.10: Concentration of selected medium-chain fatty acids (hexanoic acid, octanoic acid, and decanoic acid) in wines fermented with <i>S. cerevisiae</i> EC1118 and <i>S. uvarum</i> CN1 at varying levels of rot (0%, 20%, and 40%). ....	84
Figure 3.11: Radar plots of the mean sensory intensities for aroma attributes (left column) and flavour, taste, and tactile sensation attributes (right column) in Riesling wines fermented with either <i>Saccharomyces cerevisiae</i> EC1118 or <i>Saccharomyces uvarum</i> CN1. ....	86

Figure 3.12: Impact of yeast strain and increasing rot percentage by weight on the sensory and chemical profiles of Riesling wines as determined by PLS. ....	89
Figure A1.1: Colony morphology of <i>Saccharomyces cerevisiae</i> and <i>Saccharomyces uvarum</i> on Wallerstein Laboratories Nutrient (WLN) differential agar. ....	104
Figure A1.2, A-P: Standard curves for VOCs (ethyl acetate, 2-methyl-1-propanol, ethyl isobutyrate, ethyl butyrate, ethyl 2-methylbutyrate, ethyl isovalerate, isoamyl acetate, hexanol, ethyl hexanoate, hexyl acetate, 2-phenylethyl ethanol, ethyl octanoate, and ethyl decanoate) and VFAs (hexanoic acid, octanoic acid, decanoic acid). ....	105
Figure A1.3: Sensory map of Riesling wines fermented with <i>S. cerevisiae</i> EC1118 and <i>S. uvarum</i> CN1 made using an increasing percentage of rot-infection by weight (control (0% rot), 20% rot, and 40% rot) via PCA on Factors 1 and 2. ....	137

## Chapter 1: Introduction and Literature Review

### 1.1.1 Introduction

The quality and outcome of alcoholic fermentation in white wine production is deeply influenced by the selection of yeast, fermentation conditions, and the chemical composition of the must, factors that are particularly critical when dealing with fruit compromised by rot. Traditional fermentations of wine rely heavily on *Saccharomyces cerevisiae*, a species valued for its robustness and predictability. However, increasing interest in microbial diversity and the challenges posed by climate change and disease pressure have prompted a re-evaluation of alternative *Saccharomyces* species. In particular, *S. uvarum*, a cryotolerant relative of *S. cerevisiae*, has emerged as a promising candidate for improving wine quality under compromised berry quality conditions and for enhancing aromatic complexity in white wine styles.

This review first outlines the foundations of conventional winemaking and yeast-driven fermentation, emphasizing the metabolic and ecological traits that underpin the success of *S. cerevisiae*. It then explores the taxonomy, physiological attributes, and fermentative potential of *S. uvarum*, including its unique metabolic profile, cryotolerance, and interaction with nitrogen sources. Special focus is given to strain CN1, a locally isolated *S. uvarum* strain with demonstrated acetic acid consumption and desirable sensory outcomes. The review culminates in a discussion of sour rot and *Botrytis cinerea*, two vineyard diseases of growing concern in cool-climate viticulture, and how their associated

changes to must chemistry affect fermentation performance and wine quality. Finally, potential mitigation strategies are considered, including the targeted use of *S. uvarum* CN1 in high-risk fruit.

By critically evaluating the current body of literature, this chapter provides a framework for understanding how *S. uvarum* CN1 may offer viable solutions to both the aromatic enhancement of white wines and the remediation of rot-affected musts. This background establishes the foundation for the experimental investigation that follows.

### 1.1.2 Study Rationale and Scope

The emergence of climate-driven challenges in viticulture, coupled with rising disease pressure from sour rot and *Botrytis cinerea*, has increased the frequency of compromised fruit reaching the winery. These conditions introduce significant obstacles to fermentation management, including elevated acetic acid levels, altered nitrogen availability, and a higher risk of sluggish or stuck fermentations. Conventional yeast strains such as *S. cerevisiae*, while reliable under ideal conditions, may struggle to perform optimally in such chemically imbalanced musts.

Recent advances in yeast ecology and strain selection have drawn attention to non-*cerevisiae* species, particularly *Saccharomyces uvarum*, for their distinct fermentative traits. Notably, the *S. uvarum* strain CN1, locally isolated from Niagara, Ontario, has demonstrated an ability to ferment under stressful conditions while simultaneously reducing volatile acidity through acetic acid uptake. These features suggest it may serve

not only as a viable alternative to *S. cerevisiae* in certain wine styles, but also as a potential biotechnological tool for managing disease-affected musts.

This literature review aims to compile current knowledge surrounding the conventional and emerging roles of wine yeasts, with a focus on *S. uvarum* and strain CN1. It encompasses yeast ecology, taxonomy, physiology, and redox metabolism, while situating these discussions within the broader context of rot-compromised fermentations and aromatic white wine production. Particular attention is given to Riesling and other cool-climate cultivars where preserving aromatic integrity and managing volatile acidity (VA) are paramount.

The scope of this review is limited to primary fermentation, excluding malolactic fermentation and broader viticultural practices, though these may be briefly referenced for context. The ultimate objective is to establish a foundation for evaluating CN1's potential to enhance wine quality and fermentation outcomes under both standard and compromised conditions, thereby guiding the design and interpretation of subsequent experimental trials.

## 1.2 Importance and Production of Aromatic White Wines

### 1.2.1 Characteristics of Aromatic White Wines

Aromatic white wines are characterized by their complex and expressive profiles, primarily derived from varietal aroma compounds, fermentation metabolites, and viticultural practices that influence grape maturity and metabolite development. These wines are often produced from grape varieties such as Riesling, Gewürztraminer, Sauvignon Blanc,

and Muscat. These wines are prized for their vibrant and complex sensory profiles, characterized by dominant fruity, floral, and occasionally spicy notes (Chen & Li, 2022). These sensory characteristics are primarily shaped by volatile organic compounds (VOCs) produced during alcoholic fermentation, especially ethyl esters, acetate esters, and higher alcohols (Carpena et al., 2020; Romano et al., 2022).

Among the most prominent contributors to aromatic white wine character are esters, which impart fruity and floral notes such as pear, banana, apple, and tropical fruit (Carpena et al., 2020). These are predominantly generated by yeast during fermentation via the esterification of fatty acids and higher alcohols, the latter of which are themselves fermentation products formed from amino acid metabolism (Chen & Li, 2022; Qu et al., 2024) (Figure 1.1).

As shown in Figure 1.1, acetate esters are synthesized via the reaction of higher alcohols with acetyl-CoA, catalyzed by alcohol acetyltransferases (AAT), and contribute intensely to banana and floral aromas (Romano et al., 2022; Qu et al., 2024). These esters are particularly sensitive to oxidation and storage conditions, which can reduce their aromatic impact post-bottling especially if they are not consumed at a young age (Gabrielli et al., 2021). Their formation and retention are optimized under low-temperature fermentation and controlled redox environments (Qu et al., 2024). Ethyl esters of straight-chain fatty acids (e.g., ethyl hexanoate, ethyl octanoate) and acetate esters of higher alcohols (e.g., isoamyl acetate, phenylethyl acetate) are particularly important to wine aroma for their low sensory thresholds and contribution to the varietal and fermentative bouquet (He et al., 2023). These compounds are highly volatile and aroma-active, and their production is

strongly modulated by fermentation conditions, such as yeast strain selection, temperature, and oxygen availability (Chen & Li, 2022; Gabrielli et al., 2021). Consequently, wines with prominent ester-derived aromas are designed for early consumption, since bottle aging often results in a marked decline of their fresh and vibrant aromatic qualities due to oxidative degeneration of these compounds.

Higher alcohols, while present in greater concentrations than esters, have a more complex impact on wine aroma. At moderate levels, compounds such as isoamyl alcohol, 2-phenylethanol, and hexanol may enhance aroma complexity and volume, contributing to desirable fruity, floral, or fusel-like characteristics, respectively (Carpena et al., 2020).

However, at elevated concentrations, generally above 300 mg/L, they may impart pungent or solvent-like off-aromas and negatively affect balance (Cordente et al., 2021). The interaction between higher alcohols and esters is also critical, as their relative ratios influence ester formation and aroma expression during aging (Carpena et al., 2020).

Microbial activity, particularly the metabolic diversity among different *Saccharomyces* species and strains, also has a profound influence on the concentration and balance of these VOCs (Carpena et al., 2020; Romano et al., 2022). Yeasts vary in their enzymatic capacities to produce or degrade aroma compounds, such as  $\beta$ -glycosidases ( $\beta$ G), involved in releasing monoterpenes from glycosidic precursors and AAT enzymes responsible for acetate ester formation which allows winemakers to modulate wine style through tailored strain selection (Chen & Li, 2022; Romano et al., 2022). Hence, the expression of aromatic white wine profiles is a function of both grape-derived precursors and fermentation-driven secondary metabolism (Chen & Li, 2022; Carpena et al., 2020).

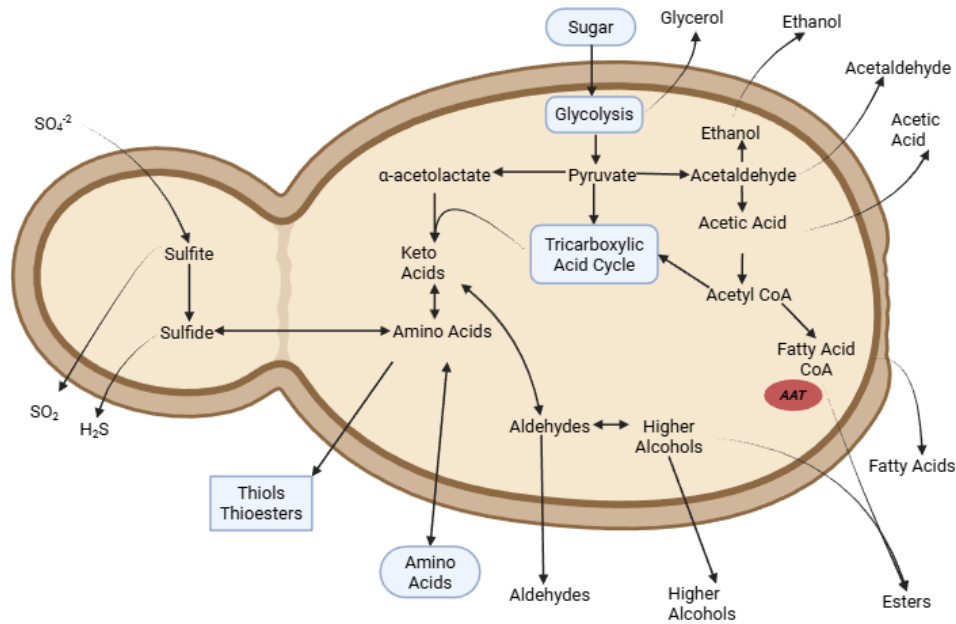


Figure 1.1: Overview of *Saccharomyces* metabolic activities influencing aromatic white wine aroma. This schematic summarizes the primary pathways linking sugar, amino acid, and fatty acid metabolism to the formation of key volatile compounds, including higher alcohols, ethyl esters, acetate esters (adapted from Bokulich and Bamforth, 2013). Created using Biorender.com.

### 1.2.2 Winemaking Techniques for Aromatic White Wines

The production of aromatic white wines requires specific winemaking techniques aimed at preserving varietal aroma compounds while enhancing fermentation-derived volatiles. The objective of this process is to retain primary fruit and floral aromas, minimize oxidative losses, and manage fermentation parameters to optimize sensory expression (Williams, 2023).

One of the earliest and most critical decisions in the production process is harvest timing, which is typically guided by assessments of grape maturity using soluble solids (°Brix) and titratable acidity (TA) (Rolle et al., 2022). Soluble solids reflects sugar content and potential alcohol, while TA indicates the acidity level, both of which are crucial for achieving the desired balance between freshness and body in the finished wine (Chen & Li, 2022). For

aromatic white wines, grapes are often harvested at moderate sugar levels (approximately 17–21 °Brix) and relatively high TA (around 7–10 g/L), which ensures bright acidity and supports the expression of aroma-active compounds (Rolle et al., 2022). The choice of harvest date is also influenced by sensory evaluations of grape flavor precursors and the degradation of methoxypyrazines or other green compounds, which may mask delicate aromatics if harvested too early (Chen & Li, 2022).

Once harvested, grapes are typically destemmed and gently pressed to limit phenolic extraction from skins and seeds, which can lead to bitterness or aromatic masking (Romano et al., 2022). Pressing is generally conducted at low pressures, often below 1.2 bar, to extract high-quality juice rich in aroma precursors while minimizing oxidation and tannin carryover (Gabrielli et al., 2021).

Fermentation temperature is a critical determinant of volatile profile development. For aromatic white wines, cool fermentation (typically 12–18°C) is widely adopted to favor the retention of esters and volatile thiols, which are susceptible to thermal degradation (Jackson, 2020; He et al., 2023). Yeast strain selection is equally important, as different *Saccharomyces* species and strains vary in their ability to synthesize and release esters, higher alcohols, and thiols (Maicas, 2021; Chen & Li, 2022). The use of non-*Saccharomyces* species in sequential or co-inoculated fermentations is also gaining interest, particularly for their enzymatic capacity to liberate bound aroma compounds and contribute to aromatic complexity (Maicas, 2021).

Redox management during fermentation and storage plays a pivotal role in preserving fruity aromas and preventing premature aging. Excessive oxygen exposure can lead to the degradation of esters and the formation of undesirable aldehydes, such as acetaldehyde, which mask fruitiness (He et al., 2023; Qu et al., 2024). As a result, reductive winemaking techniques, including the use of inert gas blanketing, low-dissolved oxygen transfer equipment, and early sulfur dioxide addition are critical to protect sensitive volatiles (Williams, 2023).

Finally, stabilization and bottling require further aromatic safeguarding. Cold stabilization, sterile filtration, and bottling under inert gas all aim to minimize microbial spoilage and oxidative degradation (Grainger & Tattersall, 2016). The cumulative effect of these techniques is to preserve the wine's varietal identity and enhance the expression of fermentation-derived aromas, culminating in a product that reflects both the grape and the winemaker's technical decisions (Carpena et al., 2020).

### 1.2.3 Riesling: A Benchmark Aromatic Variety

Riesling in particular, holds a prominent position in Canadian viticulture, particularly in Ontario, where it is regarded as one of the benchmark varieties for expressing terroir and cool climate winemaking excellence. Originally hailing from Germany's Rhine region, Riesling is a cold-hardy *Vitis vinifera* cultivar well-suited to the climatic conditions of Canada, especially in regions like the Niagara Peninsula, Prince Edward County, and Lake Erie North Shore (Haeger, 2016).

In Ontario, Riesling is one of the most widely planted white grape varieties and is prized for its high natural acidity, aromatic complexity, and ability to produce a broad spectrum of wine styles from dry table wines to sweet late harvest and Icewine (Willwerth et al., 2015; Haeger, 2016). Its versatility, combined with the province's climatic conditions, such as large diurnal temperature ranges, prolonged ripening periods, and moderated growing seasons due to proximity to the Great Lakes, facilitates the development of desirable volatile compounds, phenolic maturity, and sugar-acid balance (Douglas et al., 2001).

According to the Ontario Wine Appellation Authority (OWAA), in 2024, Riesling accounted for the largest share of VQA-certified wine production, representing 15% of all VQA wines produced that year (OWAA, 2024). This dominance was also reflected in grape processing data, with Grape Growers of Ontario (GGO) reporting that Riesling was the most heavily processed *Vitis vinifera* variety by volume, surpassing other white and red cultivars in tonnage (Grape Growers of Ontario, 2024).

Riesling's suitability to Ontario terroirs has made it a vital component of research and quality assessment within the Canadian wine industry. The Vintners Quality Alliance (VQA) frequently uses Riesling in its regional comparative tastings and sensory evaluations due to its ability to reflect site-specific characteristics (Willwerth et al., 2015). Moreover, its prominence in both academic and commercial research is underscored by its frequent use in viticultural studies, such as those exploring sub-appellation differentiation (Willwerth et al., 2015), sensory typicity (Douglas et al., 2001), and economic branding strategies (Barbe et al., 2016).

#### 1.2.4 Challenges in Riesling Production

Despite its prominence in cool climate viticulture, Riesling is notably susceptible to rot-related diseases, particularly *Botrytis cinerea* (noble and grey rot) and sour rot—a complex disease often involving yeasts, acetic acid bacteria, and opportunistic fungi (Hall et al., 2018). This susceptibility presents significant challenges for grape growers and winemakers, as these infections can adversely affect fruit quality, must chemistry, fermentation outcomes, and ultimately wine sensory attributes (Carpena et al., 2020).

Several factors contribute to Riesling's heightened vulnerability to rot. First is the compactness of its grape clusters, which promotes poor airflow and creates microenvironments conducive to fungal proliferation (Keller, 2020). Tight bunch architecture, combined with the thin skins of Riesling berries, facilitates the entry and spread of rot organisms, particularly in humid or rainy pre-harvest conditions (Barata et al., 2012). These characteristics are exacerbated under conditions of high crop load or inadequate canopy management, which reduce sunlight penetration and delay drying of the fruit zone (Bhandari et al., 2024). A comparison of healthy versus sour-rot affected Riesling clusters can be seen in Figure 1.2.



Figure 1.2: Representative Riesling grape clusters showing healthy fruit (left) and sour rot-affected fruit (right). Photo by Daniel Phillipow (2023).

Another contributing factor is Riesling's late ripening window. In Ontario, Riesling is often harvested after other white varieties to allow for full aromatic development and potential Icewine production (Bhandari et al., 2024; Willwerth et al., 2015). However, this extended hang time increases exposure to rainfall, fluctuating temperatures, and insect activity, each of which increases the likelihood of rot development (Hall et al., 2018). Sour rot has been linked to damage from fruit flies (*Drosophila spp.*), which facilitate microbial entry and trigger acetic acid formation (Barata et al., 2012).

From an enological perspective, rot infections in Riesling grapes can lead to elevated levels of undesirable metabolites, including gluconic acid, acetic acid, and ethyl acetate, which compromise fermentation kinetics and sensory quality (Bhandari et al., 2024; Jiang et al., 2023; Kelly et al., 2022). Although some winemakers selectively embrace *Botrytis cinerea* under controlled "noble rot" conditions for late-harvest or dessert wines, uncontrolled infections often lead to a degradation of varietal character and increased oxidative precursors (Gabrielli et al., 2021; Jackson, 2020).

In Ontario, climate variability and late-season rainfall remain key risk factors for rot development in Riesling vineyards (Sieczkowski et al., 2022; Mundy et al., 2022). Integrated disease management strategies, such as improved canopy architecture, judicious fungicide use, and earlier harvest of compromised blocks, are essential for maintaining fruit integrity (Brischetto et al., 2024; Neugebauer et al., 2024).

## 1.3 Conventional Winemaking and Yeast Selection

### 1.3.1 Role of Yeast in Alcoholic Fermentation

Yeasts are the primary biological catalysts responsible for alcoholic fermentation, the core biochemical process that converts grape must into wine. During this process, yeasts metabolize the primary grape sugars—glucose and fructose—into ethanol and carbon dioxide via glycolysis and alcoholic fermentation pathways (Jackson, 2020; Maicas, 2020). Glycolysis converts hexose sugars to pyruvate through a series of enzymatic reactions, which is then decarboxylated to acetaldehyde and reduced to ethanol by alcohol dehydrogenase (Walker & Walker, 2018). In addition to these major end-products, yeasts produce a variety of secondary metabolites detailed earlier including higher alcohols, esters, volatile acids, sulfur compounds, and organic acids, many of which significantly influence wine aroma, flavor, and mouthfeel (Carpena et al., 2020; He et al., 2023; Cordente et al., 2021).

The fermentation process follows a sequence of physiological phases: (1) the lag phase, during which yeast cells adapt to the fermentation environment; (2) the exponential growth phase, marked by rapid cell division and sugar consumption; (3) the stationary phase,

where growth ceases but metabolic activity remains high; and (4) the decline phase, during which cell viability decreases due to nutrient depletion and ethanol accumulation (Moimenta et al., 2023; Aiello et al., 2024; Chen & Li, 2022). Throughout these phases, yeasts shift from primarily anabolic activity (biomass production) to catabolic metabolism, driving both ethanol production and the formation of flavor-active metabolites (Comitini et al., 2021; Duncan et al., 2025).

### 1.3.2 Characteristics and Dominance of *Saccharomyces cerevisiae* strains

*S. cerevisiae* is the dominant yeast species in conventional winemaking due to several advantageous traits: its high ethanol tolerance, strong fermentative metabolism, ability to rapidly outcompete indigenous microflora, and capacity to complete fermentation under anaerobic or low-oxygen conditions (Parapouli et al., 2020). It also demonstrates adaptability across a range of winemaking conditions, including variable temperature, nitrogen availability, sugar concentration, and pH, making it a reliable and efficient fermenter in both industrial and artisanal contexts (Bruner & Fox, 2020; Peris et al., 2023).

During spontaneous fermentations, non-*Saccharomyces* yeast such as *Hanseniaspora uvarum*, *Metschnikowia pulcherrima*, and *Candida zemplinina* (synonymy with *Starmerella bacillaris*) typically dominate the early stages due to their rapid initial growth on grape surfaces (Benito-Castellanos et al., 2025; Grangeteau et al., 2016). However, as ethanol concentrations rise beyond 4–5% v/v, these species are usually outcompeted by *S. cerevisiae*, which is more tolerant to increasing alcohol levels, osmotic stress, and nutrient limitation (Costantini et al., 2021). This ecological succession is accelerated in inoculated

fermentations, where commercial *S. cerevisiae* strains are deliberately introduced and rapidly establish themselves, suppressing wild or indigenous yeasts (Parapouli et al., 2020; Marr et al., 2023).

While commercial *S. cerevisiae* strains have been selected for traits such as fast fermentation kinetics, low volatile acidity production, and consistent metabolite profiles, repeated use across different vintages or regions may limit microbial diversity and reduce expression of regional wine character (Costantini et al., 2021; Marr et al., 2023). Over time, this can lead to a homogenization of sensory profiles, particularly in large-scale production systems (Marr et al., 2023; Cordente et al., 2021).

Despite its dominance, *S. cerevisiae* is not the only member of the genus *Saccharomyces* found in wine fermentations (Bruner & Fox, 2020; Comitini et al., 2021). Species such as *S. paradoxus* and hybrids with *S. kudriavzevii* or *S. uvarum* may occasionally be isolated, particularly in cooler climates or under low-nutrient conditions, though they often display reduced ethanol tolerance or incomplete fermentation capacity (Costantini et al., 2021; Masneuf-Pomarede et al., 2010). However, growing interest in the ecological and enological roles of these non-dominant species has prompted closer examination of their potential contributions to wine character, especially when they persist naturally in vineyard environments.

Regionally adapted indigenous strains persisting in specific vineyard ecosystems without commercial inoculation have been shown to exhibit distinct fermentative kinetics, stress tolerances, and volatile compound production, contributing to site-specific wine profiles

and supporting the concept of microbial terroir (Comitini et al., 2021; Bruner & Fox, 2020; McCarthy et al., 2021). For example, Marr et al. (2023) reported that *S. cerevisiae* strains from British Columbia formed a novel, phylogenetically distinct Pacific West Coast Wine clade, suggesting local adaptation and potential for enological differentiation (McCarthy et al., 2021; Marr et al., 2023).

### 1.3.3 Yeast Selection for Sensory Profile Optimization

Yeast strains are increasingly selected not only for their technological reliability but also for their influence on sensory outcomes. While *S. cerevisiae* remains the primary species used in commercial winemaking, other *Saccharomyces* species, such as *S. uvarum* and non-*Saccharomyces* yeasts, are gaining interest for their unique contributions to aroma, mouthfeel, and fermentation dynamics, particularly in cool-climate and lower-intervention winemaking contexts (Comitini et al., 2021; Costantini et al., 2021). Within *S. cerevisiae*, strain-specific differences influence the production of aroma-active compounds including esters, higher alcohols, medium-chain fatty acids, sulfur volatiles, and volatile phenols (Carpena et al., 2020; Cordente et al., 2021). For example, some strains are known to enhance fruity ester expression in aromatic white wines, while others minimize off-flavor formation or contribute to perceived roundness and body through elevated glycerol and yeast-derived ethanol production (He et al., 2023; Aiello et al., 2024). In model wine systems, de-la-Fuente-Blanco et al. (2024) have shown that ethanol exerts perceptible effects on mouthfeel via its interaction with odor, taste, and retronasal signals, particularly when concentrations exceed ~10–11 % v/v.

Sensory-driven yeast selection also considers fermentation kinetics, nitrogen uptake preferences, and compatibility with malolactic bacteria or non-*Saccharomyces* co-inoculants (Comitini et al., 2021; Duncan et al., 2023). In cool-climate viticulture, where the preservation of varietal aroma and freshness is critical, strains are often chosen for their ability to ferment at low temperatures, retain esters, and produce low levels of volatile acidity and acetaldehyde (Kelly et al., 2020a; Gabrielli et al., 2021).

#### 1.3.4 Fermentation Metabolites and Redox Balance

The formation of fermentation metabolites is closely linked to the yeast's management of redox cofactors, particularly the balance between  $\text{NAD}^+$  and  $\text{NADH}$ , which plays a critical role in both primary and secondary metabolism (Coral-Medina et al., 2023). During alcoholic fermentation, the regeneration of  $\text{NAD}^+$  is essential for glycolytic flux, as the reduction of acetaldehyde to ethanol by alcohol dehydrogenase consumes  $\text{NADH}$  (Figure 1.1), restoring the redox balance required to sustain anaerobic metabolism (Duncan et al., 2025; Walker & Walker, 2018). This redox recycling not only ensures fermentation completion but also shapes the concentrations of key metabolic by-products that influence wine aroma and flavor (Duncan et al., 2023; He et al., 2023; Yang et al., 2017).

Redox balance influences the production of compounds such as glycerol, organic acids, and volatile esters (Duncan et al., 2023; Tyibilika et al., 2024; Yang et al., 2017). Glycerol, a product of dihydroxyacetone phosphate (DHAP) reduction, is synthesized as a mechanism for  $\text{NAD}^+$  regeneration when redox imbalances arise, particularly under osmotic or ethanol-induced stress (Aiello et al., 2024; Duncan et al., 2023). In hyperosmotic fermentations,

such as those studied by Yang et al. (2017), glycerol production plays a dual role in osmoregulation and redox homeostasis, with its accumulation directly correlating with shifts in cytosolic NADH/NAD<sup>+</sup> ratios. Similarly, acetate and succinate are generated through alternative redox-associated pathways and can accumulate depending on yeast species, oxygen availability, and the intracellular redox state (Cheraiti et al., 2005; Tybilika et al., 2024; Yang et al., 2017).

The production of volatile esters is also influenced by redox potential (Cordente et al., 2021; He et al., 2023). Specifically, oxidation-reduction potential (ORP) affects the expression of enzymes such as alcohol acetyltransferases and the availability of fatty acid precursors, thereby modulating medium-chain fatty acid ethyl ester synthesis (Qu et al., 2024; Berovic, 2024). Wines fermented under more reductive conditions often show enhanced ester retention, while oxidative environments may promote hydrolysis or volatilization of aroma-active compounds (Berovic, 2024; Gabrielli et al., 2021).

Mixed-species fermentations further complicate redox interactions (Comitini et al., 2021; Coral-Medina et al., 2023). When *S. cerevisiae* and *S. uvarum* are co-inoculated, their differing redox cofactor requirements and metabolic strategies can lead to cooperative or competitive interactions that alter metabolite profiles (Cheraiti et al., 2005; Morgan et al., 2020). For instance, *S. uvarum* tends to produce higher levels of glycerol and succinate, while *S. cerevisiae* may dominate ethanol and acetate production; together, they may redistribute redox fluxes in ways that influence fermentation kinetics and sensory outcomes (Cheraiti et al., 2005; Kelly et al., 2020a).

## 1.4 *Saccharomyces uvarum*

*Saccharomyces uvarum* is a cryotolerant yeast species, capable of maintaining efficient fermentation activity at low temperatures, often below 15 °C, and producing distinctive metabolite profiles under such conditions (Castellari et al., 1998). Cryotolerant yeasts, such as *S. uvarum*, have been reported to produce lower acetic acid and higher concentrations of glycerol and succinic acid compared to *Saccharomyces cerevisiae*, attributes that can enhance mouthfeel and mitigate certain fermentation faults (Kelly et al., 2018; Lyons et al., 2021). *S. uvarum* is closely related to *Saccharomyces cerevisiae* but possesses distinct physiological and metabolic characteristics that make it increasingly attractive for specialized winemaking applications. Traditionally associated with spontaneous fermentations in cool-climate regions, *S. uvarum* is gaining renewed attention due to its contributions to wine aroma complexity, lower ethanol production, and potential role in fermenting compromised musts (Masneuf-Pomarede et al., 2010; Albertin et al., 2014).

### 1.4.1 Taxonomy and Identification

Historically, *Saccharomyces uvarum* was classified under the broad and heterogeneous *Saccharomyces bayanus species complex*, a taxon that also encompassed *S. bayanus* var. *bayanus* and numerous interspecific hybrids. This classification reflected the limitations of early phenotypic and biochemical identification methods, which lacked the resolution to distinguish between closely related taxa within the *Saccharomyces sensu stricto* complex (Pontes et al., 2020; Franco-Duarte et al., 2019). As a result, strains with differing genetic

backgrounds were often grouped together under the umbrella of *S. bayanus*, obscuring the evolutionary and functional diversity present within the group.

The application of molecular biology techniques, particularly rDNA sequencing, multi-locus sequence typing (MLST), and whole-genome comparisons, has since clarified the taxonomic status of *S. uvarum*. Comparative genomics has revealed that *S. uvarum* is a distinct species, sharing approximately 86–89% genome identity with *S. cerevisiae*, but differing markedly in chromosomal structure, mitochondrial DNA, and gene content related to temperature tolerance, nitrogen metabolism, and sugar utilization (Pontes et al., 2020; Molinet et al., 2022). These genomic differences support the reclassification as an independent species, separate from *S. bayanus* sensu stricto, which is now recognized as a hybrid taxon composed of contributions from *S. uvarum*, *S. cerevisiae*, and *S. eubayanus* (Franco-Duarte et al., 2019).

Identification of *S. uvarum* in enological settings requires the use of molecular tools capable of differentiating it from both *S. cerevisiae* and hybrid strains. PCR-RFLP of the internal transcribed spacer (ITS) region and sequencing of the D1/D2 domain of the 26S rRNA gene are widely used for species-level resolution (Díaz et al., 2018). Additional techniques such as pulsed-field gel electrophoresis (PFGE), mitochondrial DNA restriction analysis, and microsatellite genotyping can further distinguish *S. uvarum* from related species or detect hybrid genomes (Gerard et al., 2023; Molinet et al., 2022). While culture-based methods using WL Nutrient Agar can assist in preliminary screening, molecular confirmation is essential due to the phenotypic overlap among *Saccharomyces* species (Díaz et al., 2018).

### 1.4.2 Key Physiological and Fermentative Traits

*Saccharomyces uvarum* exhibits several physiological and metabolic traits that differentiate it from *S. cerevisiae* and make it particularly well-suited to specific enological applications, especially in cool-climate white wine fermentations. These traits include strong cryotolerance, unique nitrogen assimilation pathways, altered glycerol and ethanol production kinetics, and the ability to generate distinct volatile profiles (García-Ríos et al., 2019; Kelly et al., 2018; Coral-Medina et al., 2023).

One of the most distinguishing characteristics of *S. uvarum* is its cryotolerance. Compared to *S. cerevisiae*, *S. uvarum* exhibits greater fermentative activity at low temperatures (10–15°C), a feature that is advantageous for preserving volatile aroma compounds and reducing the risk of undesirable microbial activity during cold fermentations (García-Ríos et al., 2019). This low-temperature adaptation is associated with its enhanced capacity for membrane fluidity maintenance, reduced ethanol toxicity, and altered enzyme kinetics under cold conditions (Morgan et al., 2020).

Fermentation with *S. uvarum* often results in lower ethanol yields and higher glycerol concentrations than those observed in *S. cerevisiae* fermentations, even when sugar conversion is complete (Lyons et al., 2021). This shift in carbon flux is believed to be partially driven by redox-balancing mechanisms and temperature-sensitive enzyme activity that favors glycerol production over ethanol. Glycerol, a non-volatile polyol, contributes to increased mouthfeel and perceived sweetness in wine and is typically present at 1.5–2

times higher concentrations in *S. uvarum* fermentations (Pérez et al., 2021; Gao et al., 2019; Kelly et al., 2018).

Nitrogen metabolism also differs markedly between *S. uvarum* and *S. cerevisiae* (Albertin et al., 2017; Minebois et al., 2020). While both species preferentially assimilate ammonium and amino acids during fermentation, *S. uvarum* exhibits enhanced utilization of certain amino acids (e.g., arginine, serine, threonine) at low temperatures, sustained activity of nitrogen transporters later in fermentation, and distinct regulation of Nitrogen Catabolite Repression (NCR)-sensitive genes (Albertin et al., 2017; Minebois et al., 2020). These traits influence its growth kinetics and metabolic output, particularly through the Ehrlich pathway (Gamero et al., 2013; Pérez et al., 2021). This results in altered production of volatile aroma compounds such as esters and higher alcohols (Coral-Medina et al., 2023; Pérez et al., 2021).

In competitive mixed fermentations, *S. uvarum* can persist alongside or even displace *S. cerevisiae* under certain environmental conditions, such as low temperatures or high initial nitrogen levels. However, under warmer or more nutrient-limited conditions, *S. cerevisiae* often dominates due to its faster fermentation kinetics and greater ethanol tolerance (Morgan et al., 2020). These competitive dynamics are not only strain-dependent but also influenced by inoculation timing and relative cell concentrations.

Volatile compound profiles also differ significantly between *S. uvarum* and *S. cerevisiae*, contributing to their distinct sensory signatures. Fermentations with *S. uvarum* typically yield higher concentrations of acetate esters (e.g., isoamyl acetate, 2-phenylethyl acetate)

and certain higher alcohols, while producing lower levels of acetic acid and fusel-like volatiles (Lyons et al., 2021). These differences make *S. uvarum* an attractive candidate for producing aromatic white wines with enhanced fruit-forward profiles and lower volatile acidity.

#### 1.4.3 Application in Winemaking and Potential for use in Aromatic White Wines

Building on its distinct physiological traits, *Saccharomyces uvarum* is emerging as a promising alternative or complement to *S. cerevisiae* in the production of aromatic white wines (Bruner & Fox, 2020; McCarthy et al., 2021). Its natural cryotolerance, altered carbon metabolism, and unique volatile compound production make it especially well-suited to cool-climate vinification, where the preservation of delicate varietal aromas is a central sensory objective (García-Ríos et al., 2019; Coral-Medina et al., 2023). Unlike *S. cerevisiae*, which is optimized for robust and rapid fermentation across a broad temperature range, *S. uvarum* thrives under low-temperature conditions (10–15 °C) and exhibits slower but more aroma-preserving kinetics; qualities that align well with the enological goals for cultivars such as Riesling, Chardonnay, and Muscat (García-Ríos et al., 2019; Coral-Medina et al., 2023).

Several specific fermentations have demonstrated the practical relevance and competitive viability of *S. uvarum* in commercial and experimental wine production (McCarthy et al., 2021; Morgan et al., 2020). At a commercial winery in the Okanagan Valley (British Columbia, Canada), spontaneous Chardonnay fermentations were found to be dominated by a genetically diverse population of indigenous *S. uvarum* across multiple vintages

(McCarthy et al., 2021). These fermentations, conducted at cool cellar temperatures, produced wines with reduced ethanol, elevated glycerol, and distinct fruity ester profiles, features that aligned with the stylistic goals of aromatic white winemaking (Kelly et al., 2020a; McCarthy et al., 2021). The persistence and dominance of *S. uvarum* under winery conditions suggest that this species can not only survive but actively define the fermentation trajectory in uninoculated settings (McCarthy et al., 2021; Gerard et al., 2023).

Supporting this, lab-scale fermentations have shown that *S. uvarum* strains, both commercial and indigenous, produce significantly higher levels of desirable esters such as 2-phenylethyl acetate, ethyl butanoate, and isoamyl acetate, while reducing fusel alcohols and volatile acidity compared to *S. cerevisiae* controls (Kelly et al., 2018; Coral-Medina et al., 2023). These sensory-active compounds contribute to enhanced floral and fruit-forward profiles, which are often central to consumer preference in white wine styles (Carpena et al., 2020; Cordente et al., 2021). Importantly, the higher glycerol yields of *S. uvarum*, especially under nitrogen-limited or low-temperature conditions, may improve mouthfeel in wines that would otherwise risk being thin or overly acidic (Aiello et al., 2024; Coral-Medina et al., 2023).

Further evidence of the enological utility of *S. uvarum* comes from mixed-culture fermentations (Comitini et al., 2021; Morgan et al., 2020). In studies comparing its performance in co-fermentations with *S. cerevisiae*, *S. uvarum* has demonstrated strong persistence and metabolic complementarity, particularly in low-temperature or nitrogen-variable conditions (Cheraiti et al., 2005; Morgan et al., 2020). These dynamics open

possibilities for designing sequential or co-inoculated fermentations that intentionally leverage the strengths of both species (Cheraiti et al., 2005; Kelly et al., 2020a).

## 1.5 Grape Rot in Wine Production

Grape rot is a major viticultural and enological challenge that affects both vineyard management and wine quality (Bhandari et al., 2024). Rot refers broadly to microbial infections that compromise grape integrity and must chemistry, with *Botrytis cinerea* (grey/noble rot) and sour rot representing the most economically significant forms of disease in cool-climate regions such as Ontario (Bhandari et al., 2024; Kelly et al., 2022). These rots not only reduce yield and grape marketability but also have profound effects on fermentation dynamics, microbial ecology, and the sensory profile of the final wine (Hall et al., 2018; Brischetto et al., 2024).

### 1.5.1 Sour Rot: Origin and Influence on Must Chemistry

Sour rot is a late-season grapevine disease complex characterized by the rapid degradation of berries accompanied by a distinctive vinegar-like odor, browning of the pulp, and leakage of juice (Bhandari et al., 2024). Unlike traditional fungal rots, sour rot is not caused by a single pathogen but arises from a polymicrobial interaction involving filamentous fungi (often initiating berry damage), fermentative yeasts, acetic acid bacteria (AAB), and opportunistically, insects, most notably *Drosophila spp.* (Hall et al., 2018; Bhandari et al., 2024). This complex etiology makes sour rot particularly difficult to manage and significantly impactful to grape composition and downstream wine quality (Crandall et al., 2022).

The development of sour rot is contingent upon several factors: physical damage to the grape berry cuticle, warm and humid environmental conditions, high inoculum pressure of yeasts and bacteria, and insect activity (Hall et al., 2018; Brischetto et al., 2025).

*Drosophila suzukii*, in particular, has been shown to both vector and exacerbate sour rot, facilitating the spread of microbes by ovipositing in intact berries and introducing wounds that allow microbial ingress (Ioriatti et al., 2017; Hall et al., 2018). This insect-mediated entry is critical, as intact berry skin is typically resistant to microbial colonization (Bhandari et al., 2024). When sour rot initiates, yeasts (primarily *Hanseniaspora* spp. and other apiculate genera) proliferate and begin fermentative activity within the berry, producing ethanol (Hall et al., 2018; Brischetto et al., 2025). Acetic acid bacteria (AAB) then oxidizes ethanol into acetic acid, resulting in the volatile acidity (VA) of infected fruit (Brischetto et al., 2025; Crandall et al., 2022).

Recent research has emphasized the ecological and metabolic complexity of sour rot microbiota. Culture-independent sequencing approaches have revealed a consistent microbial signature associated with diseased berries, indicating that disease progression may be mediated by a specific microbial consortium rather than random opportunistic colonization (Jumbam et al., 2025). These microbiomes not only shift the composition of must but also alter the biochemical environment, increasing the concentrations of acetic acid, acetaldehyde, and ethyl acetate—compounds that are detrimental to fermentation and sensory quality when present above threshold levels (Crandall et al., 2022; Hall et al., 2018). Importantly, these metabolites are already present in the grape must at the time of harvest, linking vineyard microbial activity directly to challenges encountered during

vinification and creating a linkage of spoilage risk from vineyard to winery. In Niagara, most wineries establish an upper allowable limit of 0.20–0.24 g/L acetic acid in grapes as a practical cut-off for accepting fruit with sour rot infection, as levels above this range are considered indicative of excessive spoilage risk (McFadden-Smith, 2010).

The chemical impact of sour rot on grape must is profound. Infected fruit typically exhibits a drop in sugar concentration due to leakage, an increase in VA, and elevated levels of gluconic acid and acetaldehyde, which are biomarkers of microbial spoilage and oxidative activity (Brischetto et al., 2024; Bhandari et al., 2024). Ethanol is sometimes present in the must prior to active fermentation, and the redox potential of juice may already be shifted, altering yeast behavior and potentially selecting for more oxidative or stress-tolerant fermentative species (Neugebauer et al., 2024; Duncan et al., 2025). These compositional changes can reduce yeast viability, slow fermentation kinetics, and increase the risk of stuck or sluggish fermentations, especially under nutrient-limited conditions (Coral-Medina et al., 2023; Tyibilika et al., 2024).

Beyond direct chemical effects, sour rot complicates winemaking by reducing grape integrity and increasing microbial load, often necessitating more aggressive sorting, sulfite addition, or antimicrobial interventions (Crandall et al., 2022; Brischetto et al., 2024). Even with triage, small percentages of rot-affected fruit (e.g., 5–10%) can elevate acetic acid concentrations above the legal threshold or produce perceptible sensory faults in wine (Crandall et al., 2022; Gabrielli et al., 2021). This risk is particularly critical in aromatic white wine production, where clean varietal expression and low thresholds for spoilage volatiles are crucial (He et al., 2023; Carpena et al., 2020).

### 1.5.2 *Botrytis cinerea*

*Botrytis cinerea*, a necrotrophic fungal pathogen, presents a paradox in viticulture and enology (Váczy et al., 2024). Under specific microclimatic conditions, namely intermittent humidity and drying, it induces “noble rot,” a process desirable for the production of sweet wines such as Sauternes (Váczy et al., 2024). However, in most cases, particularly under persistently wet conditions, *B. cinerea* causes “gray mold,” a destructive infection that compromises grape integrity and deteriorates must and wine quality (Kelly et al., 2022; Váczy et al., 2024). The distinction between these two outcomes is dictated by the interaction of environmental conditions, berry physiology, and microbial ecology (Hall et al., 2018; Jiang et al., 2023).

In gray mold scenarios, *B. cinerea* penetrates the berry cuticle, secreting a suite of cell wall-degrading enzymes and oxidases that result in tissue maceration, increased susceptibility to secondary microbial invasion, and significant leakage of juice and nutrients (Kelly et al., 2022; Váczy et al., 2024). This leads to a cascade of biochemical changes in the must, including elevated gluconic acid, laccase activity, and phenolic oxidation products, all of which interfere with fermentation and negatively affect wine stability and shelf life (Kelly et al., 2022; Bhandari et al., 2024). Wines produced from botrytized grapes exhibiting gray mold symptoms often suffer from reduced color intensity, altered tannin structure, and increased oxidative defects (Gabrielli et al., 2021; Jiang et al., 2023).

Importantly, the presence of *B. cinerea* is not always an isolated phenomenon. Sour rot-affected clusters have been found to be at increased risk for subsequent or concurrent *B. cinerea* colonization, especially during postharvest storage (Owoyemi et al., 2022; Brischetto et al., 2025). This interplay between disease complexes further complicates vineyard management and raises the stakes for rigorous harvest sorting in years with high late-season humidity (Crandall et al., 2022; Bhandari et al., 2024).

The ability to detect and manage *B. cinerea* before harvest is critical. Jiang et al. (2023) proposed the use of volatile analysis as a non-invasive, early detection tool to assess infection levels in grapes. Such technologies offer promising avenues for selective harvesting, triage, and must adjustment strategies (Jiang et al., 2023; Neugebauer et al., 2024). Still, in vintages where gray mold is unavoidable, alternative yeast selection, including cryotolerant or low-VA-producing strains, may help mitigate the impact on wine quality, particularly in aromatic white wines where *Botrytis*-related off-aromas are most perceptible (Kelly et al., 2020a; Coral-Medina et al., 2023).

### 1.5.3 Influence of Rot on Fermentation and Wine Quality

The presence of sour rot and *Botrytis cinerea* infections in harvested grapes has profound consequences for fermentation kinetics, microbial ecology, and ultimately, wine quality. These rot-related diseases alter must chemistry prior to inoculation, introducing unwanted microbial metabolites (e.g., acetic acid, gluconic acid, acetaldehyde), reducing sugar concentrations, and increasing microbial load, each of which poses risks to fermentation efficiency and sensory integrity (Crandall et al., 2022).

One of the most critical impacts of rot-affected fruit is the elevation of volatile acidity (VA), particularly from the combined activity of acetic acid bacteria and fermentative yeasts already active within damaged berries. In sour rot-infected grapes, musts may contain ethanol and acetic acid even before primary fermentation begins (Hall et al., 2018; Bhandari et al., 2024). These pre-fermentation metabolites disrupt yeast metabolism by acidifying the environment and imposing redox imbalances that stress inoculated strains. Acetic acid at concentrations above 0.5 g/L can inhibit yeast growth, particularly in *Saccharomyces cerevisiae*, and is known to induce oxidative stress and mitochondrial dysfunction (Guaragnella & Bettiga, 2021). The combination of a depleted redox potential, high VA, and fluctuating nitrogen availability can lead to sluggish or stuck fermentations.

Rot also compromises the chemical stability and organoleptic properties of wine (Crandall et al., 2022; Hall et al., 2018). In *Botrytis*-infected grapes exhibiting gray mold symptoms, oxidative enzymes such as laccase remain active even after fermentation and sulfite addition, degrading anthocyanins and phenolic compounds and accelerating wine browning and aroma loss (Kelly et al., 2022; Gabrielli et al., 2021). This oxidative spoilage is especially detrimental in white and rosé wines, which rely on delicate aromatic and visual clarity (Gabrielli et al., 2021; He et al., 2023). Wines produced from such musts often require aggressive clarification, stabilization, and antioxidant additions, which can strip varietal character (Brischetto et al., 2024; Váczy et al., 2024).

Additionally, infections by sour rot and *B. cinerea* can alter the aroma profile of the final wine. Jiang et al. (2023) demonstrated that *Botrytis*-infected grapes are associated with elevated levels of C8 volatile compounds, such as 1-octen-3-ol and octanal, which impart

musty or earthy notes. Similarly, sour rot increases the concentration of ethyl acetate and acetaldehyde, compounds that even at sub-threshold levels can suppress varietal fruit character and contribute to off-odors (Brischetto et al., 2025; Sébastien et al., 2024). These volatile markers are particularly problematic in aromatic white wines, where clean fruit expression is paramount and perception thresholds for spoilage compounds are lower (Carpena et al., 2020; He et al., 2023).

From a microbiological perspective, rot-affected musts present increased competition for inoculated yeast strains (Hall et al., 2018; Jumbam et al., 2025). Resident microbial populations including non-*Saccharomyces* yeasts, acetic acid bacteria, and filamentous fungi may reduce viable yeast counts or alter the fermentation trajectory (Bhandari et al., 2024; Neugebauer et al., 2024). This microbial instability can necessitate increased sulfite additions or selective antimicrobial agents, both of which may interfere with desirable yeast performance (Franco-Duarte et al., 2019; Díaz et al., 2018).

Moreover, grapes with even modest proportions of rot (e.g., 5–10%) have been shown to significantly shift must composition and fermentation dynamics (Crandall et al., 2022; Brischetto et al., 2024). These effects are often additive, with sour rot increasing acetic acid and microbial load, and *Botrytis* contributing oxidative enzymes, gluconic acid, and undesirable volatiles (Hall et al., 2018; Jiang et al., 2023). Together, these infections decrease fermentation predictability, increase processing costs, and result in wines that are more difficult to stabilize and less likely to meet stylistic targets, especially for aromatic white wines, where clarity, purity, and freshness are key attributes (Kelly et al., 2020a; He et al., 2023).

#### 1.5.4 Mitigation Strategies for Rot-Compromised Fruit

Given the profound enological consequences of sour rot and *Botrytis cinerea*, effective mitigation strategies are essential to reduce microbial load, preserve must quality, and support successful fermentation outcomes (Crandall et al., 2022; Hall et al., 2018).

Management approaches span both vineyard-based interventions aimed at preventing or minimizing infection, and winery-based practices focused on selective processing, microbial control, and yeast strain selection to stabilize rot-affected fruit (Hall et al., 2018; Gabrielli et al., 2021).

In the vineyard, cultural and chemical strategies form the first line of defense. For *Botrytis*, canopy management practices such as leaf removal, shoot thinning, and improved airflow have been shown to reduce humidity and delay infection onset, particularly in wet climates (Mundy et al., 2022; Brischetto et al., 2024). Timed fungicide applications can suppress *B. cinerea* sporulation during vulnerable growth stages, although overuse may contribute to resistance development or disrupt beneficial microbial communities (Crandall et al., 2022; Váczy et al., 2024). For sour rot, control is more complex due to its polymicrobial and insect-mediated nature (Hall et al., 2018; Bhandari et al., 2024). Chemical sprays initiated after symptom onset are largely ineffective (Kenney & Hall, 2021). Instead, preventative strategies, particularly targeting *Drosophila spp.* populations, are more effective (Hall et al., 2018; Ioriatti et al., 2017). Vineyard sanitation, insecticide use, and earlier harvest are among the most effective tools to reduce rot risk under high-pressure conditions (Brischetto et al., 2024; Bhandari et al., 2024).

Increasing attention is being paid to biocontrol options for sour rot suppression. A recent meta-analysis of 67 studies found promising results for yeast- and bacteria-based biocontrol agents, including strains of *Metschnikowia*, *Aureobasidium*, and *Bacillus*, which outcompete or inhibit sour rot-associated microbes on the berry surface (Brischetto et al., 2024). These organisms may be particularly valuable in organic or low-input viticulture systems, though field validation across regions remains limited (Crandall et al., 2022). Understanding the structure and dynamics of the grape microbiome is also emerging as a key strategy (Jumbam et al., 2025). Targeting known sour rot associates identified through culture-independent approaches may allow for precision microbial management at the cluster level (Jumbam et al., 2025; Bhandari et al., 2024).

In the winery, the focus shifts to minimizing the impact of infected fruit on must chemistry and fermentation (Gabrielli et al., 2021; Neugebauer et al., 2024). One of the most immediate interventions is rigorous fruit sorting (Crandall et al., 2022; Jiang et al., 2023). Hand or optical sorting to remove visibly infected berries or clusters significantly reduces microbial load and the concentration of problematic metabolites such as acetic acid, gluconic acid, and laccase (Kelly et al., 2022; Brischetto et al., 2024). Where sorting is impractical or infection is diffuse, partial juice draining (saignée), cold settling, and inert gas blanketing during pressing can help reduce the extraction of oxidative enzymes and spoilage compounds (Gabrielli et al., 2021; Váczy et al., 2024).

For microbiologically unstable musts, increased initial SO<sub>2</sub> additions may be required to suppress native microbial populations (Franco-Duarte et al., 2019; Díaz et al., 2018). However, excessive SO<sub>2</sub> can also inhibit desirable yeast activity (Comitini et al., 2021).

Therefore, targeted antimicrobial strategies such as flash pasteurization, use of lysozyme or chitosan, or inoculation with competitive, stress-tolerant yeast strains (e.g., *S. uvarum*) may offer a better balance between control and fermentation success (Kelly et al., 2020a; Coral-Medina et al., 2023). Cryotolerant or high-glycerol-producing strains are particularly useful in rot-affected fermentations, as they tend to produce lower volatile acidity and tolerate oxidative stress more effectively (Coral-Medina et al., 2023; Aiello et al., 2024).

Monitoring of volatile acidity, gluconic acid, and acetaldehyde concentrations pre-fermentation can serve as a triage tool for fruit quality (Hall et al., 2018; Jiang et al., 2023).

As discussed in Section 1.5.1, grapes with acetic acid concentrations exceeding 0.20–0.24 g/L are often rejected or downgraded due to their high spoilage risk (McFadden-Smith, 2010). Musts from borderline fruit can sometimes be salvaged through blending or the application of reductive winemaking techniques, including careful oxygen exclusion, minimal handling, and early clarification (Gabrielli et al., 2021; He et al., 2023).

## 1.6 Preliminary Research on *S. uvarum* CN1

### 1.6.1 Background on CN1

The yeast strain previously referred to as *Saccharomyces bayanus* CN1, now taxonomically identified as *Saccharomyces uvarum* CN1, was isolated from the Niagara region (Canada) from Icewine Riesling grapes and selected for its performance under cool-climate winemaking conditions (Kelly et al., 2018). Originally classified under the broader *S. bayanus* designation, subsequent molecular analyses have clarified CN1's placement within *Saccharomyces uvarum*. This species is known for its cryotolerance, lower ethanol

yield, and capacity to produce elevated levels of glycerol and fruity esters, which are traits of particular interest for stylistically delicate wines and fermentations under stressful conditions (Kelly et al., 2020a; Kelly et al., 2018).

*S. uvarum* CN1 emerged as a promising autochthonous alternative to commercial *S. cerevisiae* strains due to its resilience during fermentation of high-sugar musts and its distinct metabolite profile. This includes a reduced production of problematic oxidative compounds such as acetic acid and acetaldehyde, even under elevated volatile acidity (VA) or partial grape dehydration (Kelly et al., 2018). The ability to thrive under such stressors, alongside sensory distinctions from mainstream yeast strains, positioned CN1 as a strong candidate for further enological investigation.

### 1.6.2 Fermentations and Pilot Trials

CN1 has been evaluated across multiple pilot-scale and laboratory fermentations, most notably in high-sugar grape musts and juice with elevated starting VA (Kelly et al., 2020a; Kelly et al., 2018). In controlled trials, CN1 demonstrated the ability to complete fermentation at must concentrations up to 27.5 °Brix, a level typical of late harvest or partially dehydrated grapes (Kelly et al., 2020a). Although fermentation duration was slightly extended compared to *S. cerevisiae* EC1118, CN1 still successfully achieved dryness while exhibiting strong fermentation vigor (Kelly et al., 2020a).

One of the most notable findings from these trials is CN1's capacity to consume acetic acid during fermentation. In fermentations with starting VA levels as high as 0.48 g/L, CN1 was able to lower the final acetic acid concentration to 0.07 g/L, representing a nearly

seven-fold reduction (Kelly et al., 2020a). This metabolic trait is rare among *Saccharomyces* species and is particularly advantageous for remediating compromised musts where wineries would otherwise reject grapes exceeding VA thresholds of 0.2–0.24 g/L (McFadden-Smith, 2010; Crandall et al., 2022).

Additionally, wines produced with CN1 consistently exhibited higher glycerol content than those fermented with EC1118, enhancing body and mouthfeel (Kelly et al., 2018; Coral-Medina et al., 2023). At the same time, concentrations of volatile acidity, ethyl acetate, and acetaldehyde, previously mentioned as key contributors to oxidative spoilage, were significantly reduced (Kelly et al., 2020a; He et al., 2023). These results suggest that CN1 may be uniquely suited to scenarios where grape condition, high sugar, or elevated VA would challenge more traditional yeast strains (Kelly et al., 2020a; Coral-Medina et al., 2023).

### 1.6.3 Potential in Aromatic White Wines and Remediation of Rot-Affected Fruit

CN1's fermentative behavior within previous trials underscores its versatility across a range of enological conditions, from pristine musts to those compromised by disease pressure. *S. uvarum* cold tolerance and lower ethanol yields offer practical advantages in cool-climate white wine production, where aromatic preservation and balance are central stylistic goals (García-Ríos et al., 2019; Coral-Medina et al., 2023). More uniquely, CN1's ability to actively consume acetic acid during fermentation sets it apart from conventional *S. cerevisiae* strains and provides an effective means of mitigating volatile acidity in rot-affected musts (Kelly et al., 2020a). This rare metabolic trait, combined with elevated ester

production and enhanced glycerol synthesis, allows CN1 to transform chemically compromised juice into wines that retain aromatic freshness, mouthfeel, and varietal typicity (Kelly et al., 2018; Brischetto et al., 2024). CN1 serves not only as a sensory-enhancing yeast but also as a strategic tool for fermentation stabilization and spoilage remediation, an increasingly valuable asset in the face of climate variability and rising disease incidence.

## 1.7 Summary

This chapter has explored the enological relevance of *Saccharomyces uvarum* CN1, a locally isolated cryotolerant yeast strain with promising potential for use in cool-climate white wine production, particularly under challenging conditions such as sour rot and *Botrytis cinerea* infection. While *S. cerevisiae* remains the industry standard due to its robust fermentative performance, increasing interest in non-*cerevisiae* species reflects a growing need for strains that support greater aromatic complexity, lower ethanol yields, and improved fermentation outcomes in compromised musts.

*S. uvarum* is distinguished from other strains by its ability to ferment at low temperatures, favor ester formation, and maintain stable fermentative kinetics in musts with high volatile acidity. Unlike many traditional strains, CN1 has demonstrated the unique capacity to actively consume acetic acid during fermentation, an attribute with substantial implications for improving wine quality in rot-affected fruit. These traits position CN1 as an effective tool not only for producing fresh, fruit-forward aromatic white wines but also for

remediating problematic juice chemistries associated with microbial spoilage and climatic stress.

Taken together, the physiological, metabolic, and fermentative characteristics of CN1 support its targeted application in enology, offering both sensory enhancement and functional remediation. This lays the foundation for the following chapter, which will investigate CN1's performance in controlled laboratory white wine fermentations, assess its produced volatile compounds and sensory profiles, and evaluate its practical utility as a primary or co-inoculated yeast in high-risk juice matrices.

## 1.8 Thesis Objectives and Hypotheses

Despite the significant enological challenges posed by *Botrytis cinerea* and sour rot, few yeast-based interventions have been explored to remediate compromised fruit while maintaining desirable sensory outcomes. Previous studies have identified *Saccharomyces uvarum* CN1 as a cryotolerant strain capable of producing high levels of glycerol and esters while reducing volatile acidity, even in fermentations with elevated initial acetic acid concentrations (Kelly et al., 2020a; Kelly et al., 2018). Building on these findings, this thesis investigates the utility of *S. uvarum* CN1 in mitigating the chemical and sensory defects associated with rot-affected white grape musts, with a specific focus on acetic acid metabolism and volatile aroma development.

The first objective of this study is to evaluate the ability of the locally isolated *S. uvarum* strain CN1 to reduce acetic acid concentrations and related spoilage metabolites (e.g., acetaldehyde, ethyl acetate) in Riesling musts compromised by *Botrytis* and sour rot at

varying infection levels (0%, 20%, and 40% w/w). Rot-affected fruit is frequently associated with elevated concentrations of acetic acid and related spoilage compounds (Hall et al., 2018; Sieczkowski et al., 2022), which can inhibit yeast performance and impair wine aroma and flavour (Brischetto et al., 2025). CN1 has previously shown the ability to metabolize acetic acid during fermentation, presumably converting it into neutral or aromatic compounds via acetyl-CoA metabolism (Kelly et al., 2020a; Vasserot et al., 2010). Assessing this metabolic function under varying degrees of rot inclusion offers insight into the strain's capacity to remediate microbial spoilage in practical winemaking contexts.

The second objective is to characterize CN1's production of volatile fatty acids, higher alcohols, ethyl esters, and acetate esters, particularly those associated with fruit-forward and floral aromatic profiles. *S. uvarum* is known to favor ester formation under cold fermentation conditions, contributing to enhanced aroma retention in aromatic white wines (Lyons et al., 2021; Coral-Medina et al., 2023). Understanding how these compounds are formed relative to a benchmark *S. cerevisiae* strain (EC1118) will help determine CN1's potential for not only remediating spoilage, but also enhancing wine aroma complexity and typicality.

The central hypothesis is that fermentations conducted with *S. uvarum* CN1 will result in a net reduction in acetic acid compared to the initial concentration, and will produce higher levels of volatile aroma compounds, especially esters, associated with fruity and floral sensory profiles. These improvements are expected to have higher concentrations than in fermentations conducted with the commercial *S. cerevisiae* EC1118, which lacks the same cold tolerance and acetic acid metabolizing potential. If confirmed, these findings could

support the targeted application of CN1 as a fermentation tool for improving the quality and sensory outcomes of rot-affected aromatic white wines.

## 1.9 Literature Cited

- Aiello, E., Arena, M. P., De Vero, L., Montanini, C., Bianchi, M., Mescola, A., Alessandrini, A., Pulvirenti, A., & Gullo, M. (2024). Wine yeast strains under ethanol-induced stress: Morphological and physiological responses. *Fermentation*, 10(12), 631. <https://doi.org/10.3390/fermentation10120631>
- Albertin, W., Miot-Sertier, C., Bely, M., Marullo, P., Coulon, J., Moine, V., Colonna-Ceccaldi, B., & Masneuf-Pomarede, I. (2014). Oenological prefermentation practices strongly impact yeast population dynamics and alcoholic fermentation kinetics in Chardonnay grape must. *International Journal of Food Microbiology*, 178, 87–97. <https://doi.org/10.1016/j.ijfoodmicro.2014.03.009>
- Barata, A., Malfeito-Ferreira, M., & Loureiro, V. (2012). The microbial ecology of wine grape berries. *International Journal of Food Microbiology*, 153(3), 243–259. <https://doi.org/10.1016/j.ijfoodmicro.2011.11.025>
- Benito-Castellanos, A., Larreina, B., Banda, M. T. C. de L., Santamaría, P., González-Arenzana, L., & Gutiérrez, A. R. (2025). Biodiversity of yeast species isolated during spontaneous fermentation: Influence of grape origin, vinification conditions, and year of study. *Microorganisms*, 13(7), 1707. <https://doi.org/10.3390/microorganisms13071707>
- Berovic, M. (2024). The role and application of redox potential in wine technology. *Fermentation*, 10(6), 312. <https://doi.org/10.3390/fermentation10060312>
- Bhandari, R., Zaman, F., Hall, M., Gold, K., Wise, A., Walter-Peterson, H., & Loeb, G. (2024). Understanding grape sour rot complex. *American Journal of Enology and Viticulture*, 75(2). <https://doi.org/10.5344/ajev.2024.22072>
- Bokulich, N. A., & Bamforth, C. W. (2013). The microbiology of malting and brewing. *Microbiology and Molecular Biology Reviews*, 77(2), 157–172. <https://doi.org/10.1128/MMBR.00060-12>
- Brischetto, C., Rossi, V., & Fedele, G. (2024). A meta-analysis of 67 studies on the control of grape sour rot revealed interesting perspectives for biocontrol. *Agronomy*, 14(8), 1859. <https://doi.org/10.3390/agronomy14081859>
- Brischetto, C., Rossi, V., Salotti, I., Languasco, L., & Fedele, G. (2025). Temperature requirements can affect the microbial composition causing sour rot in grapes. *Environmental Microbiology Reports*, 17(1), e70061. <https://doi.org/10.1111/1758-2229.70061>

- Bruner, J., & Fox, G. (2020). Novel non-cerevisiae saccharomyces yeast species used in beer and alcoholic beverage fermentations. *Fermentation*, 6(4), 116. <https://doi.org/10.3390/fermentation6040116>
- Carpena, M., Fraga-Corral, M., Otero, P., Nogueira, R. A., Garcia-Oliveira, P., Prieto, M. A., & Simal-Gandara, J. (2020). Secondary aroma: Influence of wine microorganisms in their aroma profile. *Foods*, 10(1), 51. <https://doi.org/10.3390/foods10010051>
- Castellari, L., Tini, V., Zambonelli, C., & Rainieri, S. (1998). Oenological properties of cryotolerant and thermotolerant *Saccharomyces* strains. *Food Technology and Biotechnology*, 36(1), 59–65.
- Chen, K., & Li, J. (2022). A glance into the aroma of white wine. In *White Wine Technology* (pp. 313–326). Elsevier. <https://doi.org/10.1016/B978-0-12-823497-6.00018-1>
- Cheraiti, N., Guezenec, S., & Salmon, J.-M. (2005). Redox interactions between *Saccharomyces cerevisiae* and *Saccharomyces uvarum* in mixed culture under enological conditions. *Applied and Environmental Microbiology*, 71(1), 255–260. <https://doi.org/10.1128/AEM.71.1.255-260.2005>
- Comitini, F., Agarbati, A., Canonico, L., & Ciani, M. (2021). Yeast interactions and molecular mechanisms in wine fermentation: A comprehensive review. *International Journal of Molecular Sciences*, 22(14), 7754. <https://doi.org/10.3390/ijms22147754>
- Coral-Medina, A., Morrissey, J. P., & Camarasa, C. (2023). The growth and metabolome of *Saccharomyces uvarum* in wine fermentations are strongly influenced by the route of nitrogen assimilation. *Journal of Industrial Microbiology & Biotechnology*, 49(6), kuac025. <https://doi.org/10.1093/jimb/kuac025>
- Cordente, A. G., Espinase Nandorfy, D., Solomon, M., Schulkin, A., Kolouchova, R., Francis, I. L., & Schmidt, S. A. (2021). Aromatic higher alcohols in wine: Implication on aroma and palate attributes during chardonnay aging. *Molecules*, 26(16), 4979. <https://doi.org/10.3390/molecules26164979>
- Costantini, A., Cravero, M. C., Panero, L., Bonello, F., Vaudano, E., Pulcini, L., & Garcia-Moruno, E. (2021). Wine fermentation performance of indigenous *Saccharomyces cerevisiae* and *Saccharomyces paradoxus* strains isolated in a Piedmont vineyard. *Beverages*, 7(2), 30. <https://doi.org/10.3390/beverages7020030>
- Crandall, S. G., Spsychalla, J., Crouch, U. T., Acevedo, F. E., Naegele, R. P., & Miles, T. D. (2022). Rotting grapes don't improve with age: Cluster rot disease complexes, management, and future prospects. *Plant Disease*, 106(8), 2013–2025. <https://doi.org/10.1094/PDIS-04-21-0695-FE>

- Díaz, C., Badalyan, G., & Bücking, M. (2018). Molecular techniques for the detection and identification of yeasts in wine. In A. F. El Sheikha, R. Levin, & J. Xu (Eds.), *Molecular Techniques in Food Biology* (1st ed., pp. 323–340). Wiley.  
<https://doi.org/10.1002/9781119374633.ch14>
- Duncan, J. D., Ortiz-Julien, A., Setati, M. E., & Divol, B. (2023). Production of flavour compounds by wine yeasts is dependent on the management of their intracellular redox balance: Sourced from the research article: “Redox cofactor metabolism in *Saccharomyces cerevisiae* and its impact on the production of alcoholic fermentation end-products” (*Food research international*, 2023). IVES Technical Reviews, Vine and Wine.  
<https://doi.org/10.20870/IVES-TR.2023.7725>
- Duncan, J. D., Setati, M. E., & Divol, B. (2025). The cellular symphony of redox cofactor management by yeasts in wine fermentation. *International Journal of Food Microbiology*, 427, 110966. <https://doi.org/10.1016/j.ijfoodmicro.2024.110966>
- Franco-Duarte, R., Černáková, L., Kadam, S., Kaushik, K. S., Salehi, B., Bevilacqua, A., Corbo, M. R., Antolak, H., Dybka-Stępień, K., Leszczewicz, M., Relison Tintino, S., de Souza, V. C. A., Sharifi-Rad, J., Coutinho, H. D. M., Martins, N., & Rodrigues, C. F. (2019). Advances in chemical and biological methods to identify microorganisms—From past to present. *Microorganisms*, 7(5), 130. <https://doi.org/10.3390/microorganisms7050130>
- Gabrielli, M., Fracassetti, D., Romanini, E., Colangelo, D., Tirelli, A., & Lambri, M. (2021). Oxygen-induced faults in bottled white wine: A review of technological and chemical characteristics. *Food Chemistry*, 348, 128922.  
<https://doi.org/10.1016/j.foodchem.2020.128922>
- Gamero, A., Tronchoni, J., Querol, A., & Belloch, C. (2013). Production of aroma compounds by cryotolerant *Saccharomyces* species and hybrids at low and moderate fermentation temperatures. *Journal of Applied Microbiology*, 114(5), 1405–1414.  
<https://doi.org/10.1111/jam.12126>
- Gao, Y., Zhang, Y., Wen, X., Song, X., Meng, D., Li, B., Wang, M., Tao, Y., Zhao, H., Guan, W., & Du, G. (2019). The glycerol and ethanol production kinetics in low-temperature wine fermentation using *Saccharomyces cerevisiae* yeast strains. *International Journal of Food Science & Technology*, 54(1), 102–110. <https://doi.org/10.1111/ijfs.13910>
- García-Ríos, E., Guillén, A., de la Cerda, R., Pérez-Través, L., Querol, A., & Guillamón, J. M. (2019). Improving the cryotolerance of wine yeast by interspecific hybridization in the genus *Saccharomyces*. *Frontiers in Microbiology*, 9. <https://doi.org/10.3389/fmicb.2018.03232>

- Gerard, L. M., Corrado, M. B., Davies, C. V., Soldá, C. A., Dalzotto, M. G., & Esteche, S. (2023). Isolation and identification of native yeasts from the spontaneous fermentation of grape musts. *Archives of Microbiology*, 205(9), 302. <https://doi.org/10.1007/s00203-023-03646-1>
- Grainger, K., & Tattersall, H. (2016). *Wine production and quality* (1st ed.). Wiley. <https://doi.org/10.1002/9781118934562>
- Grangeteau, C., Gerhards, D., Von Wallbrunn, C., Alexandre, H., Rousseaux, S., & Guilloux-Benatier, M. (2016). Persistence of two non-saccharomyces yeasts (*Hanseniaspora* and *starmerella*) in the cellar. *Frontiers in Microbiology*, 7. <https://doi.org/10.3389/fmicb.2016.00268>
- Guaragnella, N., & Bettiga, M. (2021). Acetic acid stress in budding yeast: From molecular mechanisms to applications. *Yeast* (Chichester, England), 38(7), 391–400. <https://doi.org/10.1002/yea.3651>
- Hall, M. E., Loeb, G. M., Cadle-Davidson, L., Evans, K. J., & Wilcox, W. F. (2018). Grape sour rot: A four-way interaction involving the host, yeast, acetic acid bacteria, and insects. *Phytopathology*®, 108(12), 1429–1442. <https://doi.org/10.1094/PHYTO-03-18-0098-R>
- He, Y., Wang, X., Li, P., Lv, Y., Nan, H., Wen, L., & Wang, Z. (2023). Research progress of wine aroma components: A critical review. *Food Chemistry*, 402, 134491. <https://doi.org/10.1016/j.foodchem.2022.134491>
- Ioriatti, C., Guzzon, R., Anfora, G., Ghidoni, F., Mazzoni, V., Villegas, T. R., Dalton, D. T., & Walton, V. M. (2017). *Drosophila suzukii* (Diptera: Drosophilidae) contributes to the development of sour rot in grape. *Journal of Economic Entomology*, 111(1), 283–292. <https://doi.org/10.1093/jee/tox292>
- Jackson, R. S. (2020). Chapter 7—Fermentation. In R. S. Jackson (Ed.), *Wine Science* (Fifth Edition) (pp. 461–572). Academic Press. <https://doi.org/10.1016/B978-0-12-816118-0.00007-6>
- Jiang, L., Qiu, Y., Dumlao, M. C., Donald, W. A., Steel, C. C., & Schmidtke, L. M. (2023). Detection and prediction of *Botrytis cinerea* infection levels in wine grapes using volatile analysis. *Food Chemistry*, 421, 136120. <https://doi.org/10.1016/j.foodchem.2023.136120>
- Jumbam, B., Toro, M., & Hu, M. (2025). Comparative analysis of grape berry microbiota uncovers sour rot associates from a Maryland vineyard. *PLOS ONE*, 20(2), e0314397. <https://doi.org/10.1371/journal.pone.0314397>
- Kelly, J., Inglis, D., Dowling, L., & Pickering, G. (2022). Impact of *Botrytis cinerea*-infected grapes on quality parameters of red wine made from withered grapes. *Australian Journal of Grape and Wine Research*, 28(3), 439–449. <https://doi.org/10.1111/ajgw.12545>

- Kelly, J., Van Dyk, S., Dowling, L., Pickering, G., Kemp, B., & Inglis, D. (2020a). *Saccharomyces uvarum* yeast isolate consumes acetic acid during fermentation of high sugar juice and juice with high starting volatile acidity. *OENO One*, 54(2). <https://doi.org/10.20870/oeno-one.2020.54.2.2594>
- Kelly, J. M., Inglis, D. L., & Pickering, G. J. (2020b). Sensorial and volatile analysis of wines made from partially dehydrated grapes: An ontario case study. *Journal of Food Quality*, 2020, 1–12. <https://doi.org/10.1155/2020/8861185>
- Kelly, J., Yang, F., Dowling, L., Nurgel, C., Beh, A., Di Profio, F., Pickering, G., & Inglis, D. L. (2018). Characterization of *Saccharomyces bayanus* CN1 for fermenting partially dehydrated grapes grown in cool climate winemaking regions. *Fermentation*, 4(3), 77. <https://doi.org/10.3390/fermentation4030077>
- Kenney, P., & Hall, M. (2021). Reducing sour rot spray applications initiated after symptom development does not impact disease control. *American Journal of Enology and Viticulture*, 5(Suppl 1), 22–28. <https://doi.org/10.5344/catalyst.2021.20008>
- Masneuf-Pomarede, I., Bely, M., Marullo, P., Pons, M., & Duchiron, F. (2010). Evidence for the existence of a genetically diverse *Saccharomyces bayanus* species in enology revealed by comparative genome hybridization. *FEMS Yeast Research*, 10(4), 439–448. <https://doi.org/10.1111/j.1567-1364.2010.00618.x>
- McCarthy, G. C., Morgan, S. C., Martiniuk, J. T., Newman, B. L., McCann, S. E., Measday, V., & Durall, D. M. (2021). An indigenous *Saccharomyces uvarum* population with high genetic diversity dominates uninoculated Chardonnay fermentations at a Canadian winery. *PLOS ONE*, 16(2), e0225615. <https://doi.org/10.1371/journal.pone.0225615>
- McFadden-Smith, W. (2010). *New Initiatives in the Management of Grape Sour Rot*. Ontario Ministry of Agriculture, Food and Rural Affairs.
- Mira, N. P., Palma, M., Guerreiro, J. F., & Sá-Correia, I. (2010). Genome-wide identification of *Saccharomyces cerevisiae* genes required for tolerance to acetic acid. *Microbial Cell Factories*, 9(1), 79. <https://doi.org/10.1186/1475-2859-9-79>
- Molinet, J., Urbina, K., Villegas, C., Abarca, V., Oporto, C. I., Villarreal, P., Villarroel, C. A., Salinas, F., Nespolo, R. F., & Cubillos, F. A. (2022). A *Saccharomyces eubayanus* haploid resource for research studies. *Scientific Reports*, 12(1), 5976. <https://doi.org/10.1038/s41598-022-10048-8>
- Morgan, S. C., Haggerty, J. J., Jiranek, V., & Durall, D. M. (2020). Competition between *Saccharomyces cerevisiae* and *Saccharomyces uvarum* in controlled Chardonnay wine

- fermentations. *American Journal of Enology and Viticulture*.  
<https://doi.org/10.5344/ajev.2020.19072>
- Mundy, D. C., Elmer, P., Wood, P., & Agnew, R. (2022). A review of cultural practices for Botrytis bunch rot management in New Zealand vineyards. *Plants*, 11(21), 3004.  
<https://doi.org/10.3390/plants11213004>
- Neugebauer, K. A., Perkins, J. A., Sysak, R., Isaacs, R., & Miles, T. D. (2024). Reducing cluster rots in Michigan wine grapes using combined pathogen and vinegar fly control. *Crop Protection*, 177, 106528. <https://doi.org/10.1016/j.cropro.2023.106528>
- Ontario Wine Appellation Authority. (2024). 2024 Annual Report.  
<https://www.ontariowineappellation.ca/>
- Owoyemi, A., Lapidot, O., Kochanek, B., Zahavi, T., Salzer, Y., Porat, R., & Lichter, A. (2022). Sour rot in the vineyard is an indicator of Botrytis rot in grapes after storage. *Postharvest Biology and Technology*, 191, 111980. <https://doi.org/10.1016/j.postharvbio.2022.111980>
- Palma, M., Guerreiro, J. F., & Sá-Correia, I. (2018). Adaptive response and tolerance to acetic acid in *Saccharomyces cerevisiae* and *Zygosaccharomyces bailii*: A physiological genomics perspective. *Frontiers in Microbiology*, 9. <https://doi.org/10.3389/fmicb.2018.00274>
- Pontes, A., Hutzler, M., Brito, P. H., & Sampaio, J. P. (2020). Revisiting the taxonomic synonyms and populations of *Saccharomyces cerevisiae*—Phylogeny, phenotypes, ecology and domestication. *Microorganisms*, 8(6), 903.  
<https://doi.org/10.3390/microorganisms8060903>
- Qu, J., Chen, X., Wang, X., He, S., Tao, Y., & Jin, G. (2024). Esters and higher alcohols regulation to enhance wine fruity aroma based on oxidation-reduction potential. *LWT*, 200, 116165.  
<https://doi.org/10.1016/j.lwt.2024.116165>
- Rolle, L., Río Segade, S., Paissoni, M. A., Giacosa, S., & Gerbi, V. (2022). Assessment and control of grape maturity and quality. In *White Wine Technology* (pp. 1–16). Elsevier.  
<https://doi.org/10.1016/B978-0-12-823497-6.00001-6>
- Sieczkowski, N., Wang, X., Hall, M., & Inglis, D. (2022). Managing sour rot in Niagara: A 3-year study on harvest date and nitrogen additions. *Catalyst*, 6(4), 35–43.  
<https://doi.org/10.5344/catalyst.2022.21007>
- Vasserot, Y., Mornet, F., & Jeandet, P. (2010). Acetic acid removal by *Saccharomyces cerevisiae* during fermentation in oenological conditions. Metabolic consequences. *Food Chemistry*, 119(3), 1220–1223. <https://doi.org/10.1016/j.foodchem.2009.08.008>

- Wang, K., Wu, Z., Du, J., Liu, Y., Zhu, Z., Feng, P., Bi, H., Zhang, Y., Liu, Y., Chen, B., Wang, M., & Tan, T. (2023). Metabolic engineering of *Saccharomyces cerevisiae* for conversion of formate and acetate into free fatty acids. *Fermentation*, 9(11), 984. <https://doi.org/10.3390/fermentation9110984>
- Willwerth, J. J., Reynolds, A. G., & Lesschaeve, I. (2015). Sensory analysis of Riesling wines from different sub-appellations in the Niagara Peninsula in Ontario. *American Journal of Enology and Viticulture*, 66(3), 279–293. <https://doi.org/10.5344/ajev.2015.14081>
- Williams, P. W. (2023). White winemaking. In *The Oxford Companion to Wine*. Oxford University Press. <https://www.oxfordreference.com/display/10.1093/acref/9780198871316.001.0001/acref-9780198871316-e-3843>
- Yang, F., Heit, C., & Inglis, D. L. (2017). Cytosolic redox status of wine yeast (*Saccharomyces cerevisiae*) under hyperosmotic stress during icewine fermentation. *Fermentation*, 3(4), 61. <https://doi.org/10.3390/fermentation3040061>

## Chapter 2 – Materials & Methods

### 2.1 Grape Harvest, Sorting, and Processing

A combination of healthy and rot-affected *Vitis vinifera* Riesling grapes was manually harvested over two consecutive days from Seeger Vineyards, located in Niagara-on-the-Lake, Ontario, Canada. On the first day, 790 kg of visually clean fruit was collected in perforated plastic bins, transported to the Cool Climate Oenology and Viticulture Institute (CCOVI) at Brock University (St. Catharines, ON, Canada), and stored in a 4 °C cold room. The following day, 248 kg of rot-affected fruit was selectively harvested and similarly transported to CCOVI. On the day after the final harvest, the rot-affected clusters were further hand-sorted to ensure that only those with more than 50% visible rot coverage were retained for processing. Clean and rot-affected grapes were then processed separately, beginning with the clean fruit. Each batch was crushed and destemmed using a Gamma 50 crusher-destemmer (Mori-TEM, Florence, Italy) into sanitized plastic buckets. Pressing was carried out with an 80 L bladder press (Enotecnica Pillan, Vicenza, Italy) at a pressure of 1 bar for two minutes, with juice collected into separate stainless steel tanks for each fruit category. The total mass of grapes and the corresponding juice yield were recorded for both clean and rot-affected lots.

Juice nitrogen levels were adjusted to 200 mg L<sup>-1</sup> using diammonium phosphate (DAP) to support adequate fermentation kinetics. From these juice fractions, three treatment groups were prepared by blending clean and rot-affected juices to achieve target inclusion levels of 0%, 20%, and 40% rot by weight. Each treatment blend was mixed in 120 L

stainless steel tanks prior to allocation. A 21 L volume of juice from each treatment was measured and transferred into individual plastic carboys for fermentation.

## 2.2 Winemaking

As outlined in Figure 2.1, a total of six fermentation treatments were conducted in triplicate, corresponding to three levels of rot inclusion (0%, 20%, and 40%) each inoculated with one of two yeast strains: *Saccharomyces cerevisiae* EC1118 or *S. uvarum* CN1. The treatments were as follows: (i) 0% rot with EC1118, (ii) 0% rot with CN1, (iii) 20% rot with EC1118, (iv) 20% rot with CN1, (v) 40% rot with EC1118, and (vi) 40% rot with CN1.

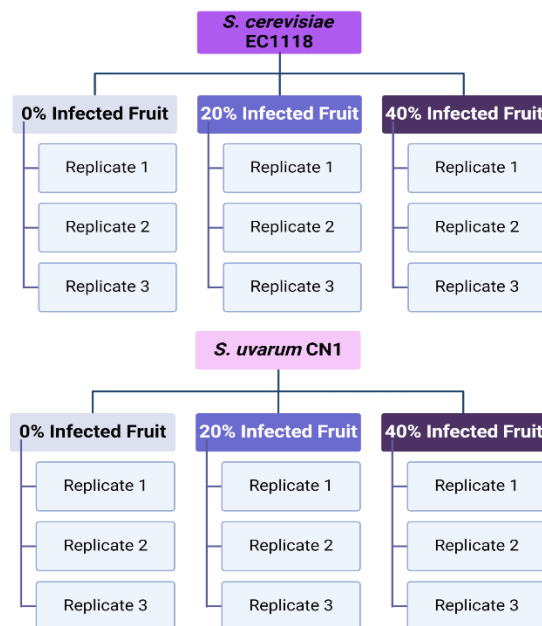


Figure 2.1: Schematic overview of the oenological treatments conducted with increasing rot percentages (0%, 20%, and 40%) inoculated using either *S. cerevisiae* EC1118 (control) or *S. uvarum* CN1. Created using Biorender.com.

Preparation of *S. cerevisiae* EC1118 followed the manufacturer's rehydration protocol. The culture was streaked onto yeast extract peptone dextrose (YPD) agar plates (1% yeast extract, 2% peptone, 2% dextrose, 2% agar). The CN1 isolate, stored in glycerol stocks at

-80 °C, was similarly revived and plated on YPD. Both yeast strains were incubated until individual colonies reached suitable size for propagation. Colonies were transferred into 300 mL of sterile-filtered Riesling juice (10 °Brix) supplemented with 2 g L<sup>-1</sup> diammonium phosphate (DAP) and incubated aerobically in 1L Erlenmeyer flasks at 25 °C with agitation (130 rpm) until cell densities reached approximately 2 × 10<sup>8</sup> cells mL<sup>-1</sup>, as determined via haemocytometer counts.

Following this, 300 mL of sterile-filtered control juice (18 °Brix, 0% rot) was added to each culture and held for 1 hour at 25 °C, with gentle swirling after 30 minutes for acclimatization (adapted from Kontkanen et al., 2004). After this build-up phase, 600 mL of each respective yeast starter was added to its corresponding must to achieve an inoculation rate of 2 × 10<sup>6</sup> cells mL<sup>-1</sup> in 21 L fermentation volumes contained in plastic carboys.

After inoculation, carboys were gently mixed by swirling and transferred to a temperature-controlled fermentation chamber set to 17 °C. On Day 1 of fermentation, 80 mg L<sup>-1</sup> of DAP was added to each fermentation to supplement yeast assimilable nitrogen (YAN).

Fermentation progress was monitored daily by measuring soluble solids (°Brix) with a hydrometer and temperature (°C) with a thermometer. Dedicated equipment was used for each yeast treatment group and sterilized between uses with 70% ethanol to prevent cross-contamination. Fermentations were deemed complete when Brix readings fell below 0 ° or remained stable for three consecutive days.

Upon completion, wines were racked off lees into sanitized 21 L plastic carboys, sparged with CO<sub>2</sub>, and stabilized with 50 mg L<sup>-1</sup> sulfur dioxide (as potassium metabisulfite). Wines

were stored at 4 °C to settle before being transferred to a -2 °C chamber for cold stabilization. Once cold-stable, wines were racked again and assessed for protein stability using bench trials with bentonite and turbidity measurements. Free sulfur dioxide levels were monitored every three weeks to ensure wine stability and protection. Immediately before bottling, free SO<sub>2</sub> was adjusted to 35–45 mg L<sup>-1</sup> to maintain protection during post-bottling storage.

Final wines were sterile-filtered through 0.45 µm filter pads, bottled into 750 mL glass bottles using a manual bottler (Criveller Group, Niagara Falls, ON, Canada), sealed with Diam 10 corks using an automated corker (STSILON-R, Bertolaso, San Vito, Italy), and stored in the CCOVI wine cellar under controlled conditions (14 °C, 74.5% relative humidity).

### 2.2.1 Additional Fermentations Not Included in Final Dataset

An additional set of fermentations was conducted in response to a temperature spike observed on Day 2 of fermentation set 1 experimental trials and excessive hydrogen sulfide production (see Figure 3.2), which raised concerns regarding the viability and fermentative capacity of the cryotolerant yeast strain *S. uvarum* CN1 under elevated thermal conditions. To address this, a new batch of fruit was collected from King and Victoria Estate Winery (Beamsville, ON) and Nomad at Hinterbrook Winery (Niagara-on-the-Lake, ON). Fruit processing and sorting followed the same protocols described in Section 2.1. However, due to elevated levels of volatile acidity in the harvested grapes, the rot proportions were adjusted to lower levels than originally planned to reach target acetic acid values in the

processed juice, resulting in treatments of 0%, 15%, and 30% w/w rot inclusion. These fermentations made up fermentation set 2.

During blending and distribution of the juice for fermentation set 2, an accidental spill of the large-format stainless steel container containing the 30% rot treatment occurred. To compensate for the loss, a clean juice sample was amended with glacial acetic acid to a final concentration of 0.35 g/L in order to approximate the volatile acidity expected in the 30% rot-affected must for fermentation set 3.

### 2.3 Microbial Implantations and Yeast Identification

To monitor yeast implantations throughout fermentation and enable species-level identification, methods were followed as outlined in McCarthy et al. (2021). Samples from the early (18-20°Brix), mid (10-12°Brix), and late stages (<5°Brix) of fermentation were serially-diluted and plated onto yeast extract peptone dextrose medium (1% yeast extract, 2% peptone, 2% dextrose, 2% agar, with the addition of 0.01% chloramphenicol (Sigma-Aldrich, St. Louis, MO, USA) to prevent bacterial growth, and 0.015% biphenyl (Sigma-Aldrich, St. Louis, MO, USA) to prevent filamentous fungal growth. Plates were incubated at 28°C for 48 h and subsequently stored at 4 °C. Plates containing 30–300 colonies were selected for replica plating onto differential media and DNA extraction for identification.

From the early, mid, and late stage plates, selected YPD plates were replica plated onto Wallerstein Nutrient Media (WLN), a differential medium used to identify non-*S. cerevisiae* yeasts. Two controls were used to distinguish between *S. cerevisiae* and *S. uvarum* colonies: EC1118 (Lallemand, Montreal, QC, Canada) and CN1, respectively. The WLN

plates were incubated at 28 °C for 24 h, and then stored at 4 °C. *S. cerevisiae* isolates appeared cream-coloured, while presumed *S. uvarum* isolates appeared green (Figure A2.1)

The yeast genus/species identity of the isolates was confirmed using whole-colony PCR, performed directly on single colonies without prior DNA extraction, following the method of Kelly et al. (2018). Initial genus/species-level screening targeted the D1/D2 domain of the large subunit rRNA gene. PCR amplification of this region was conducted using standard thermal cycling conditions, and the resulting amplicons were purified using the QIAquick PCR Purification Kit (QIAGEN, Cat. No. 28104). Sequencing was performed by the Centre for Applied Genomics (The Hospital for Sick Children, Peter Gilgan Centre for Research and Learning, Toronto, Canada). The obtained sequences were aligned and compared against reference databases using the Basic Local Alignment Search Tool (BLAST) to determine if the isolates belonged to the *Saccharomyces* genus.

To refine the *Saccharomyces* species identification, the  $\beta$ -tubulin gene was amplified using the primer pair  $\beta$ tub3 (5'-TGGGCYAAGGGTYAYTAYAC) and  $\beta$ tub4r (5'-GCCTCAGTRAAYTCCATYTCRTCCAT), following the approach described by Huang et al. (2009). Although this gene reliably differentiates among *S. cerevisiae*, *S. bayanus*, and *S. pastorianus*, it cannot distinguish between *S. bayanus* sensu stricto and *S. uvarum*. Therefore, isolates presumptively identified as either *S. bayanus* or *S. uvarum* were further analyzed through amplification of three regions of the Glutamate Dehydrogenase 1 (GDH1 gene): the open reading frame (ORF), promoter (Pro), and intergenic spacer (IGS), as described by Nguyen and Gaillardin (2005). Primer sequences for the GDH1 ORF and

promoter regions were not explicitly listed, as conserved primers were used and species differentiation was based on sequence variation rather than primer specificity. For the IGS region, which provides diagnostic resolution between *S. bayanus* and *S. uvarum*, the primer set SuglgU (5'-GCCAAGAAGTACACTAAGG) and SuglgL (5'-CTGTTCGATGCTTTACAAAAC) was used.

All PCR reactions were carried out in 25  $\mu\text{L}$  volumes consisting of 19.75  $\mu\text{L}$  sterile  $\text{dH}_2\text{O}$ , 2.5  $\mu\text{L}$  10 $\times$  PCR buffer, 1.0  $\mu\text{L}$  each of forward and reverse primers (10  $\mu\text{M}$ ), 0.5  $\mu\text{L}$  dNTP mix (10 mM), and 0.25  $\mu\text{L}$  Taq DNA polymerase (Roche, 5 U/ $\mu\text{L}$ ). Thermocycling parameters for all amplifications were as follows: initial denaturation at 94°C for 3 minutes, followed by 35 cycles of 94°C for 30 seconds, gene-specific annealing temperature for 45 seconds (e.g., 58°C for  $\beta$ -tubulin; 45°C for GDH1 IGS), and 72°C for 1 minute. A final elongation step was conducted at 72°C for 10 minutes. All purified PCR products were sequenced and analyzed by BLAST to confirm species-level identity.

#### 2.4 Grape, Must, and Fermentation Analysis

Fermentation temperature was recorded daily using a standard thermometer (°C). Soluble solids were measured throughout fermentation using a degree Brix hydrometer to monitor sugar depletion over time (°Brix). The pH of juice and wine samples was determined using a benchtop pH meter (SympHony SB70P; VWR, Mississauga, ON, Canada), while titratable acidity (TA) was assessed by titration with 0.1 mol L<sup>-1</sup> sodium hydroxide (NaOH) to a pH endpoint of 8.2. All TA measurements were recorded in units of g/L tartaric acid.

Chemical analyses of fermentation metabolites were performed using enzymatic assay kits from Megazyme International (Bray, County Wicklow, Ireland). The analytes quantified included glucose and fructose (K-FRUGL), glycerol (K-GCROL), acetaldehyde (K-ACHD), ethanol in must (K-ETOH), amino acid nitrogen (K-PANOPA), ammonia nitrogen (K-AMIAR), acetic acid (K-ACET), gluconic acid (K-GATE), succinic acid (K-SUCC), following the manufacturer's protocols.

Ethanol concentrations in finished wines were measured using gas chromatography (GC-FID). Analyses were conducted on a Hewlett-Packard 6890 Series gas chromatograph (Agilent Technologies Inc., Santa Clara, CA, USA) equipped with a flame ionization detector (FID), split/splitless injector, and operated via ChemStation software (version E.02.00.493). Separations were achieved using a DB-WAX capillary column (30 m length × 0.25 mm ID × 0.25 µm film thickness; Agilent Technologies, model 122-7032), with helium used as the carrier gas at a flow rate of 1.5 mL min<sup>-1</sup>.

## 2.5 Volatile Organic Compounds and Volatile Fatty Acid Analysis

Volatile compound analysis was performed using a modified version of the protocol described by Tomasino et al. (2015), targeting compounds relevant to the aromatic and flavour profile of Riesling wines. A selection of representative volatile classes was chosen for analysis, based on their known contributions to varietal character as listed in Table 2.1.

Table 2.1: Categories, CAS Numbers, odour descriptors and sensory threshold ( $\mu\text{g/L}$ ) of all VOCs and VFAs measured in wines made from increasing rot levels.

Category	Compound	CAS Number	Sensory Threshold	Purity (%)	Odour Descriptor
<i>Volatile Organic Compounds (VOCs)</i>					
Internal Standard	1-Hexan-d <sub>13</sub> -ol ISTD	204244-84-8	N/A	98	N/A
	1-Phenyl-d <sub>5</sub> -ethanol ISTD	90162-45-1	N/A	100	N/A
	Ethyl hexanoate-d <sub>11</sub> ISTD	2159-19-5	N/A	98	N/A
	3-Methylbutyl Acetate-d <sub>3</sub> ISTD	1219804-75-7	N/A	98	N/A
	Hexanoic-d <sub>11</sub> -acid	95348-44-0	N/A	100	N/A
Acetate Esters	Isoamyl acetate	123-92-2	30 <sup>f</sup>	100	Fruity, banana <sup>f</sup>
	Hexyl acetate	142-92-7	670 <sup>f</sup>	100	Pear <sup>f</sup>
	Ethyl acetate	141-78-6	7,500 <sup>f</sup>	100	Fruity, pineapple, varnish, pungent <sup>f</sup>
Ethyl Esters	Ethyl Isobutyrate	97-62-1	15 <sup>f</sup>	99	Sweet, rubber <sup>f</sup>
	Ethyl butyrate	105-54-4	20 <sup>f</sup>	99.5	Apple <sup>f</sup>
	Ethyl isovalerate	108-64-5	3 <sup>b</sup>	98	Apple, fruit, pineapple <sup>b</sup>
	Ethyl 2-methylbutyrate	7452-79-1	18 <sup>b</sup>	99	Fruity, sweet, apple <sup>b</sup>
	Ethyl hexanoate	123-66-0	14 <sup>c</sup>	100	Green apple <sup>c</sup>
	Ethyl octanoate	106-32-1	580 <sup>b</sup>	99	Fruity, strawberry <sup>b</sup>
	Ethyl decanoate	110-38-3	200 <sup>e</sup>	99	Soap, floral <sup>e</sup>
Alcohol	Hexanol	111-27-3	8,000 <sup>a</sup>	100	Herbaceous, resin, flower <sup>a</sup>
	2-methylpropanol	78-83-1	40,000 <sup>e</sup>	99.5	Green <sup>e</sup>
	2-phenylethanol	60-12-18	14,000 <sup>b</sup>	99	Rose, honey <sup>b</sup>
<i>Volatile Fatty Acids (VFAs)</i>					
	Hexanoic acid	142-62-1	420 <sup>d</sup>	100	Sweat <sup>d</sup>
	Octanoic acid	124-07-2	500 <sup>d</sup>	100	Sweat, cheese <sup>d</sup>
	Decanoic acid	334-48-5	1000 <sup>d</sup>	98	Rancid fat <sup>d</sup>

<sup>a</sup>Bellincontro et al., 2016

<sup>b</sup>Francis and Newton, 2005

<sup>c</sup>López et al., 2012

<sup>d</sup>Pérez-Navarro et al., 2020

<sup>e</sup>Noguerol-Pato et al., 2009

<sup>f</sup>Rice et al., 2018

<sup>g</sup>Suklje et al., 2016

Concentrations of analytical standards were prepared following Tomasino et al. (2015), with adjustments for matrix effects using a model wine derived from the 0% rot EC1118 treatment. All preparations used Milli-Q water (Biocel MilliQ, EMD Millipore, Cillerica, MA, USA) filtered through a 0.22  $\mu\text{m}$  membrane (Millipore). Stock standard solutions (Standard A) were prepared in Chromasolv<sup>®</sup> HPLC-grade ethanol (Sigma-Aldrich, Oakville, ON, Canada) and used to formulate a composite standard (Standard C), which was diluted to prepare a fresh working standard daily.

For calibration and sample preparation, 3 g of reagent-grade NaCl (BioShop, Burlington, ON, Canada) was added to 20 mL amber glass vials (MicroLiter Analytical Supplies Inc., Millville, NJ, USA) with 8.06 mL Milli-Q water and model wine. The model wine was produced by de-aromatizing a base wine via rotary evaporation (40 °C, 30 min) and adjusting ethanol to 10% (v/v). Standards received an appropriate volume of Standard C and 40  $\mu\text{L}$  of an internal standard mixture, then were sealed with PTFE/silicone-lined magnetic headspace caps. Calibration curves were generated by plotting analyte concentration against the response factor, defined as the ratio of analyte peak area to internal standard peak area. Wine samples were diluted tenfold with Milli-Q water (VOCs) or pH 3.5 acidified matrix (VFAs) and prepared identically to standards.  $d_{11}$ -Hexanoic acid served as the internal standard for VFAs.

Extraction was performed via headspace solid-phase microextraction (HS-SPME) using a 2 cm DVB/CAR/PDMS 24-gauge fiber (Supelco). Vials were equilibrated at 40 °C for 1 min (500 rpm) before a 30 min headspace exposure. Desorption occurred in the GC inlet for 10 min. Analyses were conducted on an Agilent 7890B GC coupled to a 5977B MS with a CTC

Analytics PAL RSI 85 autosampler, fitted with a DB-624 UI capillary column (30 m × 0.25 mm i.d., 1.40 µm film; Agilent Technologies). Helium was used as the carrier gas (1 mL/min). The oven program began at 35 °C (5.66 min hold), ramped 8.8 °C/min to 100 °C (1.5 min hold), 13.3 °C/min to 220 °C (3.43 min hold), and 22.1 °C/min to 250 °C (3.43 min hold), for a total run time of 80 min. Inlet and transfer line temperatures were 250 °C, with splitless injection, a 5 min solvent delay, and fiber bake-out before (10 min) and after (20 min) each run. Detection was performed in both full scan (35–400 m/z) and SIM modes (EMV gain factor = 7).

VFA analysis followed the same GC-MS parameters with adaptations specific to this compound class. Compounds were identified using full-scan (SCAN) mode, matched to spectral data from the NIST17 mass spectral library, and confirmed by retention time, diagnostic ion fragments, and comparison with authentic standards. Quantification was achieved by comparing peak areas of analytes to those of deuterated internal standards, using up to six-point calibration curves prepared in model wine ( $r^2 > 0.90$ ). All samples were analyzed in duplicate, with coefficients of variation ranging from 1% to 12%.

## 2.6 Sensory Evaluation

A preliminary bench tasting (n = 5) was conducted to evaluate the sensory consistency among winemaking replicates within each treatment and to determine if any faults were present in the wine. Wines were assessed for similarity in aroma, taste, and mouthfeel. Based on the consensus of this informal assessment, the triplicate fermentations for each treatment were deemed sufficiently similar to be blended into six representative wines for

sensory evaluation: EC1118 0% Rot, CN1 0% Rot, EC1118 20% Rot, CN1 20% Rot, EC1118 40% Rot, and CN1 40% Rot. No faults were reported.

Quantitative descriptive analysis (QDA) was conducted by a trained panel of 14 participants (eight males and six females) recruited from the student and staff community at the Cool Climate Oenology and Viticulture Institute (CCOVI), Brock University. Sensory testing was carried out approximately six months post-bottling, following ten preparatory training sessions. Panelists were selected based on previous wine tasting experience, availability, and willingness to participate. Ethics approval for sensory testing was granted by the Brock University Research Ethics Board (File No. 22-308 – KELLY).

Training followed the procedures outlined in the Manual on Descriptive Analysis Testing for Sensory Evaluation (Hootman, 1992). The first two one-hour training sessions involved exposure to all six wines, during which replicates were blended and assessed for the presence of faults unrelated to experimental treatment (e.g., cork taint). These sessions were used to generate an initial descriptor pool for aroma, flavour, and mouthfeel attributes. Through group discussion, redundant or overlapping terms were removed, resulting in a finalized consensus lexicon.

The final list of aroma descriptors included: lemon/lime, green apple, tropical, stone fruit, honey, floral, rubber, soya sauce, oxidized fruit, and musty. Flavour descriptors included: lemon/lime, green apple, tropical, stone fruit, honey, floral, oxidized fruit, and rubber. Additional tactile and taste descriptors included sweetness, acidity, bitterness, alcohol, and body. Reference standards for all aroma descriptors were developed using bulk

Riesling wine fermented with EC1118 as the base. Recipes and preparation procedures are provided in Table 2.2. Panelists evaluated and refined these reference standards over the course of the next six one-hour sessions.

*Table 2.2: Complete list of reference standards and describing terms used for descriptive analysis of Riesling wines made from partially rot-affected grapes.*

<b>Attribute</b>	<b>Includes Terms</b>	<b>Reference Standard Composition</b>
Lemon/Lime	Lemon, lime, citrus	100mL wine + one quarter diced lemon + one quarter diced lime. Left overnight to steep.
Green Apple	Apple, green apple, apple skin	100mL wine + one quarter green apple sliced. Left overnight to steep.
Stone Fruit	Peach, apricot	100mL wine + one quarter apricot sliced + one quarter peach sliced. Left overnight to steep.
Tropical	Pineapple, passionfruit	100mL wine + one drop pineapple aroma standard + one drop passionfruit aroma standard.
Honey		100mL wine + two drops honey aroma standard.
Floral	White blossom, rose	100mL wine + one drop mixed floral standard.
Oxidized Fruit	Bruised apple, sherry	100mL wine + 5mL Fino Sherry.
Rubber	Petrol, elastic, rubber band	100mL wine + 4 elastic bands. Left overnight to steep.
Soya Sauce	Olive, soya sauce, BBQ sauce	100mL wine + 5mL soya sauce.
Musty	Wet basement, soil, damp clothing	100mL wine + two drops must aroma standard + one drop mushroom standard
Sweet	N/A	100mL wine + 6g/L sucrose.
Sour	N/A	100mL wine + 2g/L tartaric acid.
Bitter	N/A	100mL wine + 50mg/L caffeine.
Alcohol	N/A	100mL wine + 8mL of 70% ethanol.
Body	N/A	100mL wine + 5g/L food grade glycerol.
The base wine used for sensory analysis consisted of bulk Riesling wine obtained from previous research projects conducted at CCOVI, representing blended lots from multiple vintages		

Panelist performance was monitored throughout the training phase using 15 cm anchored line scales (low to high intensity) divided into quadrants, provided on paper ballots. By the eighth session, consistency across panelist ratings indicated readiness for data collection. An additional training session was held to introduce panelists to the Compusense™ system and familiarize them with the electronic interface and sensory booths.

Formal evaluation of the wines was carried out in duplicate over four sessions, with panelists evaluating three wines per session (one flight per session). Wines were presented in a complete randomized block design to minimize presentation order effects. Prior to each session, wines were opened and screened for non-treatment-related faults. Panelists were instructed to assess samples in the order presented and to take a two-minute forced break between wines to mitigate sensory fatigue. Each panelist was assigned an individual booth equipped with a computer, mouse, spittoon, water, unsalted crackers, and a breathalyzer (BACtrack S80). Participants were required to expectorate all samples and confirm blood alcohol levels before leaving each session. Wines (30 mL per sample) were served at room temperature in International Standards Organization (ISO) wine glasses, covered with petri dish lids, and labeled with random three-digit codes. The sensory laboratory was illuminated with red lighting to minimize colour bias.

Descriptive analysis data were collected using Compusense™ software (Guelph, ON, Canada). Panelists rated the intensity of each attribute using a 15 cm unstructured line scale anchored at “low” and “high,” with responses recorded in millimeter values. The final attribute list used for evaluation was refined from those generated during training;

descriptors that did not reach panel consensus were excluded prior to formal data collection.

## 2.7 Statistical Analysis

Statistical analyses were performed in XLSTAT (Addinsoft, Paris, France) at a 95% confidence level ( $p < 0.05$ ). One-way ANOVA was used to assess differences among volatile compound concentrations, while two-way ANOVA evaluated the effects of tasting replicate, winemaking replicate, and their interaction. A three-way ANOVA was also conducted to account for the effects of tasting replicate, judge, wine treatment, and all associated two-way interactions (Tasting Replicate  $\times$  Judge, Tasting Replicate  $\times$  Wine, Judge  $\times$  Wine). When significant effects were observed, post-hoc comparisons were conducted using least significant difference (LSD) tests.

Principal component analysis (PCA) was conducted to explore associations between chemical compounds (observations/variables) and winemaking treatments (included as supplementary variables). The analysis used Pearson (n) correlation matrices without rotation and was visualized using correlation biplots. Partial least squares (PLS) regression was also performed to model the relationship between chemical (Y) and sensory (X) variables. The PLS algorithm used fast computation with automatic stopping conditions, Jackknife (leave-one-out) cross-validation, and autoscaling (centering and reduction of variables). All multivariate analyses were performed using XLSTAT (version 2024.4.2, build 1426; Addinsoft, Paris, France).

## 2.8 Statement of Ethics

All participants provided informed consent prior to their involvement in the study. The research protocol was reviewed and approved by the Brock University Research Ethics Board (File No. 22-308 – KELLY).

## Chapter 3: Results

### 3.1 Microbial Implantations and Yeast Identification

The implantation success of the inoculated yeast strains, *S. cerevisiae* EC1118 and *S. uvarum* CN1, was evaluated across three fermentation sets corresponding to the experimental trials previously described. Briefly, set 1 represented the initial fermentation series, set 2 the repeat trial performed under controlled conditions following the temperature spike observed in set 1, and set 3 the acetic-acid-amended replacement for the lost 30% rot treatment. For each fermentation set, samples were removed for microbial evaluation from the original (Riesling must pre-inoculation, and at early, middle, and late fermentation time points). The proportions of *S. cerevisiae*, *S. uvarum*, and other yeast species were quantified as percentages of total colony-forming units (CFUs) recovered per treatment (Figure 3.1).

#### 3.1.1 Fermentation Set 1

In fermentation set 1, at the early sampling timepoint in Figure 3.1b, all six treatments showed 100% implantation success of the intended inoculated strain, with no detection of unintended yeast species or contaminants. EC1118 fermentations at 0%, 20%, and 40% rot inclusion yielded exclusively *S. cerevisiae* colonies, whereas CN1 fermentations across

all rot levels resulted exclusively in *S. uvarum* colonies. These results indicate complete implantation fidelity during this fermentation round.

The Riesling middle time point for fermentation set 1 (Figure 3.1c) revealed minor deviations from complete implantation. EC1118 fermentations at 20% and 40% rot levels exhibited small proportions of *S. uvarum* (4% and 2%, respectively), suggesting possible low-level cross-contamination or persistence of native yeasts. *S. cerevisiae* remained the dominant species, with implantation levels  $\geq 96\%$  across all rot levels. CN1 fermentations again resulted in 100% *S. uvarum* recovery across all treatments, indicating consistent implantation success.

In the Riesling late time point analysis for fermentation set 1 of Figure 3.1d, implantation success returned to 100% fidelity across all treatments. All EC1118 fermentations yielded exclusively *S. cerevisiae* colonies, and all CN1 fermentations yielded exclusively *S. uvarum*. No other yeast species were recovered in any treatment, and no implantation failures or deviations were observed.

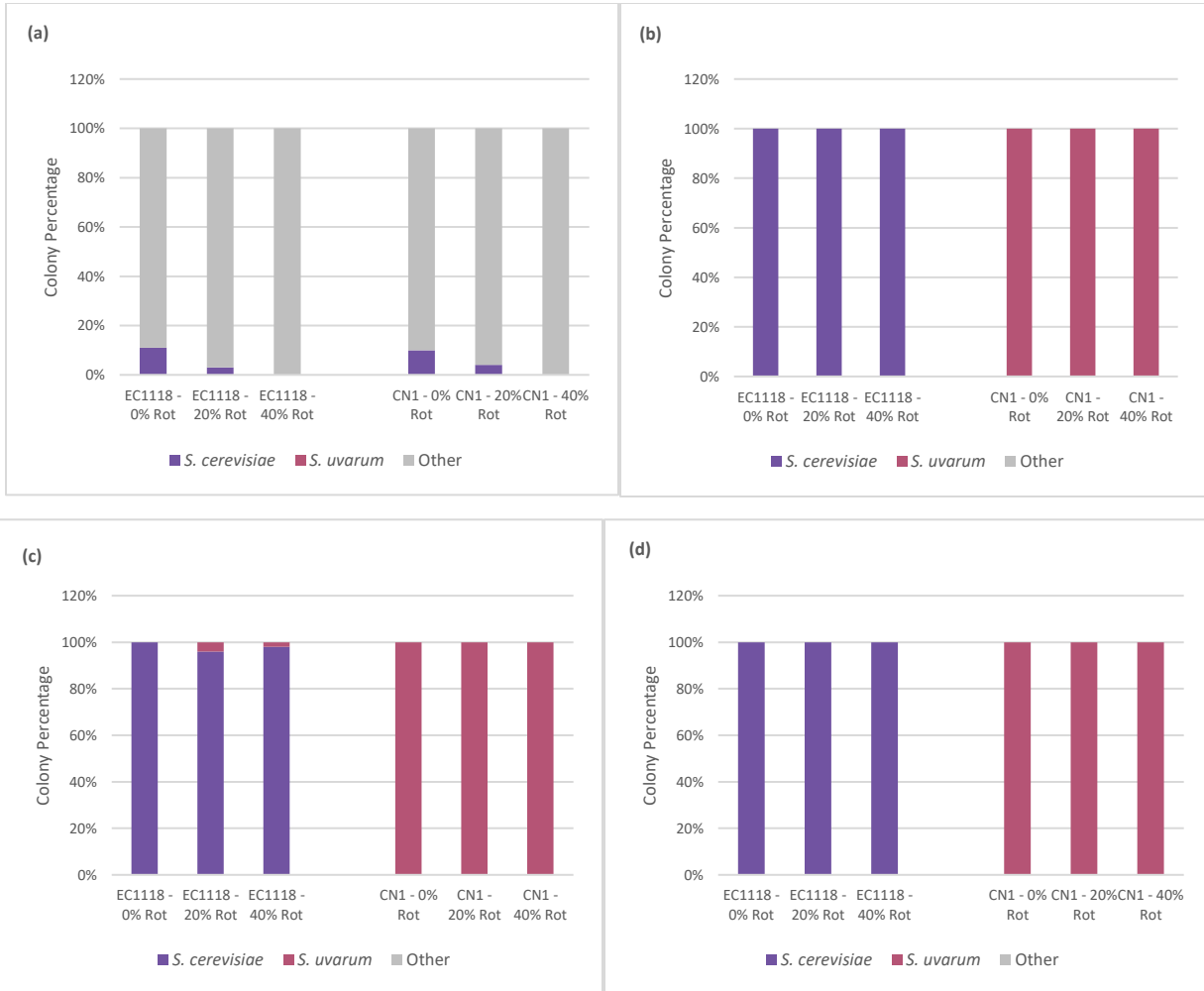


Figure 3.1: Proportional distribution of yeast species recovered from implantation plating across six wine fermentation treatments for Fermentation set 1. Treatments included three levels of rot infection (0%, 20%, and 40%) and two inoculated yeast strains: *Saccharomyces cerevisiae* EC1118 and *S. uvarum* CN1. Bars represent the relative abundance of *S. cerevisiae*, *S. uvarum*, and other yeast species identified through replicate plating on WLN differential media. Yeast implantations were measured at four different timepoints throughout the fermentation: Juice (pre-inoculation) (a), Early (18-20°Brix) (b), Middle (10-12°Brix) (c), and Late (<5°Brix) (d).

The  $\beta$ -tubulin and GDH1 intergenic spacer (*igs*) gene regions were amplified and sequenced for yeast isolates from the CN1 and EC1118 fermentations, along with their respective positive controls. These markers were selected for their ability to reliably discriminate between closely related *Saccharomyces* species.

For the  $\beta$ -tubulin region, all CN1 isolates (20% rot, 40% rot treatments and the positive control) matched *S. uvarum* strain CBS7001 with 99–100% query coverage and high sequence identities (99.77–99.88%) (Table 3.1). Pairwise alignment of these  $\beta$ -tubulin contigs revealed no nucleotide substitutions and only minor single-based insertions/deletions (9-10 bp total across the alignment) (Table A1.1). The CN1 0% rot isolate also returned *S. uvarum* CBS7001 as the top BLAST hit but with but with reduced sequence identity (84.23%) and 95% query coverage (Table 3.1). Alignment of this contig to the CN1  $\beta$ -tubulin consensus sequence revealed a higher number of differences including 86 nucleotide substitutions and 86bp of insertions/deletions (Table A1.1). Inspection of the raw Sanger chromatograms showed poor signal quality and unreliable base calls at positions corresponding to the apparent substitutions and indels, indicating sequencing artefacts rather than true  $\beta$ -tubulin polymorphisms. In combination with the high identity of the corresponding GDH1 *igs* sequence and the conservation of other CN1  $\beta$ -tubulin sequences, the reduced identity of the CN1 0% rot  $\beta$ -tubulin sequence is therefore attributed to poor-quality sequencing rather than genetic divergence.

For the GDH1 *igs* region, all CN1 isolates (0%, 20%, 40% rot) and the positive control matched *S. uvarum* strain CBS7001 with 99–100% coverage and high sequence identities ranging from 99.24% to 99.74%, confirming species-level identity across all treatments

(Table 3.1). Alignment of the GDH1 igs contigs revealed no nucleotide substitutions among isolates and only a small number of single-base insertions/deletions ( $\leq 10$  bp per alignment) (Table A1.1).

For EC1118,  $\beta$ -tubulin sequences from the 0% rot, 20% rot, and positive control isolates matched *S. cerevisiae* strain KSD-Yc with 98–100% coverage and sequence identities between 99.09% and 99.88% (Table 3.1). The EC1118 40% rot isolate matched *S. cerevisiae* strain YJM270 with 100% coverage and 97.64% sequence identity. Alignment of EC1118  $\beta$ -tubulin contigs revealed modest numbers of nucleotide substitutions and short insertions/deletions, with fewer than 20 substitutions and fewer than 25 bp of indels observed across all comparisons (Table A1.1).

GDH1 igs sequences from all EC1118 isolates (0%, 20%, 40% rot) and the positive control matched *S. cerevisiae* strain CEN.PK113-7D with 99–100% coverage and 100% sequence identity in every case (Table 3.1). Direct comparison of the GDH1 igs contigs revealed no substitutions and only minimal terminal indels providing consistent confirmation of strain identity regardless of rot level.

Overall, both  $\beta$ -tubulin and GDH1 igs sequencing confirmed that CN1 isolates belonged to *S. uvarum* and EC1118 isolates to *S. cerevisiae*, with the only deviation being a reduced  $\beta$ -tubulin sequence identity for the CN1 0% rot sample (Table 3.1).

Table 3.1: Sequence homology of isolates from the *Saccharomyces uvarum* CN1 and *S. cerevisiae* EC1118 2023 Riesling fermentations, including positive control stocks, against reference strains in the NCBI GenBank database.

Gene Region	Sample	NCBI Database Strain for Sequence Comparison	Max Score	Query Coverage	Sequence Identity	GenBank Accession Number
B-tubulin	CN1_0% rot	<i>Saccharomyces uvarum</i> Strain CBS7001	817	95%	84.23%	CP113769.1
	CN1_20% rot	<i>Saccharomyces uvarum</i> Strain CBS7001	1580	99%	99.77%	CP113769.1
	CN1_40% rot	<i>Saccharomyces uvarum</i> Strain CBS7001	1561	100%	99.88%	CP113769.1
	CN1 positive control	<i>Saccharomyces uvarum</i> Strain CBS7001	1572	99%	99.88%	CP113769.1
	EC1118_0% rot	<i>Saccharomyces cerevisiae</i> Strain KSD-Yc	1568	99%	99.09%	CP024000.1
	EC1118_20% rot	<i>Saccharomyces cerevisiae</i> Strain KSD-Yc	1591	100%	99.77%	CP024000.1
	EC1118_40% rot	<i>Saccharomyces cerevisiae</i> Strain YJM270	1520	100%	97.64%	CP004895.2
	EC1118 positive control	<i>Saccharomyces cerevisiae</i> Strain KSD-Yc	1530	98%	99.88%	CP024000.1
GDH1 igs Region	CN1_0% rot	<i>Saccharomyces uvarum</i> Strain CBS7001	721	99%	99.24%	CP113771.1
	CN1_20% rot	<i>Saccharomyces uvarum</i> Strain CBS7001	701	100%	99.74%	CP113771.1
	CN1_40% rot	<i>Saccharomyces uvarum</i> strain CBS7001	712	99%	99.74%	CP113771.1
	CN1 positive control	<i>Saccharomyces uvarum</i> strain CBS7001	717	100%	99.74%	CP113771.1
	EC1118_0% rot	<i>Saccharomyces cerevisiae</i> strain CEN.PK113-7D	734	99%	100.00%	CP046095.1
	EC1118_20% rot	<i>Saccharomyces cerevisiae</i> strain CEN.PK113-7D	732	100%	100.00%	CP046095.1
	EC1118_40% rot	<i>Saccharomyces cerevisiae</i> strain CEN.PK113-7D	734	99%	100.00%	CP046095.1
	EC1118 positive control	<i>Saccharomyces cerevisiae</i> strain CEN.PK113-7D	745	99%	100.00%	CP046095.1

### 3.1.2 Fermentation Set 2 and 3

Despite the corrective efforts attempted in the second and third trial fermentations previously mentioned in the methodology, post-fermentation analyses revealed critical procedural errors. Microbial implantation plating (Figure 3.2), followed by molecular identification via ITS sequencing (Table 3.2) for fermentation set 2, indicated that all fermentations had been inadvertently inoculated with *S. uvarum* CN1, rather than the intended *S. cerevisiae* EC1118 control. This error rendered the dataset unsuitable for comparative purposes, as strain-specific effects could not be evaluated under the new fermentation conditions. In addition, since fermentation set 3 had been inoculated with the same mislabeled plates as fermentation set 2, the dataset was also not suitable for comparative purposes. Consequently, fermentation set 2 and 3 were excluded from all chemical and sensory analyses and are reported here for the purpose of methodological transparency and to illustrate that the yeast identification assay worked.

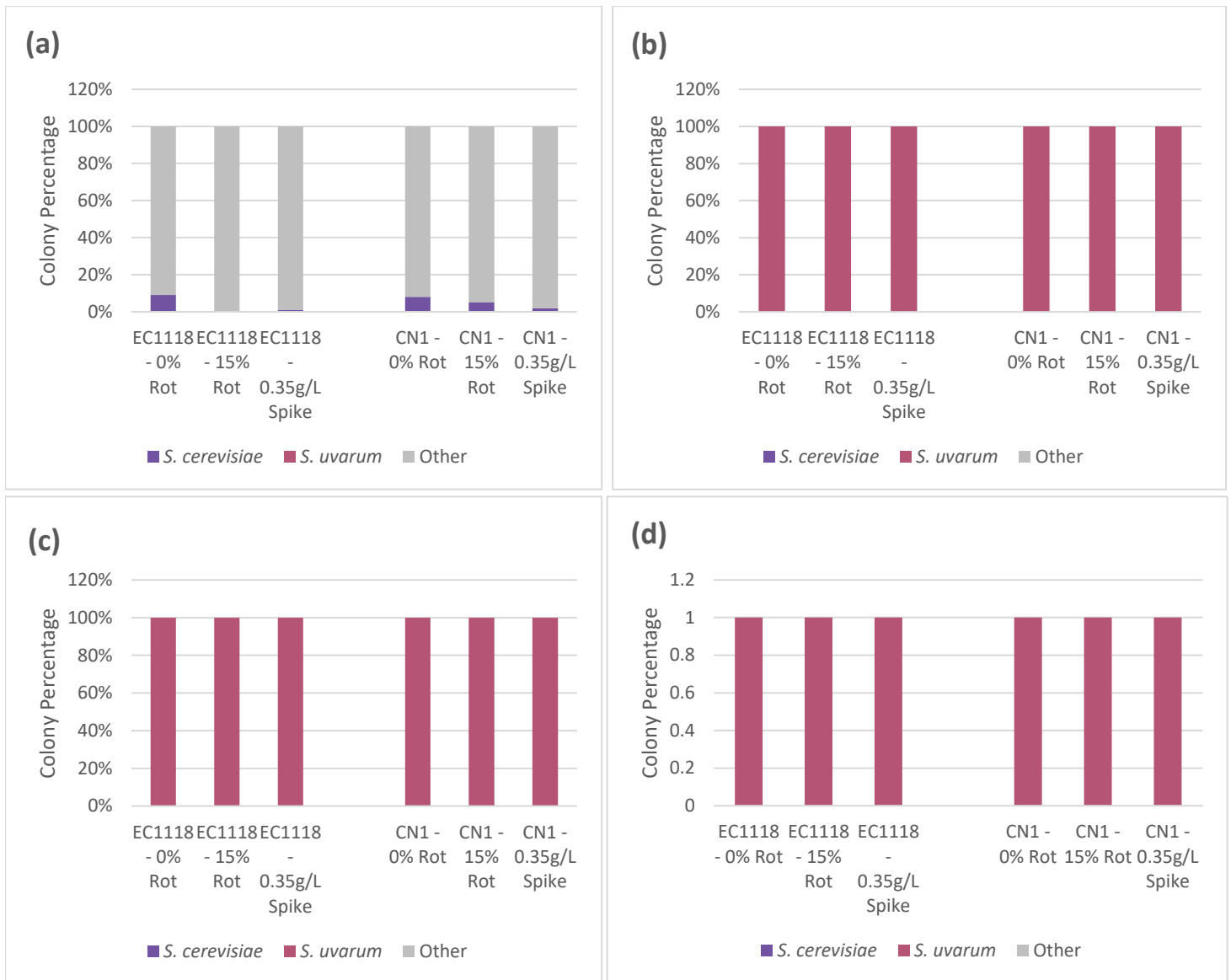


Figure 3.2: Proportional distribution of yeast species recovered from implantation plating across six additional wine fermentation treatments from set 2 and 3. Treatments included three levels of rot infection (0%, 20%, and 40%) and two inoculated yeast strains: *Saccharomyces cerevisiae* EC1118 and *S. uvarum* CN1. Bars represent the relative abundance of *S. cerevisiae*, *S. uvarum*, and other yeast species identified through replicate plating on WLN differential media. Yeast implantations were measured at four different timepoints throughout the fermentation: Juice (pre-inoculation) (a), Early (18-20°Brix) (b), Middle (10-12°Brix) (c), and Late (<5°Brix) (d).

Table 3.2: Sequence homology of isolates from the *Saccharomyces uvarum* CN1 and *S. cerevisiae* EC1118 second and third trial 2023 Riesling fermentations, including positive control stocks, against reference strains in the NCBI GenBank database

Gene Region	Sample	NCBI Database Strain for Sequence Comparison	Max Score	Query Coverage	Sequence Identity	GenBank Accession Number
B-tubulin	CN1_0% rot	<i>Saccharomyces uvarum</i> strain CBS7001 chromosome VI, complete sequence	1576	100%	99.88%	CP113769.1
	CN1_15% rot	<i>Saccharomyces uvarum</i> strain CBS7001 chromosome VI, complete sequence	1557	100%	99.88%	CP113769.1
	CN1_30% rot	<i>Saccharomyces uvarum</i> strain CBS7001 chromosome VI, complete sequence	1557	100%	99.42%	CP113769.1
	CN1_0.35g/L spike	<i>Saccharomyces uvarum</i> strain CBS7001 chromosome VI, complete sequence	1565	99%	99.65%	CP113769.1
	CN1 positive control	<i>Saccharomyces uvarum</i> strain CBS7001 chromosome VI, complete sequence	1572	99%	99.88%	CP113769.1
	EC1118_0% rot	<i>Saccharomyces uvarum</i> strain CBS7001 chromosome VI, complete sequence	1321	98%	94.34%	CP113769.1
	EC1118_15% rot	<i>Saccharomyces uvarum</i> strain CBS7001 chromosome VI, complete sequence	1580	100%	99.88%	CP113769.1
	EC1118_0.35 g/L rot	<i>Saccharomyces uvarum</i> strain CBS7001 chromosome VI, complete sequence	1567	98%	99.53%	CP113769.1
	EC1118 positive control	<i>Saccharomyces cerevisiae</i> strain KSD-Yc chromosome 6	1530	98%	99.88%	CP024000.1
GDH1 igs Region	CN1_0% rot	<i>Saccharomyces uvarum</i> strain CBS7001 chromosome VIII, complete sequence	715	100%	99.88%	CP113771.1
	CN1_15% rot	<i>Saccharomyces uvarum</i> strain CBS7001 chromosome VIII, complete sequence	710	100%	99.88%	CP113771.1
	CN1_30% rot	<i>Saccharomyces uvarum</i> strain CBS7001 chromosome VIII, complete sequence	713	100%	99.42%	CP113771.1
	CN1_0.35g/L spike	<i>Saccharomyces uvarum</i> strain CBS7001 chromosome VIII, complete sequence	704	99%	99.65%	CP113771.1
	CN1 positive control	<i>Saccharomyces uvarum</i> strain CBS7001 chromosome VIII, complete sequence	717	98%	94.34%	CP113771.1
	EC1118_0% rot	<i>Saccharomyces uvarum</i> strain CBS7001 chromosome VIII, complete sequence	688	100%	99.88%	CP113771.1
	EC1118_15% rot	<i>Saccharomyces uvarum</i> strain CBS7001 chromosome VIII, complete sequence	706	98%	99.53%	CP113771.1
	EC1118_0.35 g/L spike	<i>Saccharomyces uvarum</i> strain CBS7001 chromosome VIII, complete sequence	699	99%	99.88%	CP113771.1
	EC1118 positive control	<i>Saccharomyces cerevisiae</i> strain CEN.PK113-7D chromosome XV	745	99%	99.74%	CP046095.1

Following the decision that fermentation set 2 and 3 could not be further evaluated for the comparative trial of *S. cerevisiae* versus *S. uvarum* performance, the initial experimental fermentation set 1, despite the earlier temperature fluctuation, were revisited and deemed valid for continued study based on adequate fermentation kinetics, dissipation of hydrogen

sulfide aroma, and confirmed strain-level differentiation by implantation plating and sequencing.

### 3.2 Fermentation Kinetics and Metabolites

The must composition for all treatments in fermentation set 1 is presented in Table 3.3.

Soluble solids ranged from  $17.7 \pm 0.2$  °Brix in the control EC1118 treatment to  $16.7 \pm 0.2$  °Brix in the 40% rot treatment, with minimal differences observed between yeast strains within each rot level as expected since the yeast had not yet been added to the fermentations. Reducing sugar decreased slightly with increasing rot ( $p < 0.05$ ), with the 40% rot treatment containing approximately 164 g/L compared to 175 g/L in the control. The total reducing sugar was also slightly lower at the high rot level in comparison to the control. No significant differences in total reducing sugar or monosaccharide concentrations were observed between juice lots for EC1118 and CN1 within rot levels as expected since the juice had not yet been inoculated with yeast.

The pH of the musts remained relatively stable between treatments ( $\sim 3.0$ ), while titratable acidity (TA) increased with rot severity. Notably, the 40% rot musts had significantly higher TA ( $10.1 \pm 0.1$  g/L for EC1118;  $9.7 \pm 0.5$  g/L for CN1) compared to the control ( $8.9 \pm 0.2$  g/L). Acetic acid and acetaldehyde concentrations increased markedly with higher proportions of rot, reaching up to  $0.30 \pm 0.06$  g/L and  $9.2 \pm 0.6$  mg/L respectively in EC1118 and CN1 treatments (Table 3.3).

Nitrogen content increased significantly with rot severity. Yeast assimilable nitrogen (YAN) rose from 92–96 mg N/L in the control to 130 mg N/L in the 40% rot musts for both strains,

driven by increases in both ammonia and primary amino nitrogen. Succinic acid and gluconic acid levels also rose with increased rot, with gluconic acid reaching over 1.2 g/L in the 40% rot must, highlighting microbial metabolism typical of *Botrytis*-infected fruit.

Table 3.3: Chemical composition of Riesling control must (0% Rot) and must from rot affected grapes (20% Rot and 40% Rot). Data is presented as mean  $\pm$  standard deviation from duplicate measurements for each sample, with three independent winemaking replicates per treatment. Within each parameter, different lowercase letters denote significant differences between treatments based on Fisher's protected LSD test ( $\alpha = 0.05$ ).  $n = 6$  for each measurement.

Metabolite \ Treatment	Control (0% Rot)		20% Rot		40% Rot	
	EC1118	CN1	EC1118	CN1	EC1118	CN1
Soluble solids ( $^{\circ}$ Brix)	17.7 $\pm$ 0.2	17.5 $\pm$ 0	16.8 $\pm$ 0.2	17.2 $\pm$ 0.2	16.7 $\pm$ 0.2	16.8 $\pm$ 0.2
Glucose (g/L)	88 $\pm$ 2 <sup>a</sup>	87 $\pm$ 1 <sup>a</sup>	85 $\pm$ 2 <sup>a</sup>	84 $\pm$ 2 <sup>a</sup>	82 $\pm$ 1 <sup>b</sup>	82 $\pm$ 2 <sup>b</sup>
Fructose (g/L)	88 $\pm$ 2 <sup>a</sup>	88 $\pm$ 2 <sup>a</sup>	86 $\pm$ 2 <sup>a</sup>	87 $\pm$ 3 <sup>a</sup>	83 $\pm$ 2 <sup>b</sup>	82 $\pm$ 2 <sup>b</sup>
Total reducing sugar (g/L)	175 $\pm$ 2 <sup>a</sup>	174 $\pm$ 2 <sup>a</sup>	170 $\pm$ 3 <sup>a</sup>	170 $\pm$ 3 <sup>a</sup>	165 $\pm$ 2 <sup>b</sup>	164 $\pm$ 2 <sup>b</sup>
pH	3.03 $\pm$ 0.02 <sup>a</sup>	3.03 $\pm$ 0.02 <sup>a</sup>	3.04 $\pm$ 0.1 <sup>a</sup>	3.02 $\pm$ 0.01 <sup>a</sup>	2.99 $\pm$ 0 <sup>b</sup>	2.99 $\pm$ 0 <sup>b</sup>
Titrateable Acidity (g/L)	8.9 $\pm$ 0.2 <sup>b</sup>	8.9 $\pm$ 0.2 <sup>b</sup>	9.3 $\pm$ 0.2 <sup>b</sup>	9.5 $\pm$ 0.1 <sup>b</sup>	10.1 $\pm$ 0.1 <sup>a</sup>	9.7 $\pm$ 0.5 <sup>a</sup>
Glycerol (g/L)	0.1 $\pm$ 0 <sup>c</sup>	0.1 $\pm$ 0 <sup>c</sup>	0.3 $\pm$ 0 <sup>a</sup>	0.3 $\pm$ 0 <sup>b</sup>	0.3 $\pm$ 0 <sup>b</sup>	0.3 $\pm$ 0 <sup>b</sup>
Acetic Acid (g/L)	0.01 $\pm$ 0 <sup>c</sup>	0.01 $\pm$ 0 <sup>c</sup>	0.13 $\pm$ 0.02 <sup>b</sup>	0.14 $\pm$ 0.01 <sup>b</sup>	0.30 $\pm$ 0.06 <sup>a</sup>	0.29 $\pm$ 0.02 <sup>a</sup>
Acetaldehyde (mg/L)	3.3 $\pm$ 0.6 <sup>c</sup>	2.6 $\pm$ 0.2 <sup>c</sup>	5.6 $\pm$ 0.5 <sup>b</sup>	6.4 $\pm$ 0.8 <sup>b</sup>	9.2 $\pm$ 0.6 <sup>a</sup>	8.3 $\pm$ 2.0 <sup>a</sup>
Ethanol (% v/v)	0.01 $\pm$ 0 <sup>d</sup>	0.01 $\pm$ 0 <sup>d</sup>	0.02 $\pm$ 0 <sup>c</sup>	0.02 $\pm$ 0 <sup>c</sup>	0.03 $\pm$ 0 <sup>a</sup>	0.03 $\pm$ 0 <sup>b</sup>
Ammonia nitrogen (mg N/L)	55 $\pm$ 2 <sup>c</sup>	53 $\pm$ 2 <sup>c</sup>	58 $\pm$ 3 <sup>b</sup>	57 $\pm$ 3 <sup>b</sup>	63 $\pm$ 3 <sup>a</sup>	62 $\pm$ 5 <sup>a</sup>
Primary Amino nitrogen (mg N/L)	40 $\pm$ 2 <sup>c</sup>	39 $\pm$ 2 <sup>c</sup>	46 $\pm$ 2 <sup>b</sup>	49 $\pm$ 3 <sup>b</sup>	66 $\pm$ 4 <sup>a</sup>	68 $\pm$ 3 <sup>a</sup>
Yeast assimilable nitrogen (mg N/L)	96 $\pm$ 2 <sup>c</sup>	92 $\pm$ 2 <sup>d</sup>	106 $\pm$ 5 <sup>c</sup>	107 $\pm$ 3 <sup>b</sup>	130 $\pm$ 3 <sup>a</sup>	130 $\pm$ 5 <sup>a</sup>
Succinic acid (g/L)	0.06 $\pm$ 0 <sup>d</sup>	0.06 $\pm$ 0 <sup>d</sup>	0.07 $\pm$ 0 <sup>c</sup>	0.07 $\pm$ 0 <sup>c</sup>	0.09 $\pm$ 0 <sup>b</sup>	0.09 $\pm$ 0 <sup>a</sup>
Gluconic acid (g/L)	0.11 $\pm$ 0.01 <sup>e</sup>	0.12 $\pm$ 0.01 <sup>e</sup>	0.58 $\pm$ 0.05 <sup>d</sup>	0.67 $\pm$ 0.02 <sup>c</sup>	1.3 $\pm$ 0.03 <sup>a</sup>	1.23 $\pm$ 0.09 <sup>b</sup>

The final wine composition for all treatments is presented in Table 3.4. Soluble solids decreased from ~17 °Brix in the must to less than 1.0 °Brix in finished wines across all treatments, confirming near-complete fermentation in most cases. However, residual sugar remained slightly higher in CN1 wines, particularly under increased rot conditions, though these differences were not statistically significant. Glucose and fructose levels followed a similar pattern, with small amounts persisting in 40% rot treatments, likely due to incomplete fermentation of fructose by both strains.

Table 3.4: Chemical composition of Riesling control wine (0% Rot) and wine made from rot-affected fruit (20% Rot, and 40% Rot). Data is presented as mean  $\pm$  standard deviation from duplicate measurements for each sample, with three independent winemaking replicates per treatment. Within each parameter, different lowercase letters denote significant differences between treatments based on Fisher's protected LSD test ( $\alpha = 0.05$ ).  $n = 6$  for each measurement.

Metabolite \ Treatment	Control (0% Rot)		20% Rot		40% Rot	
	EC1118	CN1	EC1118	CN1	EC1118	CN1
Glucose (g/L)	0.14 $\pm$ 0.04 <sup>a</sup>	0.08 $\pm$ 0.06 <sup>b</sup>	0.09 $\pm$ 0.02 <sup>b</sup>	0.08 $\pm$ 0.01 <sup>b</sup>	0.11 $\pm$ 0.03 <sup>b</sup>	0.05 $\pm$ 0.03 <sup>b</sup>
Fructose (g/L)	5.02 $\pm$ 0.87 <sup>a</sup>	6.00 $\pm$ 0.18 <sup>a</sup>	4.56 $\pm$ 0.12 <sup>c</sup>	3.95 $\pm$ 0.18 <sup>b</sup>	3.92 $\pm$ 0.26 <sup>b</sup>	3.38 $\pm$ 0.14 <sup>b</sup>
Total residual sugar (g/L)	5.15 $\pm$ 0.91 <sup>a</sup>	6.09 $\pm$ 0.56 <sup>a</sup>	4.65 $\pm$ 0.12 <sup>c</sup>	4.04 $\pm$ 0.18 <sup>b</sup>	4.03 $\pm$ 0.26 <sup>b</sup>	3.43 $\pm$ 0.14 <sup>b</sup>
pH	2.91 $\pm$ 0 <sup>c</sup>	3.00 $\pm$ 0 <sup>a</sup>	2.91 $\pm$ 0 <sup>c</sup>	3.01 $\pm$ 0.01 <sup>b</sup>	2.94 $\pm$ 0.01 <sup>d</sup>	3.00 $\pm$ 0 <sup>a</sup>
Titrateable Acidity (g/L)	10.1 $\pm$ 0.1 <sup>b</sup>	10.3 $\pm$ 0.2 <sup>b</sup>	10.3 $\pm$ 0.1 <sup>b</sup>	10.2 $\pm$ 0.2 <sup>b</sup>	11.0 $\pm$ 0.1 <sup>a</sup>	10.7 $\pm$ 0.2 <sup>a</sup>
Glycerol (g/L)	4.7 $\pm$ 0.5 <sup>d</sup>	7.4 $\pm$ 0.2 <sup>a</sup>	4.3 $\pm$ 0.2 <sup>d</sup>	6.4 $\pm$ 0.2 <sup>b</sup>	4.2 $\pm$ 0.1 <sup>e</sup>	5.8 $\pm$ 0.4 <sup>c</sup>
Acetic Acid (g/L)	0.17 $\pm$ 0.01 <sup>a</sup>	0.05 $\pm$ 0.01 <sup>d</sup>	0.13 $\pm$ 0.01 <sup>c</sup>	0.02 $\pm$ 0 <sup>f</sup>	0.15 $\pm$ 0.01 <sup>c</sup>	0.03 $\pm$ 0.01 <sup>e</sup>
Acetaldehyde (mg/L)	18.6 $\pm$ 1.2 <sup>a</sup>	15.5 $\pm$ 2.9 <sup>b</sup>	18.0 $\pm$ 1.0 <sup>a</sup>	24.0 $\pm$ 2.0 <sup>a</sup>	17.5 $\pm$ 0.6 <sup>b</sup>	24.2 $\pm$ 2.0 <sup>a</sup>
Ethanol (% v/v)	10.5 $\pm$ 0.48 <sup>a</sup>	9.6 $\pm$ 0.84 <sup>b</sup>	10.7 $\pm$ 0.61 <sup>a</sup>	8.5 $\pm$ 0.60 <sup>b</sup>	9.9 $\pm$ 0.14 <sup>a</sup>	8.6 $\pm$ 0.27 <sup>b</sup>
Ammonia nitrogen (mg N/L)	1 $\pm$ 1 <sup>a</sup>	0 $\pm$ 0 <sup>b</sup>	1 $\pm$ 1 <sup>a</sup>	0 $\pm$ 0 <sup>b</sup>	1 $\pm$ 1 <sup>a</sup>	0 $\pm$ 0 <sup>b</sup>
Primary Amino nitrogen (mg N/L)	14 $\pm$ 1 <sup>c</sup>	12 $\pm$ 5 <sup>c</sup>	15 $\pm$ 1 <sup>c</sup>	13 $\pm$ 1 <sup>c</sup>	23 $\pm$ 3 <sup>a</sup>	18 $\pm$ 2 <sup>b</sup>
Yeast assimilable nitrogen (mg N/L)	15 $\pm$ 2 <sup>c</sup>	12 $\pm$ 5 <sup>c</sup>	16 $\pm$ 1 <sup>b</sup>	13 $\pm$ 2 <sup>c</sup>	23 $\pm$ 3 <sup>a</sup>	17 $\pm$ 3 <sup>b</sup>
Succinic acid (g/L)	0.44 $\pm$ 0.01 <sup>d</sup>	1.05 $\pm$ 0.06 <sup>a</sup>	0.51 $\pm$ 0.02 <sup>e</sup>	0.88 $\pm$ 0.02 <sup>b</sup>	0.50 $\pm$ 0.02 <sup>e</sup>	0.82 $\pm$ 0.02 <sup>c</sup>
Gluconic acid (g/L)	0.10 $\pm$ 0 <sup>d</sup>	0.09 $\pm$ 0.02 <sup>d</sup>	0.51 $\pm$ 0.05 <sup>a</sup>	0.65 $\pm$ 0.02 <sup>c</sup>	1.13 $\pm$ 0.02 <sup>b</sup>	1.13 $\pm$ 0.03 <sup>b</sup>

Significant differences in key fermentation metabolites were observed between *S. cerevisiae* EC1118 and *S. uvarum* CN1 across all rot treatments (Table 3.4). Glucose concentrations were low in all wines, indicating near-complete depletion; however, CN1 0% rot wines contained significantly less glucose than EC1118 (0.08  $\pm$  0.06 g/L vs. 0.14  $\pm$  0.04 g/L,  $p < 0.05$ ). Fructose and total residual sugar concentrations were significantly

lower in CN1 than EC1118 at both 20% and 40% rot, with no differences observed at 0% rot.

CN1 fermentations consistently produced higher glycerol than EC1118 across all treatments ( $p < 0.05$ ), with the largest difference observed at 0% rot ( $7.4 \pm 0.2$  g/L vs.  $4.7 \pm 0.5$  g/L). In contrast, CN1 produced significantly lower acetic acid concentrations in every treatment, with reductions ranging from 65–85% relative to EC1118. Acetaldehyde production differed by treatment: CN1 wines had significantly higher concentrations than EC1118 at 20% and 40% rot, but lower concentrations at 0% rot.

Ethanol concentrations were consistently lower in CN1 wines at 20% and 40% rot ( $p < 0.05$ ), with no significant difference at 0% rot. For organic acids, CN1 produced significantly more succinic acid than EC1118 in all treatments, approximately double in each case. Gluconic acid was significantly higher in CN1 wines at 20% rot but not different at 0% or 40% rot.

Nitrogen parameters showed fewer differences. YAN and PAN were significantly lower in CN1 wines at 40% rot, but no significant differences were observed in ammonia nitrogen across treatments.

Overall, CN1 fermentations were characterized by higher glycerol and succinic acid, lower ethanol and acetic acid, and reduced residual sugar at elevated rot levels.

Acetic acid concentrations in the initial must (pre-inoculation) and finished wines are shown in Figure 3.3 for fermentations conducted with EC1118 (a) and CN1 (b). In wines fermented with EC1118, acetic acid levels were significantly higher in the 0% rot treatment relative to the corresponding must, indicating net production of volatile acidity under clean fruit conditions. No significant change was observed between must and wine at 20% rot, whereas a significant decrease occurred at 40% rot. Similar overall trends were observed in fermentations inoculated with CN1; however, acetic acid concentrations were significantly lower across all treatments when compared with EC1118 (Table 3.4). The most pronounced reduction was observed in the 40% rot treatment, where CN1 exhibited substantial acetic acid consumption relative to the initial must.

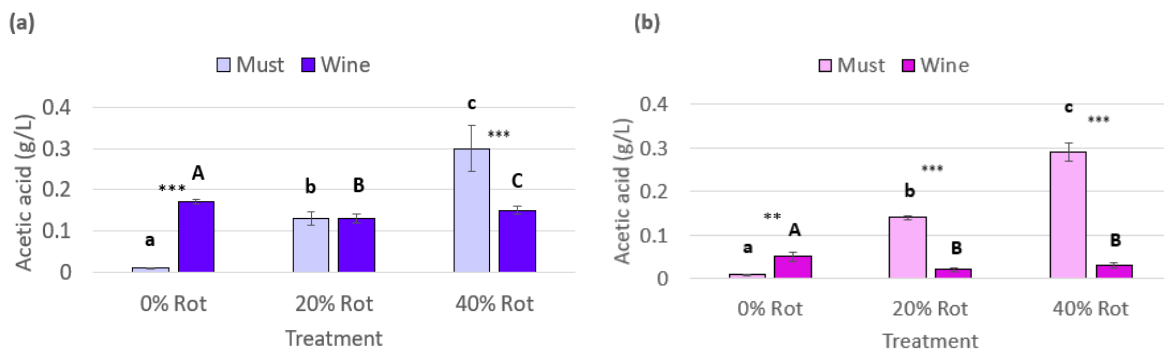


Figure 3.3: Acetic acid (g/L) in initial must and finished wines made from juice of increasing rot levels vinified with either EC1118 (a) or CN1 (b). Data represent the mean value  $\pm$  standard deviation of duplicate measurements per sample (three winemaking replicates per treatment). Significant differences were determined through ANOVA followed by Fisher's LSD. \*( $\alpha < 0.05$ ), \*\*( $\alpha < 0.01$ ), and \*\*\* ( $\alpha < 0.001$ ) show significant difference between yeast within the same rot treatments.

Fermentation temperature profiles for all treatments are presented in Figure 3.4. Across both yeast strains and rot inclusion levels, temperature remained stable at approximately 17 °C throughout fermentation, consistent with controlled cool-fermentation conditions. The only deviation occurred on Day 2 of the initial fermentation set, where a transient temperature spike to ~20 °C was recorded before returning to baseline levels. No further fluctuations were observed.

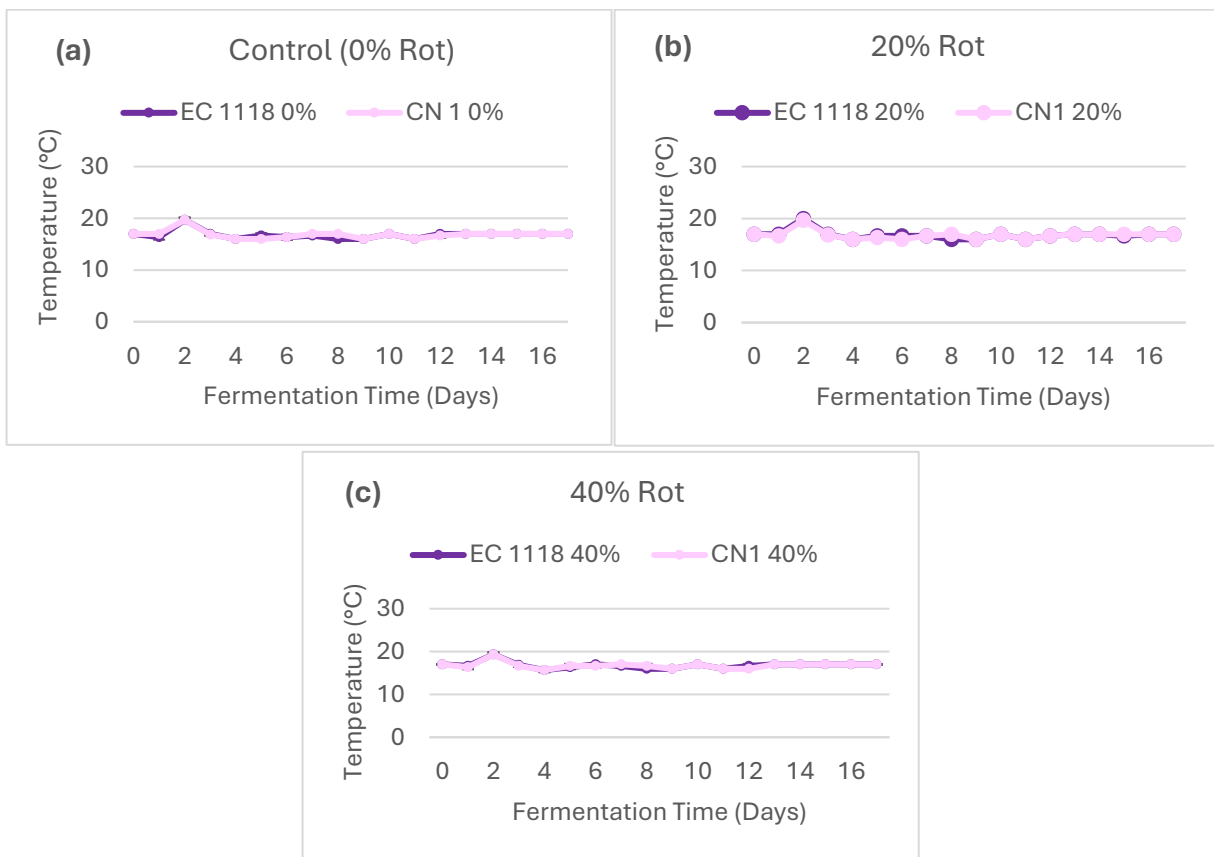


Figure 3.4: Temperature (°C) during fermentation. (a) *Saccharomyces cerevisiae* EC1118 (dark purple) and *Saccharomyces uvarum* CN1 (light pink) under three rot conditions: (a) 0% rot (control), (b) 20% rot, and (c) 40% rot.

Soluble solid ( $^{\circ}$ Brix) trends during fermentation are shown in Figure 3.5. Both EC1118 and CN1 demonstrated similar rates of sugar consumption under all rot conditions, with rapid declines in soluble solids during the first 4-7 days followed by gradual stabilization toward dryness. Complete fermentation was achieved after approximately 16 days for both yeast across all rot treatments.

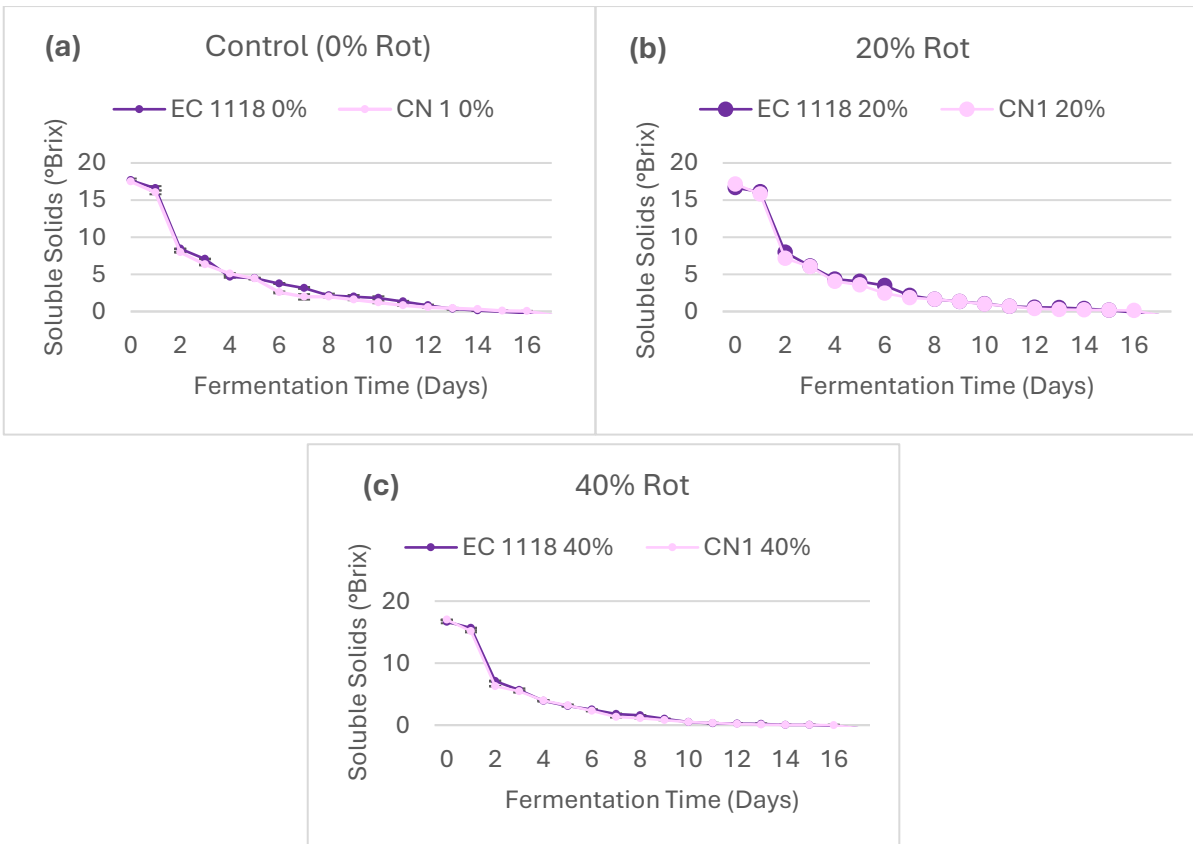


Figure 3.5: Soluble solid levels during fermentation. *Saccharomyces cerevisiae* EC1118 (dark purple) and *Saccharomyces uvarum* CN1 (light pink) under three rot conditions: (a) 0% rot (control), (b) 20% rot, and (c) 40% rot.

### 3.2.1 Fermentation Set 2 and 3

In the second and third fermentation trials, conducted to account for the temperature deviations observed in Trial 1 (Figure 3.6), the acetic acid values were quite low in the wines and no significant differences in final acetic acid concentrations were observed between wines fermented with *S. cerevisiae* EC1118 and *S. uvarum* CN1. This is because both fermentations were mistakenly inoculated with CN1 as outlined in section 3.1. As a result of the inoculation error, fermentation sets 2 and 3 were not further evaluated.

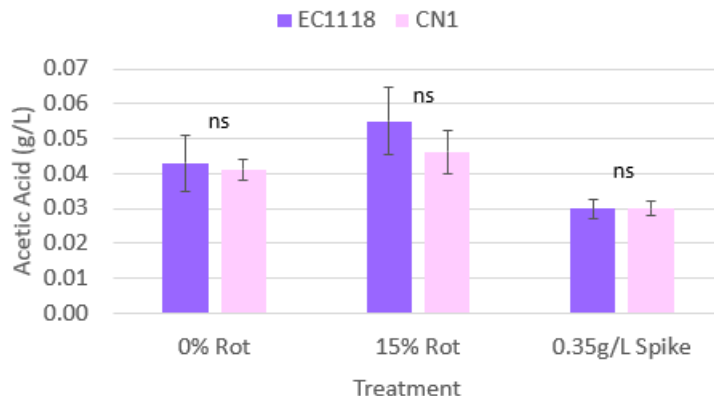


Figure 3.6: Acetic acid (g/L) in finished wines made from juice of increasing rot levels (second trial; 0% and 15% rot) and juice spiked with 0.35g/L acetic acid (third trial). Data represent the mean value  $\pm$  standard deviation of duplicate measurements per sample (three winemaking replicates per treatment). Significant differences were determined through ANOVA followed by Fisher's LSD. No significance (ns), \*( $\alpha < 0.05$ ), \*\*( $\alpha < 0.01$ ), and \*\*\* ( $\alpha < 0.001$ ) show significant difference between yeast within the same rot treatments.

### 3.3 Volatile Organic Compounds and Volatile Fatty Acids

Volatile compound analysis revealed distinct differences in higher alcohol production between yeast strains and across varying levels of rot severity in Riesling wines (Figure 3.7 and Table A1.3 in appendix). *S. cerevisiae* EC1118 fermentations consistently produced lower and relatively stable concentrations of higher alcohols, including 2-methyl-1-

propanol ( $14,832 \pm 1,149 \mu\text{g/L}$  to  $16,073 \pm 1,205 \mu\text{g/L}$ ) and 2-phenylethanol ( $15,847 \pm 2,384 \mu\text{g/L}$  to  $17,821 \pm 2,026 \mu\text{g/L}$ ) across the 0–40% rot treatments. In contrast, *S. uvarum* CN1 produced significantly higher levels of these compounds, particularly 2-phenylethanol, which reached more than 10X the concentration than that found in EC1118 fermentations at  $211,971 \pm 35,455 \mu\text{g/L}$  in the 0% rot treatment and remained elevated in the 20% and 40% treatments ( $217,916 \pm 57,604 \mu\text{g/L}$  and  $172,838 \pm 14,004 \mu\text{g/L}$ , respectively). Similarly, CN1 produced more 2-methyl-1-propanol than EC1118 across all treatments, though concentrations declined from  $54,936 \pm 7,915 \mu\text{g/L}$  at 0% rot to  $39,070 \pm 1,358 \mu\text{g/L}$  at 40% rot. Hexanol concentrations were also consistently higher in CN1 wines, whereas EC1118 showed a slight increase with rising rot levels.

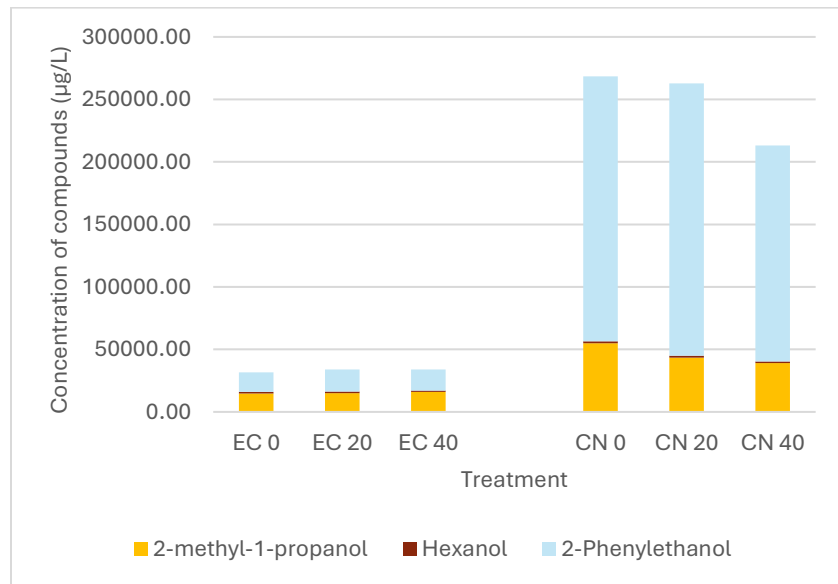


Figure 3.7: Concentration of selected higher alcohols (2-methyl-1-propanol, hexanol, and 2-phenylethanol) in wines fermented with *S. cerevisiae* EC1118 and *S. uvarum* CN1 across increasing levels of rot infection (0%, 20%, and 40%).

While CN1 generated higher concentrations of higher alcohols, the production of acetate esters showed the opposite trend (Figure 3.8 and Table A1.3 in appendix). EC1118 wines contained markedly greater concentrations of ethyl acetate, isoamyl acetate, and hexyl acetate than those fermented with CN1. Ethyl acetate, the most abundant acetate ester, ranged from  $42,406 \pm 2,448 \mu\text{g/L}$  to  $52,528 \pm 3,839 \mu\text{g/L}$  in EC1118 wines, while CN1 treatments ranged from  $21,856 \pm 3,054 \mu\text{g/L}$  to  $25,546 \pm 3,710 \mu\text{g/L}$ . Isoamyl acetate was likewise higher in EC1118 wines, with concentrations ranging from  $2,944 \pm 274 \mu\text{g/L}$  to  $3,688 \pm 349 \mu\text{g/L}$ , compared to CN1 wines, which declined from  $2,682 \pm 79 \mu\text{g/L}$  to  $1,627 \pm 79 \mu\text{g/L}$  as rot severity increased. Hexyl acetate followed a similar pattern, ranging from  $366 \pm 45 \mu\text{g/L}$  to  $500 \pm 36 \mu\text{g/L}$  in EC1118, and  $189 \pm 28 \mu\text{g/L}$  to  $216 \pm 22 \mu\text{g/L}$  in CN1 wines. Overall, the EC1118 strain produced higher levels of acetate esters across all rot conditions for the acetate esters measured.

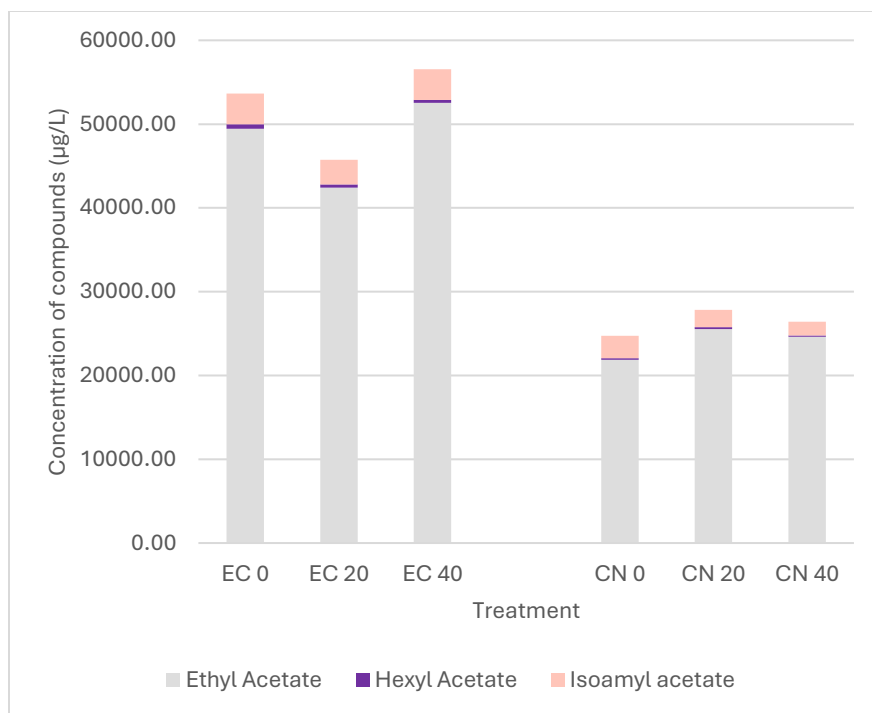


Figure 3.8: Concentration of selected acetate esters and ethyl in Riesling wines fermented with *S. cerevisiae* EC1118 and *S. uvarum* CN1 across increasing levels of rot infection (0%, 20%, and 40%).

A comparable trend was observed for most ethyl esters, which were generally more abundant in EC1118 wines than in those fermented with CN1 (Figure 3.9 and Table A1.3 in appendix). Ethyl hexanoate concentrations ranged from  $1,252 \pm 37 \mu\text{g/L}$  to  $1,772 \pm 190 \mu\text{g/L}$  in EC1118 wines, while CN1 wines remained below  $151 \pm 10 \mu\text{g/L}$  across all treatments. Likewise, EC1118 wines exhibited higher concentrations of ethyl octanoate ( $607 \pm 176 \mu\text{g/L}$  to  $653 \pm 66 \mu\text{g/L}$ ) and ethyl decanoate ( $131 \pm 12 \mu\text{g/L}$  to  $172 \pm 23 \mu\text{g/L}$ ), compared to CN1 wines ( $174 \pm 16 \mu\text{g/L}$  to  $200 \pm 20 \mu\text{g/L}$  for ethyl octanoate;  $110 \pm 6 \mu\text{g/L}$  to  $141 \pm 28 \mu\text{g/L}$  for ethyl decanoate). Exceptions to this trend included ethyl isobutyrate, which was higher in CN1 wines across all rot levels ( $5,478 \pm 141 \mu\text{g/L}$  at 0% rot), compared to EC1118 ( $4,187 \pm 279 \mu\text{g/L}$  at 0% rot). For other minor ethyl esters such as ethyl butyrate, ethyl 2-

methylbutyrate, and ethyl isovalerate, EC1118 wines consistently showed higher concentrations than CN1.

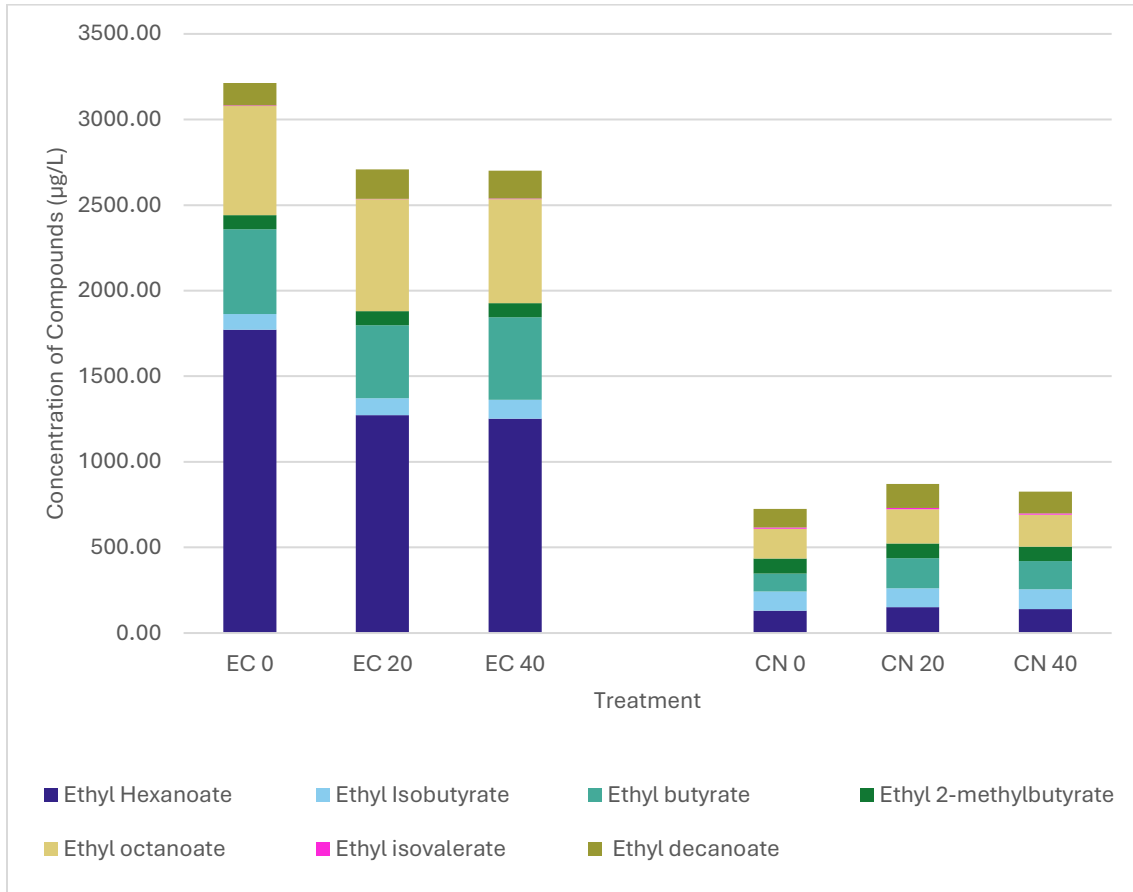


Figure 3.9: Concentration of selected ethyl esters in Riesling wines fermented with *S. cerevisiae* EC1118 and *S. uvarum* CN1 across increasing levels of rot infection (0%, 20%, and 40%).

Volatile fatty acid (VFA) concentrations, including hexanoic, octanoic, and decanoic acids, were quantified across yeast treatments and increasing levels of rot (Figure 3.10 and Table A1.3 in appendix). Across all rot levels, wines fermented with *S. cerevisiae* EC1118 exhibited substantially higher VFA concentrations than those fermented with *S. uvarum* CN1. Octanoic acid was consistently the most abundant of the VFAs, with EC1118 wines at 0% rot containing  $10,459 \pm 11.58 \mu\text{g/L}$ , decreasing to  $7,942 \pm 4.42 \mu\text{g/L}$  at 40% rot. Hexanoic acid similarly decreased with rot, from  $8,683 \pm 8.91 \mu\text{g/L}$  to  $5,904 \pm 4.50 \mu\text{g/L}$  in

EC1118 wines. Decanoic acid also declined from  $4,631 \pm 9.00 \mu\text{g/L}$  at 0% rot to  $3,130 \pm 2.66 \mu\text{g/L}$  at 40% rot. In comparison, CN1 fermentations showed considerably lower levels of all three VFAs, with octanoic acid ranging from  $2,270 \pm 2.43 \mu\text{g/L}$  to  $2,773 \pm 2.36 \mu\text{g/L}$  across rot treatments. This trend was consistent for hexanoic and decanoic acids, which both remained below  $700 \mu\text{g/L}$  and  $3,500 \mu\text{g/L}$ , respectively, in all CN1 fermentations.

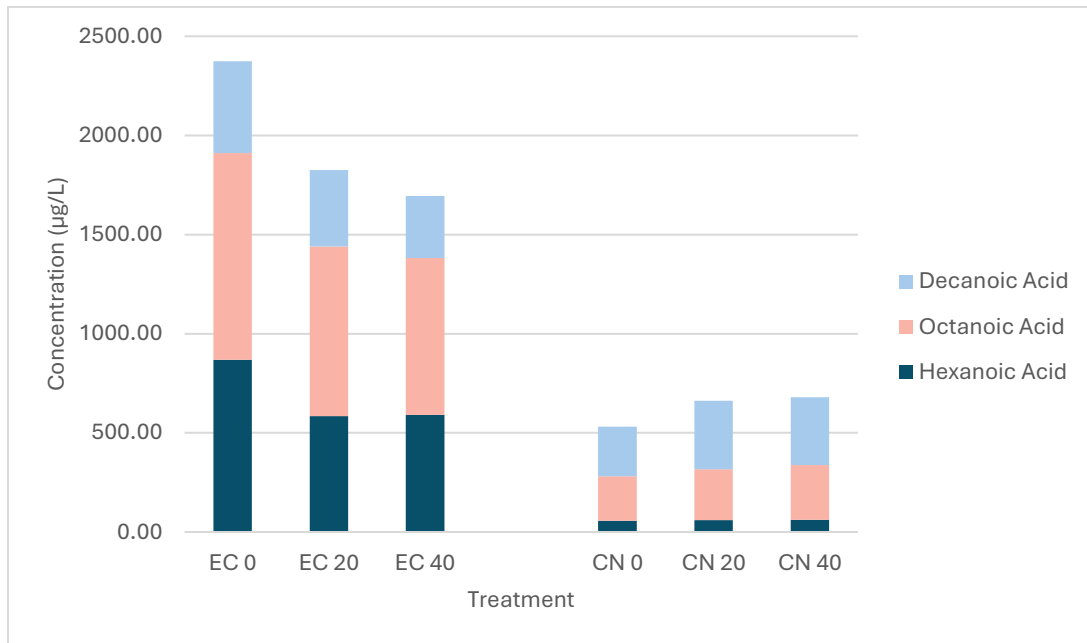


Figure 3.10: Concentration of selected medium-chain fatty acids (hexanoic acid, octanoic acid, and decanoic acid) in wines fermented with *S. cerevisiae* EC1118 and *S. uvarum* CN1 at varying levels of rot (0%, 20%, and 40%).

### 3.4 Sensory Evaluation

For aroma attributes, in the control wines (0% rot), EC1118 produced a significantly higher intensity of Tropical aroma (mean score = 6.08) compared to CN1 (mean score = 4.35; Figure 3.11a). At 40% rot, EC1118 again exhibited a significantly higher Tropical aroma intensity (mean score = 5.90) than CN1 (mean score = 3.97), while CN1 produced a significantly higher Musty aroma intensity (mean score = 4.30) than EC1118 (mean score =

2.29; Figure 3.11c). No other aroma attributes were significantly different between yeast strains within any rot treatment.

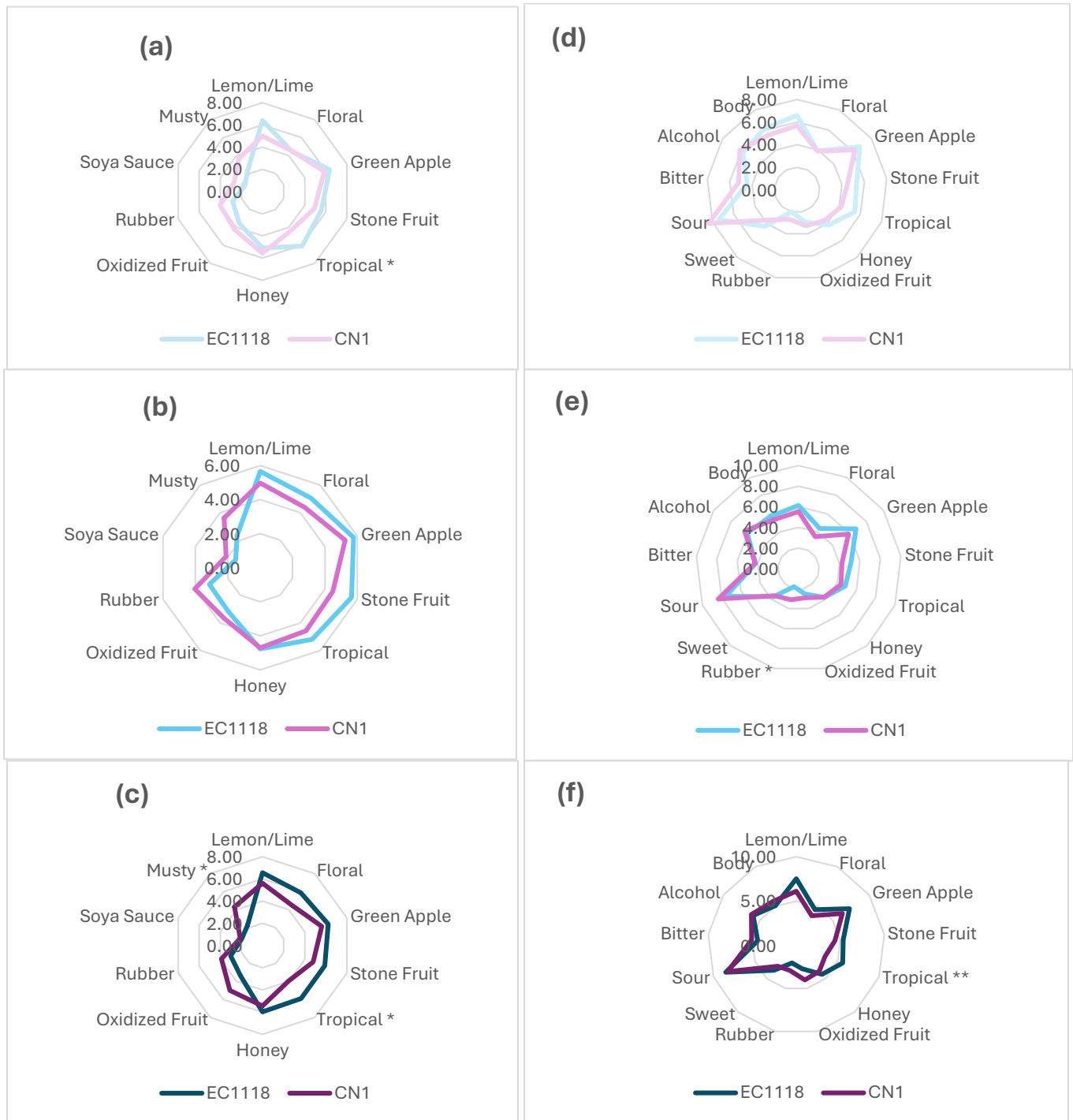


Figure 3.11: Radar plots of the mean sensory intensities for aroma attributes (left column) and flavour, taste, and tactile sensation attributes (right column) in Riesling wines fermented with either *Saccharomyces cerevisiae* EC1118 or *Saccharomyces uvarum* CN1. Sensory evaluations were conducted for three levels of rot severity, arranged in rows from top to bottom: 0% rot inclusion (top row), 20% rot inclusion (middle row), and 40% rot inclusion (bottom row). Descriptive analysis (DA) was conducted with a trained panel ( $n = 14$ ) to evaluate the aroma, flavour, and mouthfeel attributes of wines produced with *S. cerevisiae* EC1118 and *S. uvarum* CN1 across 0%, 20%, and 40% rot treatments. Mean scores represent the average intensity ratings from panelists, collected and quantified using Compusense software.

For flavour and in-mouth sensations, no significant differences were observed between yeast strains in the 0% rot treatment (Figure 3.11d). At 20% rot, CN1 wines were rated significantly higher in Rubber flavour (mean score = 3.13) compared to EC1118 wines (mean score = 1.82) (Figure 3.11e). At 40% rot, EC1118 wines were rated significantly higher in Tropical flavour (mean score = 5.62) compared to CN1 wines (mean score = 3.48) (Figure 3.11f). No other flavour or mouthfeel attributes differed significantly between yeast strains within any rot treatment.

Figure 3.12 presents a biplot from a Partial Least Squares (PLS) regression, integrating volatile compound concentrations and sensory attribute intensities across fermentations with *S. cerevisiae* EC1118 and *S. uvarum* CN1 under varying degrees of rot (0%, 20%, 40%). The first two components (t1 and t2) explain the majority of variance in the dataset, allowing for multivariate comparison of sensory and chemical drivers across treatments.

Based on the spatial distribution of the plot, clear separation is observed between treatment groups, with EC1118 fermentations clustering on the right side of the t1 axis and CN1 fermentations grouped to the left. Along the positive t1 axis, wines fermented with EC1118, particularly at 20% and 40% rot, are associated with elevated fruit-related sensory attributes including tropical aroma, stone fruit aroma, lemon/lime aroma and flavor, floral aroma, and honey flavor. These samples also exhibit strong associations with several key volatile esters, including ethyl hexanoate, ethyl octanoate, ethyl butyrate, and isoamyl acetate, as well as acetic acid and ethanol. These compounds are known contributors to fruity and floral aromatic expression, suggesting that EC1118 fermentation preserves or enhances these qualities, especially in moderately rot-affected fruit.

Conversely, CN1 fermentations at 0%, 20%, and 40% rot are grouped in the negative t1 and positive t2 quadrants, associated with oxidized fruit aroma and flavor, musty aroma, rubber flavor, and soya sauce aroma, as well as higher levels of volatile fatty acids (e.g., hexanoic acid, octanoic acid) and higher alcohols (e.g., 2-phenylethanol, 2-methyl-1-propanol).

Despite these associations, the reported intensities of fault-related attributes remained low across samples, as indicated in Figure 3.11, suggesting CN1's performance was not overtly detrimental. Importantly, CN1 wines were also aligned with succinate and glycerol, compounds associated with mouthfeel enhancement and lower ethanol production, indicating a potentially distinct metabolic profile under stress conditions.

Notably, EC1118 0% rot separated strongly along the positive t1 and negative t2 axis, showing unique alignment with the sensory attribute body and elevated decanoic acid concentrations. This suggests the commercial *S. cerevisiae* strain may contribute to a fuller mouthfeel in clean fruit, likely through combined effects of ethanol, fatty acid, and ester production.

In contrast, CN1 samples maintained a more compact grouping across all rot levels, especially under moderate and high rot (20% and 40%), indicating a potentially more consistent sensory–chemical profile under spoilage pressure. These groupings were also located closer to the origin of the plot, suggesting that CN1 exerted less influence on the overall variance structure relative to EC samples, which were positioned further from the origin. This pattern implies that CN1 may confer greater fermentation resilience or modulate undesirable compound expression during stress, albeit at the expense of some fruity esters.

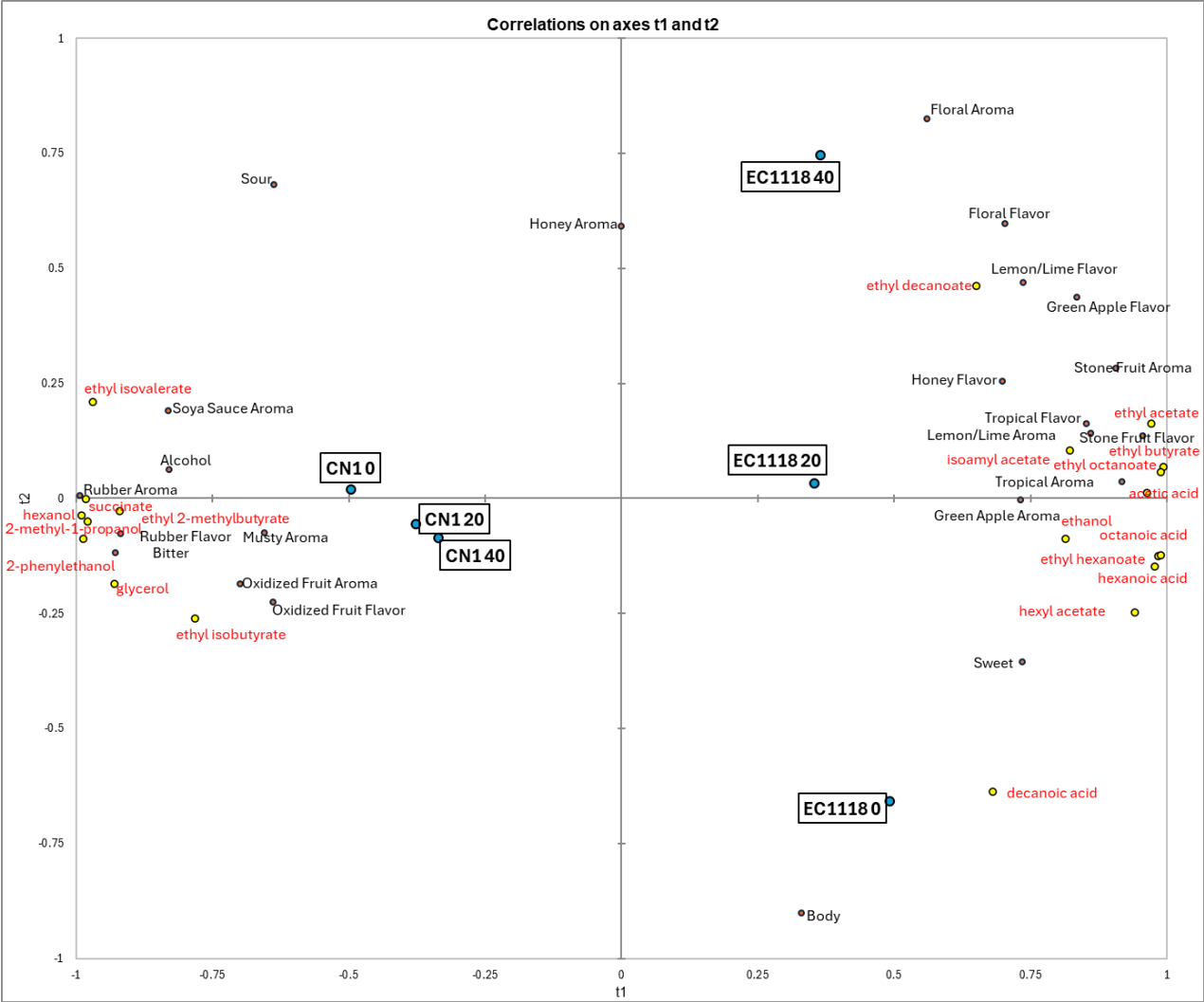


Figure 3.12: Impact of yeast strain and increasing rot percentage by weight on the sensory and chemical profiles of Riesling wines as determined by PLS. Each treatment point is the mean of attribute intensity rating of three winemaking replicates.

## Chapter 4: Discussion & Conclusion

### 4.1: Discussion

This study assessed the performance of a locally isolated *S. uvarum* strain (CN1) in mitigating the adverse chemical and sensory effects of grape rot infections in cool-climate Riesling fermentations. In comparison to the industry-standard *S. cerevisiae* EC1118, CN1 showed unique and desirable responses to elevated volatile acidity, stress conditions, and compromised fruit, contributing to improved fermentation profiles and potentially higher quality in rot-affected wines. These findings align with emerging literature that supports the strategic application of cryotolerant and non-traditional *Saccharomyces* species for enhancing wine quality under suboptimal fruit conditions (Bruner & Fox, 2020; Duncan et al., 2023).

Fermentations inoculated with CN1 exhibited a reduction in acetic acid concentrations relative to initial values, particularly in rot-affected treatments, where volatile acidity was expected to be most problematic due to the metabolic activity of acetic acid bacteria and rot-associated yeasts (Hall et al., 2018; Bhandari et al., 2024). In contrast, fermentations with EC1118 retained elevated acetic acid, especially at higher rot levels, suggesting less efficient acetate removal under these conditions. Similar results were reported by Kelly et al. (2020) in red wines, where *S. uvarum* consumed appreciable amounts of acetic acid in musts with high starting VA and/or sugar concentrations.

The underlying mechanism for acetic acid reduction in *S. uvarum* fermentations may be linked to redox-associated acetate assimilation pathways, which are activated under

oxygen-limited and stress-prone enological conditions (Cheraiti et al., 2005; Guaragnella & Bettiga, 2021; Duncan et al., 2025). In yeast cells, acetic acid can be transported across the plasma membrane in its undissociated form, then converted to acetyl-CoA by acetyl-CoA synthetase. In *S. uvarum*, this acetyl-CoA can be directed toward multiple metabolic fates, including fatty acid biosynthesis, storage lipid formation, or ester synthesis (Wang et al., 2023).

The combined effect is a net reduction in acetic acid levels while simultaneously supporting intracellular redox balance via  $\text{NAD}^+/\text{NADH}$ , potentially improving wine stability and mitigating sensory defects. Elevated volatile acidity (VA), primarily from acetic acid, is associated with vinegar-like aromas when concentrations exceed  $\sim 0.7\text{--}1.1$  g/L, while its ester derivative, ethyl acetate, imparts nail polish remover-like notes above  $\sim 150\text{--}200$  mg/L (Zoecklein et al., 1999; Waterhouse et al., 2016). By maintaining acetic acid below these sensory thresholds, CN1 may help preserve freshness and suppress fault expression in wine.

It was initially hypothesized that the consumed acetic acid would be converted into acetyl-CoA and subsequently channeled into the production of acetate esters from higher alcohols through esterification and Ehrlich pathway routes (Duncan et al., 2023). While modest levels of certain higher alcohols were observed in CN1 fermentations, the corresponding increase in acetate esters was not evident. This suggests that alternative metabolic routes for acetyl-CoA assimilation may have been active, potentially involving pathways for fatty acid biosynthesis, storage lipid formation, stress response intermediates, or other acetate esters that were not measured (Coral-Medina et al., 2023;

Wang et al., 2023). One possibility is the formation of phenylacetic acid and phenylethyl acetate from the relatively high concentrations of 2-phenylethanol present in these wines, as *Saccharomyces* species can oxidize or esterify 2-phenylethanol to yield these compounds via phenylalanine catabolism and subsequent acetylation reactions (Styger et al., 2011; Pires et al., 2014). Notably, phenylacetic acid has been described as contributing honey-like, floral, and sometimes musty or hay-like aromas (Pires et al., 2014; Hernández-Orte et al., 2008), which could explain the higher musty notes detected by the panel in certain CN1 treatments (Figure 3.9a-c). Coral-Medina et al. (2023) emphasized that nitrogen assimilation and intracellular metabolic regulation strongly modulate *S. uvarum* fermentation profile. The absence of a clear correlation between acetic acid depletion and ester formation implies that CN1 may prioritize redox balance and carbon flow toward stress mitigation and energy maintenance rather than aroma compound synthesis under rot-affected conditions (Duncan et al., 2025; Aiello et al., 2024).

Strains of *S. uvarum* possess an increased capacity for redox cofactor rebalancing via NADH-linked pathways, including glycerol and succinate formation, which may support intracellular acetate utilization as a compensatory response under redox stress (Duncan et al., 2025). Aiello et al. (2024) demonstrated that cryotolerant *Saccharomyces* species sustain membrane integrity and enzymatic function during ethanol-induced oxidative stress, conditions relevant to the present study. Acetic acid removal by *S. cerevisiae* has been previously documented (Vasserot et al., 2010), though the net removal in EC1118 fermentations was minimal in this case. This outcome reflects the potential for further

strain-level differences in acetate metabolism or inhibition under rot-induced stressors (Guaragnella & Bettiga, 2021; Kelly et al., 2020).

Sensory evaluation revealed that fermentations with *S. uvarum* CN1 were consistently rated lower in fruit-associated aroma and flavor intensity, including citrus, tropical, and floral descriptors, compared to fermentations conducted with *S. cerevisiae* EC1118. This pattern was observed across all levels of rot infection and was most pronounced in the 20% and 40% rot treatments. Conversely, EC1118 fermentations retained higher intensities of these positive sensory attributes but also exhibited greater intensities of off-aromas such as oxidized and sour notes at elevated rot levels.

One possible explanation for the diminished expression of fruit-driven characters in CN1 wines specifically, is the temperature spike recorded on Day 2 of fermentation (Figure 2.2). The brief spike to 21°C (and possibly higher before recording was performed) exceeded the cryotolerant range preferred by *S. uvarum*, which is typically optimized for fermentation between 10–17 °C (Masneuf-Pomarede et al., 2010; García-Ríos et al., 2019). As a cryotolerant species, *S. uvarum* exhibits increased sensitivity to thermal fluctuations, with elevated temperatures associated with reductions in volatile ester biosynthesis, particularly ethyl and acetate esters, due to compromised acetyltransferase activity and disrupted redox balance (Duncan et al., 2023; Coral-Medina et al., 2023).

To confirm whether CN1's acetic acid attenuation observed in Trial 1 was reproducible under stable thermal conditions, Trials 2 and 3 were performed later in the vintage. However, these subsequent trials were compromised due to improper inoculation. In both

cases, fermentation dominance by the intended inoculated strains was not achieved. Implantation plating and genetic sequencing revealed inconsistencies with EC1118 fermentations, likely indicating improper inoculation with CN1 rather than the intended yeast. This explains why no significant differences in final acetic acid concentrations were detected between treatments in Trials 2 and 3.

Thermal stress may also result in the upregulation of stress response pathways and altered carbon partitioning, limiting the production of desirable aroma-active metabolites and potentially leading to the accumulation of less favorable compounds, including acetaldehyde and higher alcohols (Aiello et al., 2024; Chen & Li, 2022). This shift in metabolic activity under stress could partially explain the subdued aromatic profile observed in CN1 fermentations, despite the strain's established capacity for enhanced ester production under optimal conditions (Kelly et al., 2020; Morgan et al., 2020).

These findings underscore the importance of stringent temperature control when applying cryotolerant yeast strains in winemaking. The early disruption to thermal stability may have impaired the ability of CN1 to express its full aromatic potential and contributed to the lower fruit-related sensory scores observed.

Implantation plating and further genetic sequencing confirmed that all CN1 fermentations were successfully dominated by *S. uvarum* with no detection of *S. cerevisiae* or other yeast species. EC1118 fermentations were likewise dominated by the inoculated strain, with minor detection (2–4%) of *S. uvarum* in select replicates. This may indicate transient carry-over or background persistence of natural *S. uvarum* from shared facilities. McCarthy et al.

(2021) demonstrated that *S. uvarum* can persist in winery environments and dominate spontaneous fermentations under cool conditions. The absence of non-*Saccharomyces* species reflects stringent fermentation control, despite elevated microbial load and VA precursors in rot-affected fruit.

The results of this study suggest that *S. uvarum* CN1 may offer enological advantages in mitigating acetic acid accumulation during fermentation of rot-affected Riesling grapes. Across all levels of sour rot and *Botrytis* infection, fermentations conducted with CN1 exhibited lower final concentrations of acetic acid compared to those inoculated with *S. cerevisiae* EC1118. These findings are consistent with previous work by Kelly et al. (2020), which demonstrated the capacity of *S. uvarum* to consume acetic acid under challenging fermentation conditions. Given the increasing prevalence of sour rot in cool-climate viticulture and its known association with acetic acid bacteria and yeast-insect interactions (Hall et al., 2018; Bhandari et al., 2024), the implementation of CN1 could represent a practical biotechnological strategy to reduce volatile acidity and improve overall wine quality.

However, as previously mentioned several limitations would likely constrain the immediate application of CN1 at the commercial scale. Future trials should include a second set of fermentations incorporating improved thermal regulation and additional biological replicates to validate the consistency of acetic acid attenuation by CN1. Alternative inoculation strategies may also enhance its performance. Co-inoculation or sequential inoculation with commercial *S. cerevisiae* strains could enable robust fermentation kinetics while preserving the capacity of CN1 to remediate volatile acidity. Cheraiti et al.

(2005) demonstrated that redox interactions between *S. cerevisiae* and *S. uvarum* in mixed cultures influence metabolite partitioning and acetate consumption. Duncan et al. (2025) further emphasized that interspecies differences in redox cofactor metabolism may complement one another when managed effectively. These strategies may improve both the sensory complexity and stability of wines made from compromised fruit, while leveraging the respective strengths of each species.

The use of *S. uvarum* CN1 thus holds promise for application in sour rot-affected musts; however, additional research is needed to determine whether the sensory attributes observed in this study are truly yeast-derived or instead fermentative issues such as fermentation stress and must condition. Some negative descriptors may arise from interactions between CN1 and rot-affected substrates rather than from the yeast itself. A second set of fermentations conducted under strict temperature control will be critical for isolating yeast-specific effects and accounting for vintage-driven variation, thereby providing a more reliable representation of the sensory and chemical profile of CN1. Further work focused on nutrient management, regulated temperatures, and sensory outcomes across vintages will support consistent interpretation of CN1 performance under variable production conditions. A clearer understanding of how CN1 responds to environmental and microbial stress will support its practical use in sustainable winemaking under increasing disease pressure.

## 4.1 Conclusions and Future Research

The use of *Saccharomyces uvarum* CN1 in the fermentation of rot-affected Riesling grapes offers a promising strategy for mitigating the negative chemical and sensory impacts associated with sour rot and *Botrytis cinerea* infection. In this study, wines fermented with CN1 exhibited significantly lower final concentrations of acetic acid compared to those fermented with the commercial *S. cerevisiae* EC1118 strain, particularly at higher levels of rot. This reduction in acetic acid may contribute to improved wine stability and sensory quality, supporting the hypothesis that CN1 could metabolize volatile acidity even under compromised fruit conditions.

While CN1 showed a capacity to reduce undesirable volatile fatty acids and suppress oxidized aromas, its fermentations were not consistently associated with elevated fruit-forward esters or higher alcohols. This outcome may be partially attributed to an early fermentation temperature spike, which likely interfered with the metabolic potential of the cryotolerant CN1 strain. These results highlight the importance of stringent temperature control when working with cryotolerant yeasts and suggest that optimal expression of CN1's capacity for ester synthesis may depend on more favorable fermentation conditions.

Despite these limitations, the findings demonstrate the potential utility of *S. uvarum* CN1 in managing microbial spoilage and acetic acid accumulation in white wine production.

Future studies should investigate optimized inoculation strategies, such as sequential or co-inoculation with *S. cerevisiae* and assess CN1 performance under more controlled environmental conditions. As disease pressure from sour rot continues to increase in cool-

climate regions, the development of tailored microbial solutions such as CN1 may provide winemakers with novel tools for enhancing wine quality and production resilience.

This work contributes to the growing body of literature on non-*Cerevisiae* *Saccharomyces* strains and their role in modern enology. By characterizing a locally isolated *S. uvarum* strain in a practical winemaking context, the study bridges fundamental yeast ecology with applied fermentation science, laying the groundwork for future research and industry adoption of alternative yeast strategies for rot-impacted fruit.

## Literature Cited

- Aiello, E., Arena, M. P., De Vero, L., Montanini, C., Bianchi, M., Mescola, A., Alessandrini, A., Pulvirenti, A., & Gullo, M. (2024). Wine yeast strains under ethanol-induced stress: Morphological and physiological responses. *Fermentation*, *10*(12), 631.  
<https://doi.org/10.3390/fermentation10120631>
- Bellincontro, A., Matarese, F., D'Onofrio, C., Accordini, D., Tosi, E., & Mencarelli, F. (2016). Management of postharvest grape withering to optimise the aroma of the final wine: A case study on Amarone. *Food Chemistry*, *213*, 378–387.  
<https://doi.org/10.1016/j.foodchem.2016.06.098>
- Bhandari, R., Zaman, F., Hall, M., Gold, K., Wise, A., Walter-Peterson, H., & Loeb, G. (2024). Understanding grape sour rot complex. *American Journal of Enology and Viticulture*, *75*(2), 0750026. <https://doi.org/10.5344/ajev.2024.22072>
- Bruner, J., & Fox, G. (2020). Novel non-cerevisiae saccharomyces yeast species used in beer and alcoholic beverage fermentations. *Fermentation*, *6*(4), 116.  
<https://doi.org/10.3390/fermentation6040116>
- Chen, K., & Li, J. (2022). A glance into the aroma of white wine. In *White Wine Technology* (pp. 313–326). Elsevier. <https://doi.org/10.1016/B978-0-12-823497-6.00018-1>
- Cheraiti, N., Guezenec, S., & Salmon, J.-M. (2005). Redox Interactions between *Saccharomyces cerevisiae* and *Saccharomyces uvarum* in Mixed Culture under Enological Conditions. *Applied and Environmental Microbiology*, *71*(1), 255–260.  
<https://doi.org/10.1128/AEM.71.1.255-260.2005>

- Coral-Medina, A., Morrissey, J. P., & Camarasa, C. (2023). The growth and metabolome of *Saccharomyces uvarum* in wine fermentations are strongly influenced by the route of nitrogen assimilation. *Journal of Industrial Microbiology and Biotechnology*, 49(6), kuac025. <https://doi.org/10.1093/jimb/kuac025>
- De-la-Fuente-Blanco, A., Arias-Pérez, I., Escudero, A., Sáenz-Navajas, M.-P., & Ferreira, V. (2024). The relevant and complex role of ethanol in the sensory properties of model wines. *OENO One*, 58(3). <https://doi.org/10.20870/oenone.2024.58.3.7864>
- Duncan, J. D., Ortiz-Julien, A., Setati, M. E., & Divol, B. (2023). Production of flavour compounds by wine yeasts is dependent on the management of their intracellular redox balance. *IVES Technical Reviews, Vine and Wine*. <https://doi.org/10.20870/IVES-TR.2023.7725>
- Duncan, J. D., Setati, M. E., & Divol, B. (2025). The cellular symphony of redox cofactor management by yeasts in wine fermentation. *International Journal of Food Microbiology*, 427, 110966. <https://doi.org/10.1016/j.ijfoodmicro.2024.110966>
- Francis, I. L., & Newton, J. L. (2005). Determining wine aroma from compositional data. *Australian Journal of Grape and Wine Research*, 11(2), 114–126. <https://doi.org/10.1111/j.1755-0238.2005.tb00283.x>
- García-Ríos, E., Guillén, A., De La Cerda, R., Pérez-Través, L., Querol, A., & Guillamón, J. M. (2019). Improving the cryotolerance of wine yeast by interspecific hybridization in the genus *saccharomyces*. *Frontiers in Microbiology*, 9, 3232. <https://doi.org/10.3389/fmicb.2018.03232>
- Guaragnella, N., & Bettiga, M. (2021). Acetic acid stress in budding yeast: From molecular mechanisms to applications. *Yeast*, 38(7), 391–400. <https://doi.org/10.1002/yea.3651>

- Hall, M. E., Loeb, G. M., Cadle-Davidson, L., Evans, K. J., & Wilcox, W. F. (2018). Grape sour rot: A four-way interaction involving the host, yeast, acetic acid bacteria, and insects. *Phytopathology*<sup>®</sup>, 108(12), 1429–1442. <https://doi.org/10.1094/PHYTO-03-18-0098-R>
- Hernández-Orte, P., Cersosimo, M., Loscos, N., Cacho, J., Garcia-Moruno, E., & Ferreira, V. (2008). The development of varietal aroma from non-floral grapes by yeasts of different genera. *Food Chemistry*, 107(3), 1064–1077. <https://doi.org/10.1016/j.foodchem.2007.09.032>
- Kelly, J., Van Dyk, S., Dowling, L., Pickering, G., Kemp, B., Inglis, D. (2020). *Saccharomyces uvarum* yeast isolate consumes acetic acid during fermentation of high sugar juice and juice with high starting volatile acidity. *OENO One*, 54(2). <https://doi.org/10.20870/oeno-one.2020.54.2.2594>
- López de Lerma, N., García-Martínez, T., Moreno, J., Mauricio, J. C., & Peinado, R. A. (2012). Volatile composition of partially fermented wines elaborated from sun dried Pedro Ximénez grapes. *Food Chemistry*, 135(4), 2445–2452. <https://doi.org/10.1016/j.foodchem.2012.07.058>
- McCarthy, G. C., Morgan, S. C., Martiniuk, J. T., Newman, B. L., McCann, S. E., Measday, V., & Durall, D. M. (2021). An indigenous *Saccharomyces uvarum* population with high genetic diversity dominates uninoculated Chardonnay fermentations at a Canadian winery. *PLOS ONE*, 16(2), e0225615. <https://doi.org/10.1371/journal.pone.0225615>
- Morgan, S. C., Haggerty, J. J., Jiranek, V., & Durall, D. M. (2020). Competition between *Saccharomyces cerevisiae* and *Saccharomyces uvarum* in Controlled Chardonnay Wine

Fermentations. *American Journal of Enology and Viticulture*, 71(3), 198–207.

<https://doi.org/10.5344/ajev.2020.19072>

Noguerol-Pato, R., González-Barreiro, C., Cancho-Grande, B., & Simal-Gándara, J. (2009).

Quantitative determination and characterisation of the main odourants of Mencía monovarietal red wines. *Food Chemistry*, 117(3), 473–484.

<https://doi.org/10.1016/j.foodchem.2009.04.014>

Pérez-Navarro, J., Izquierdo-Cañas, P., Mena-Morales, A., Chacón-Vozmediano, J., Martínez-

Gascueña, J., García-Romero, E., Hermosín-Gutiérrez, I., & Gómez-Alonso, S. (2020).

Comprehensive chemical and sensory assessment of wines made from white grapes of vitis vinifera cultivars albillo dorado and montonera del casar: A comparative study with airén. *Foods*, 9(9), 1282. <https://doi.org/10.3390/foods9091282>

Pires, E. J., Teixeira, J. A., Brányik, T., & Vicente, A. A. (2014). Yeast: The soul of beer's aroma--a

review of flavour-active esters and higher alcohols produced by the brewing yeast. *Applied*

*Microbiology and Biotechnology*, 98(5), 1937–1949. <https://doi.org/10.1007/s00253-013-5470-0>

Rice, S., Lutt, N., Koziel, J., Dharmadhikari, M., & Fennell, A. (2018). Determination of selected

aromas in marquette and frontenac wine using headspace-spme coupled with gc-ms and simultaneous olfactometry. *Separations*, 5(1), 20.

<https://doi.org/10.3390/separations5010020>

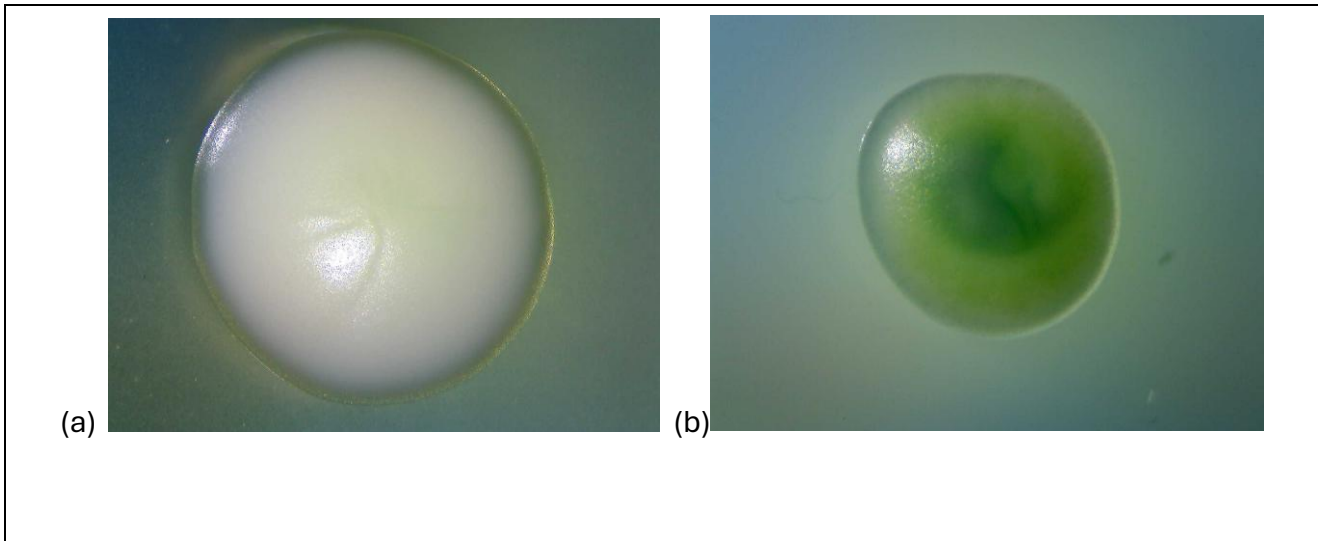
Styger, G., Prior, B., & Bauer, F. F. (2011). Wine flavor and aroma. *Journal of Industrial*

*Microbiology & Biotechnology*, 38(9), 1145–1159. [https://doi.org/10.1007/s10295-011-](https://doi.org/10.1007/s10295-011-1018-4)

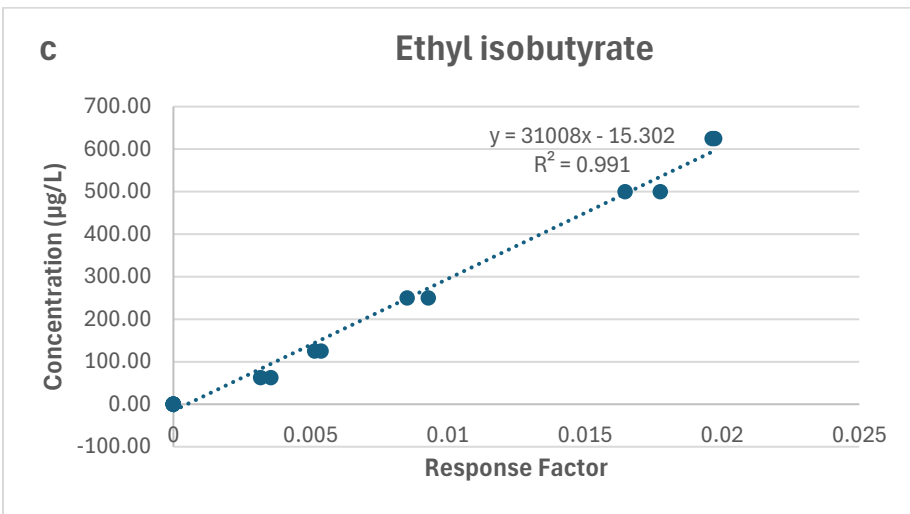
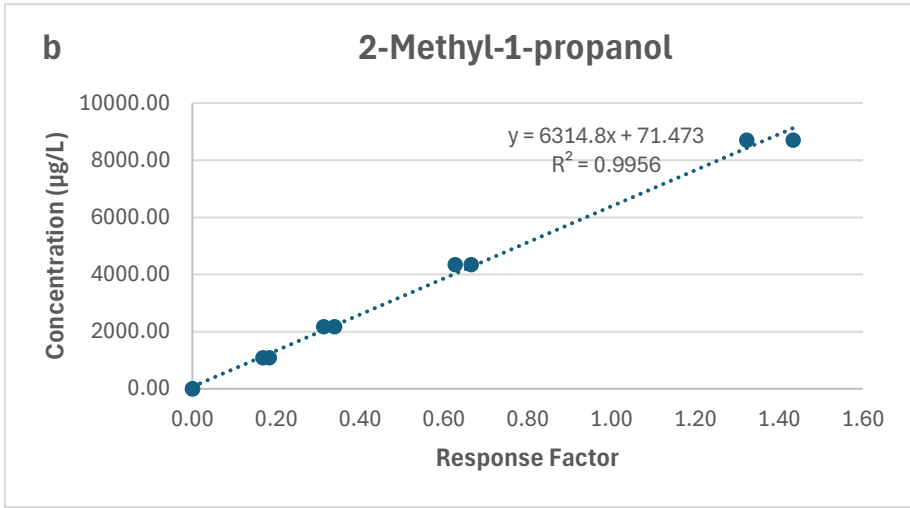
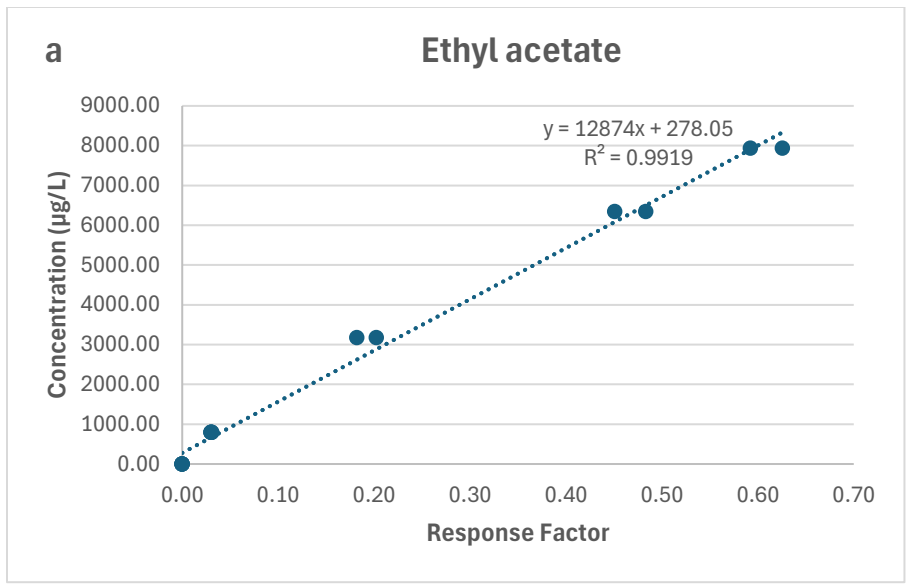
1018-4

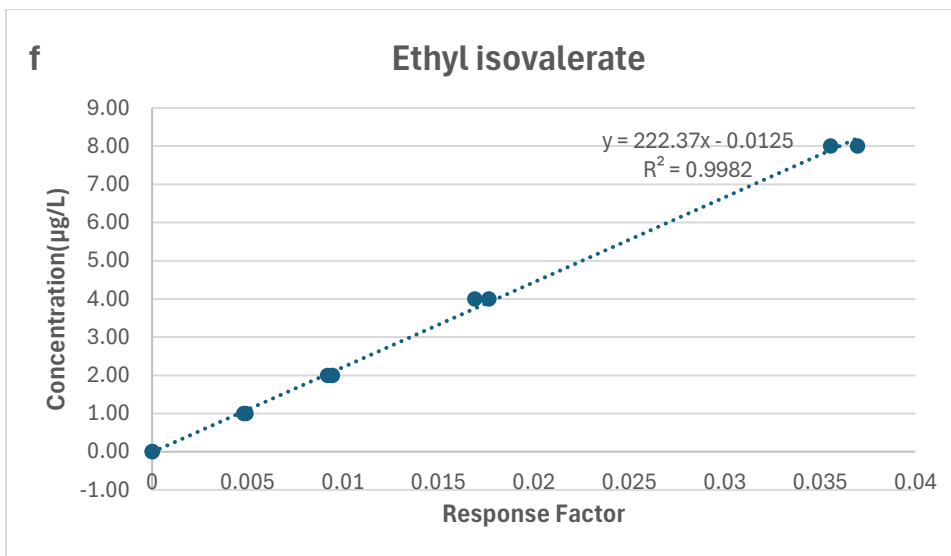
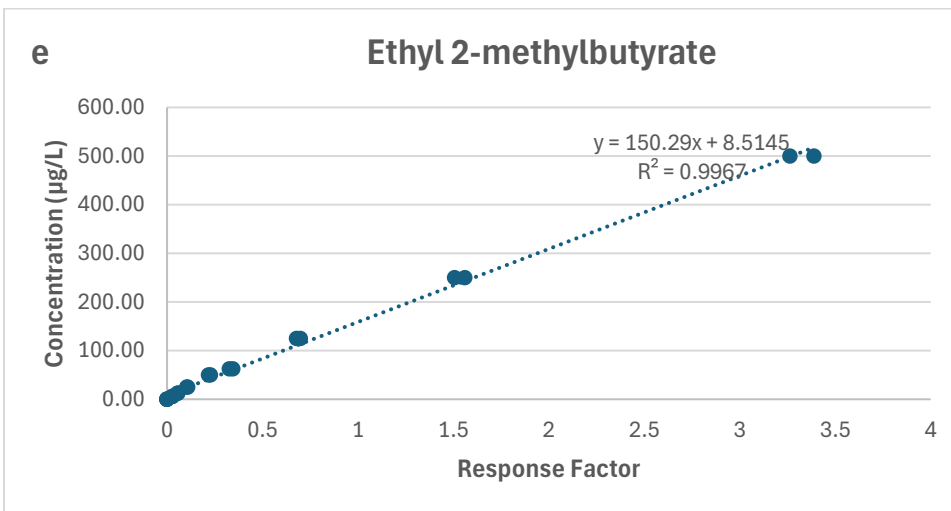
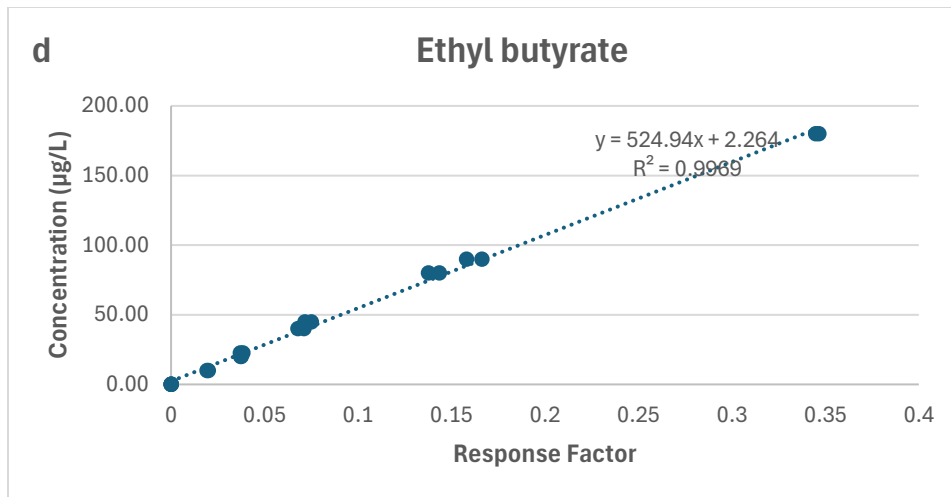
- Šuklje, K., Zhang, X., Antalick, G., Clark, A. C., Deloire, A., & Schmidtke, L. M. (2016). Berry shriveling significantly alters shiraz (*vitis vinifera* L.) grape and wine chemical composition. *Journal of Agricultural and Food Chemistry*, 64(4), 870–880.  
<https://doi.org/10.1021/acs.jafc.5b05158>
- Tomasino, E., Harrison, R., Breitmeyer, J., Sedcole, R., Sherlock, R., & Frost, A. (2015). Aroma composition of 2-year-old New Zealand Pinot Noir wine and its relationship to sensory characteristics using canonical correlation analysis and addition/omission tests: Chemistry and sensory of New Zealand Pinot Noir. *Australian Journal of Grape and Wine Research*, 21(3), 376–388. <https://doi.org/10.1111/ajgw.12149>
- Vasserot, Y., Mornet, F., & Jeandet, P. (2010). Acetic acid removal by *Saccharomyces cerevisiae* during fermentation in oenological conditions. Metabolic consequences. *Food Chemistry*, 119(3), 1220–1223. <https://doi.org/10.1016/j.foodchem.2009.08.008>
- Wang, K., Wu, Z., Du, J., Liu, Y., Zhu, Z., Feng, P., Bi, H., Zhang, Y., Liu, Y., Chen, B., Wang, M., & Tan, T. (2023). Metabolic engineering of *saccharomyces cerevisiae* for conversion of formate and acetate into free fatty acids. *Fermentation*, 9(11), 984.  
<https://doi.org/10.3390/fermentation9110984>
- Waterhouse, A. L., Sacks, G. L., & Jeffery, D. W. (2016). *Understanding wine chemistry*. John Wiley & Sons.
- Zoecklein, B. W., Fugelsang, K. C., Gump, B. H., & Nury, F. S. (1999). *Wine analysis and production* (2nd ed.). Springer Science & Business Media.

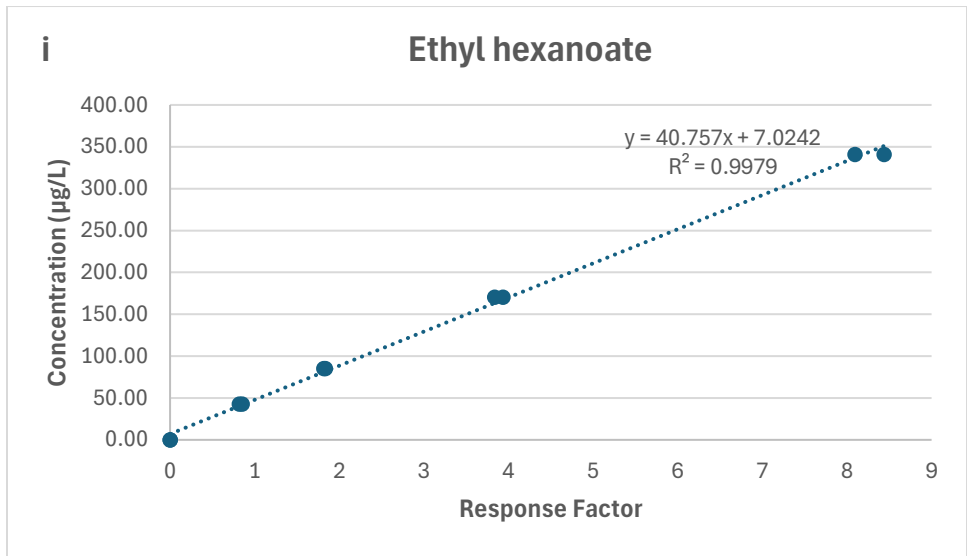
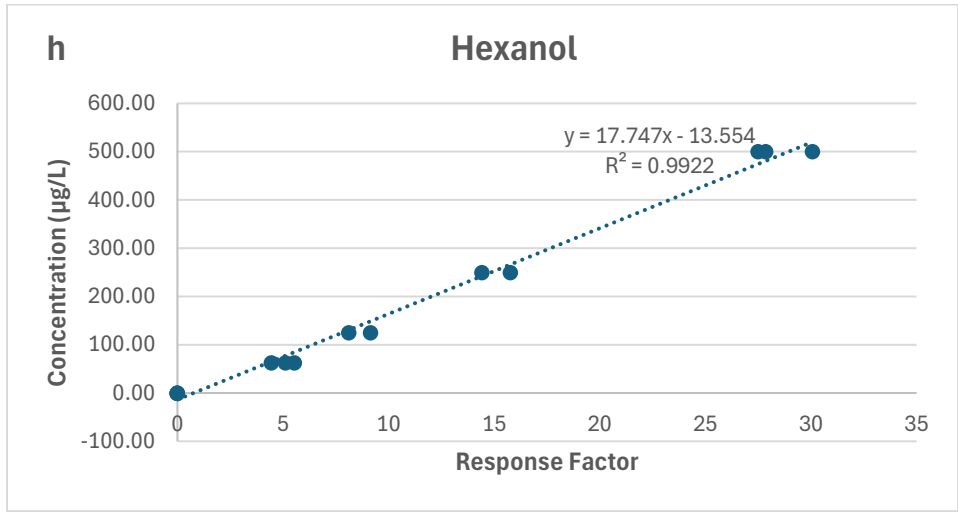
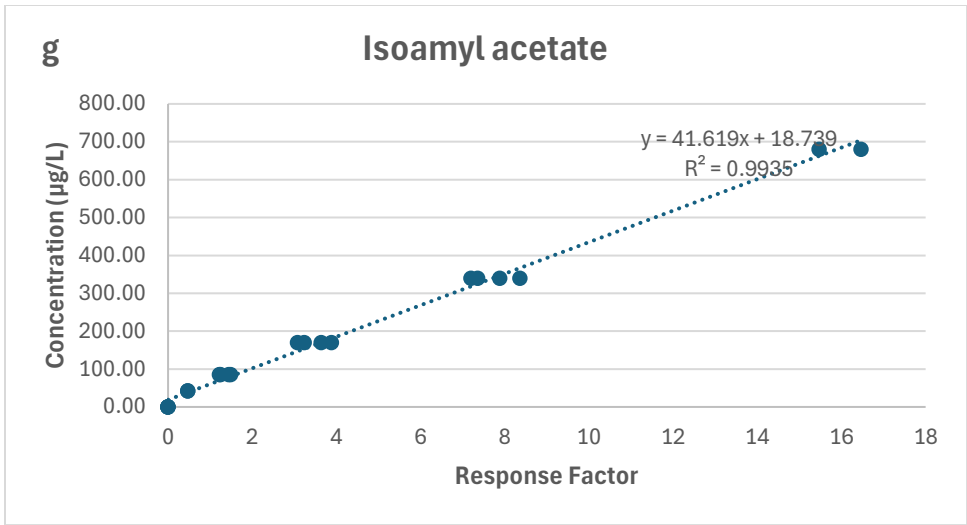
## Appendix

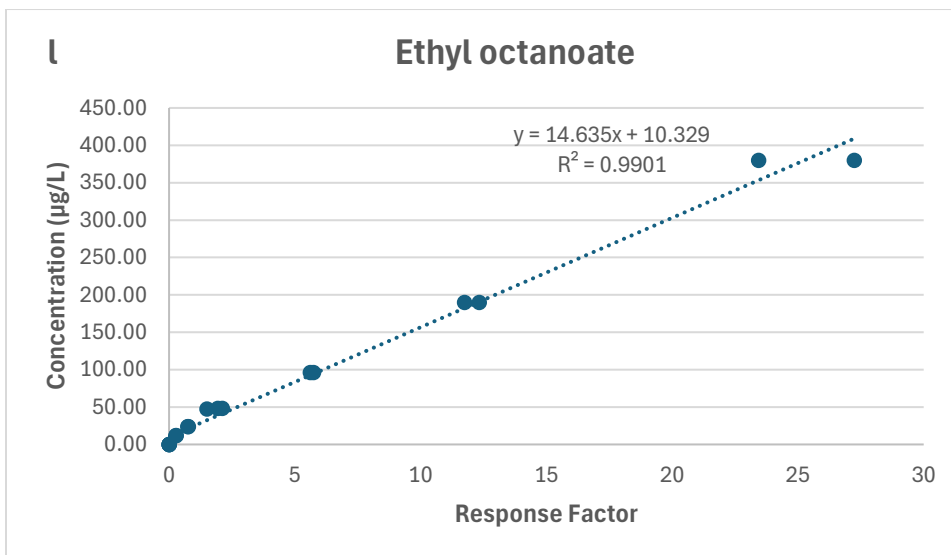
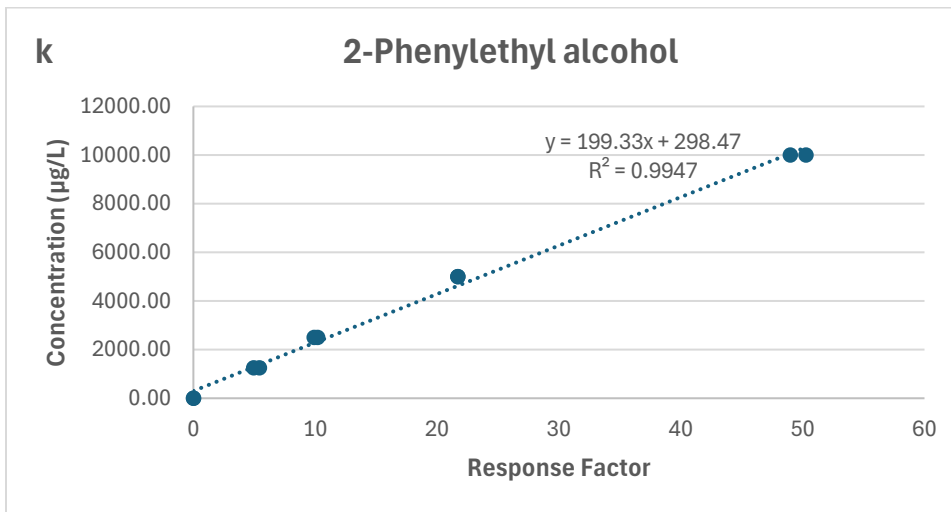
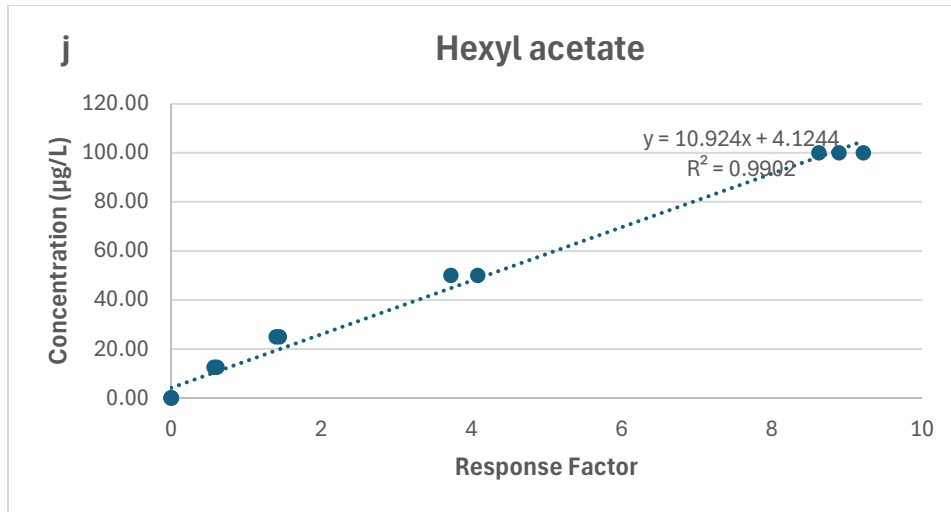


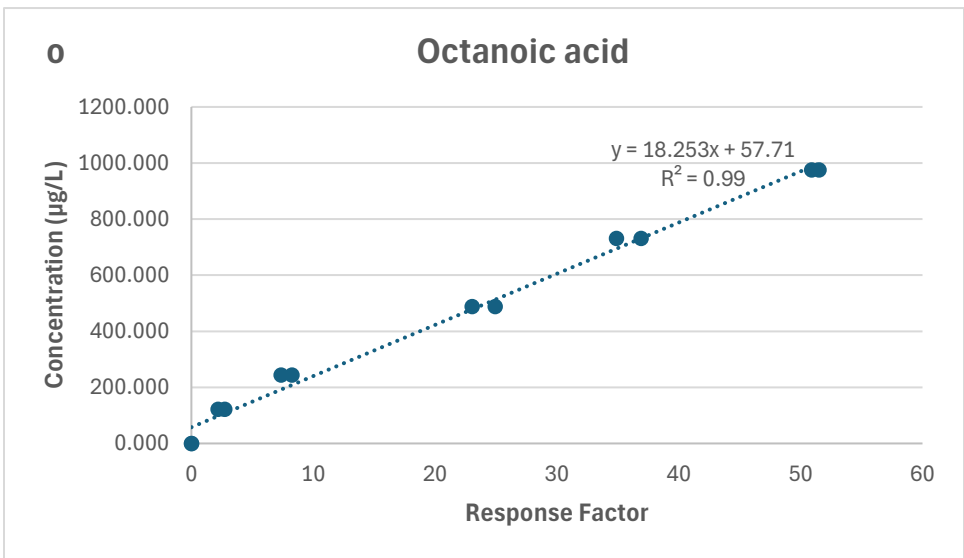
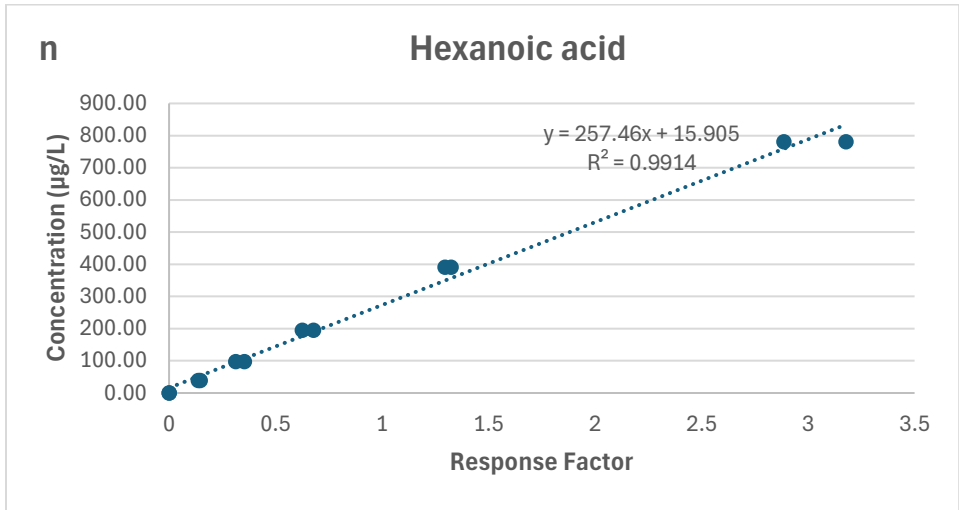
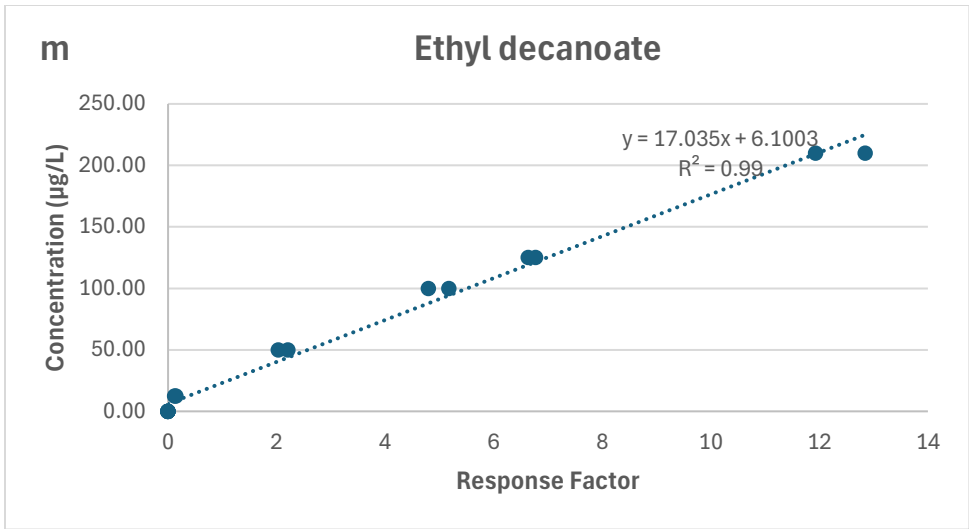
*Figure A1.1: Colony morphology of Saccharomyces cerevisiae and Saccharomyces uvarum on Wallerstein Laboratories Nutrient (WLN) differential agar. Colonies of S. cerevisiae appear cream-colored (a), whereas S. uvarum colonies exhibit a darker green hue (b).*











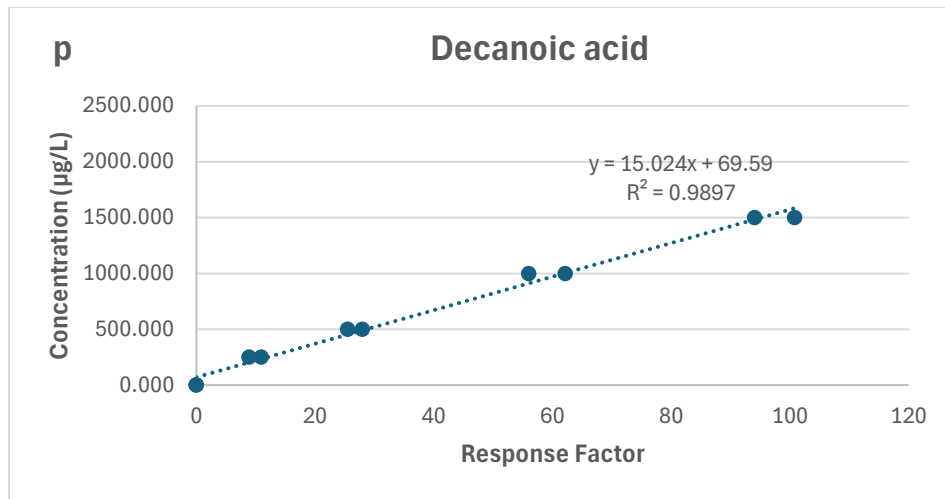


Figure A1.2, A-P: Standard curves for VOCs (ethyl acetate, 2-methyl-1-propanol, ethyl isobutyrate, ethyl butyrate, ethyl 2-methylbutyrate, ethyl isovalerate, isoamyl acetate, hexanol, ethyl hexanoate, hexyl acetate, 2-phenylethyl ethanol, ethyl octanoate, and ethyl decanoate) and VFAs (hexanoic acid, octanoic acid, decanoic acid).

Table A1.1: Number of nucleotide differences observed in  $\beta$ -tubulin and GDH1 igs sequences from CN1 and EC1118 fermentation set 1 isolates relative to their strain-specific positive controls. Sequences were trimmed to remove low-quality regions at the ends and aligned using the same alignment settings for all samples. Single-base differences are reported as substitutions, inserted or deleted bases are reported as indels (total number of affected base pairs), and ambiguous bases, represented as N in the sequence, are listed separately. Query coverage (%) and sequence identity (%) were obtained from pairwise alignments to the corresponding positive-control sequences.

Gene Region	Sample	Substitutions (n)	Indels (Total bp)	Ambiguous Bases	Query Coverage	Sequence Identity
B-tubulin	CN1 0% rot	86	86	3	95%	84.23%
	CN1 20% rot	2	9	0	99%	99.77%
	CN1 40% rot	0	10	0	100%	99.88%
	CN1 positive control	0	0	0	99%	99.88%
	EC1118 0% rot	4	10	1	99%	99.09%
	EC1118 20% rot	18	21	1	100%	99.77%
	EC1118 40% rot	6	11	1	100%	97.64%
	EC1118 positive control	0	0	1	98%	99.88%
GDH1 igs Region	CN1 0% rot	0	10	2	99%	99.24%
	CN1 20% rot	0	9	1	100%	99.74%
	CN1 40% rot	0	3	1	99%	99.74%
	CN1 positive control	0	0	1	100%	99.74%
	EC1118 0% rot	0	8	0	99%	100.00%
	EC1118 20% rot	0	8	0	100%	100.00%
	EC1118 40% rot	2	5	0	99%	100.00%
	EC1118 positive control	0	0	0	99%	100.00%



Query 503 TAGGTCGANCCATCATTGACTGCGATTGGTTCTCAATCGTATCNCAGATCGTTGCATCAA 562  
 || || | |||||||||||||||||||||||||||| || |||||||| | |  
 Sbjct 36527 TATG-CG--C---CATTGACTGCGATTGGTTCTCAATCGT-TC--AGATCGTTG-ACC-- 36574

Query 563 GGTCTNNGNGAATTTGACCCAGCCTAGGATATGTTTCGACTAAAAAGTNTAAAATGAAA 622  
 | |||| | |||| |||||| | | |||| |||| || | || || | |  
 Sbjct 36575 GTTCCT--G--AATT-GACCCAGC--A--A-ATGTT-CGACTCCAA-G---AATATG--A 36617

Query 623 TAAAAGATGCTGACCCAAGAAACAGTAAAACTTGACCGTTGCGGCATTCTTTAGTNAGA 682  
 | | |||||||||||||| || | |||||||||||||||||| || ||  
 Sbjct 36618 TGGCCGCTGCTGACCCAAGAAACGGTAGATACTTGACCGTTGCGGCATTCTTCAG--AG- 36674

Query 683 AAGTAAAGATACCGTAGAAGGAAGAAGTAAAACGAAATGAATCATAAGTCCAATCCAAGT 742  
 |||| | |||| |||||| || || |||||| | || ||||||||||||  
 Sbjct 36675 --GTAAAGTTCCGTA-AAGGAAGTAG-AAGACGAAATGCA-CA-AAGTCCAATCCAAG- 36727

Query 743 ANACTCAGGAATACTTGGATCGAAGGGATTCCCTAACAAAATGCAATTTTNTATCCGCCGT 802  
 | |||| | |||| | |||| |||||||||| |||| | |||||  
 Sbjct 36728 A-ACTCAG-ACTACTTTG-TCGAATGGATTCCCTAACACGTCGAA-----A-CCGCCGT 36777

Query 803 GTGTTCTGTAGCTCCACAAGGCATGGAACATGGACTGCTACGAACATAGCTAATCCTACA 862  
 |||||| |||||| |||| |||| |||||| || || |||| ||||  
 Sbjct 36778 GTGTTCTGTGCTCCACAAGGCTTGGA-CATGG-CTGCTACTTTCATTGCTAATTCTACA 36835

Query 863 TCCATCCAAGAACTGTTGAAGAGAGTCGGTGACCAACCTCCGGCCATGATCAAA-GAACA 921  
 |||||||||||||| |||||||||||||| | |||||| |||| || | |  
 Sbjct 36836 TCCATCCAAGAACTGTTTAAGAGAGTCGGTGACCAATTTTCGGCCATGTTCAAAGAA-A 36894

Query 922 AGCTTTC 928  
 |||||  
 Sbjct 36895 AGCTTTC 36901



```

Query 541 AATGTTTCGACTCCAAGAATATGATGGCCGCTGCTGACCCAAGAAACGGTAGATACTTGAC 600
          |||
Sbjct 36595 AATGTTTCGACTCCAAGAATATGATGGCCGCTGCTGACCCAAGAAACGGTAGATACTTGAC 36654

Query 601 CGTTGCGGCATTCTTTAGAGGTAAAGTTTCCGTAAAGGAAGTAGAAGACGAAATGCACAA 660
          |||
Sbjct 36655 CGTTGCGGCATTCTTCAGAGGTAAAGTTTCCGTAAAGGAAGTAGAAGACGAAATGCACAA 36714

Query 661 AGTCCAATCCAAGAACTCAGACTACTTTGTGCGAATGGATTCCCTAACACGTGCAAACCGC 720
          |||
Sbjct 36715 AGTCCAATCCAAGAACTCAGACTACTTTGTGCGAATGGATTCCCTAACACGTGCAAACCGC 36774

Query 721 CGTGTGTTCTGTGCGCTCCACAAGGCTTGGACATGGCTGCTACTTTCATTGCTAATTCTAC 780
          |||
Sbjct 36775 CGTGTGTTCTGTGCGCTCCACAAGGCTTGGACATGGCTGCTACTTTCATTGCTAATTCTAC 36834

Query 781 ATCCATCCAAGAACTGTTTAAAGAGAGTCGGTGACCAATTTTCGGCCATGTTCAAAGAAA 840
          |||
Sbjct 36835 ATCCATCCAAGAACTGTTTAAAGAGAGTCGGTGACCAATTTTCGGCCATGTTCAAAGAAA 36894

Query 841 AGCTTTCTTGCAATTGGTATACT 862
          |||
Sbjct 36895 AGCTTTCTTGCAATTGGTATACT 36916

```



Sbjct 36542 GCGATTGGTTCTCAATCGTTCAGATCGTTGACCGTTCCTGAATTGACCCAGCAAATGTTTC 36601  
  
 Query 541 GACTCCAAGAATATGATGGCCGCTGCTGACCCAAGAAACGGTAGATACTTGACCGTTGCG 600  
 |||  
 Sbjct 36602 GACTCCAAGAATATGATGGCCGCTGCTGACCCAAGAAACGGTAGATACTTGACCGTTGCG 36661  
  
 Query 601 GCATTCTTTAGAGGTAAAGTTTCCGTAAAGGAAGTAGAAGACGAAATGCACAAAAGTCCAA 660  
 |||  
 Sbjct 36662 GCATTCTTCAGAGGTAAAGTTTCCGTAAAGGAAGTAGAAGACGAAATGCACAAAAGTCCAA 36721  
  
 Query 661 TCCAAGAACTCAGACTACTTTGTGCAATGGATTCCCTAACACGTGCAAACCGCCGTGTGT 720  
 |||  
 Sbjct 36722 TCCAAGAACTCAGACTACTTTGTGCAATGGATTCCCTAACACGTGCAAACCGCCGTGTGT 36781  
  
 Query 721 TCTGTCGCTCCACAAGGCTTGGACATGGCTGCTACTTTCATTGCTAATTCTACATCCATC 780  
 |||  
 Sbjct 36782 TCTGTCGCTCCACAAGGCTTGGACATGGCTGCTACTTTCATTGCTAATTCTACATCCATC 36841  
  
 Query 781 CAAGAACTGTTTAAAGAGAGTCGGTGACCAATTTTCGGCCATGTTCAAAGAAAAGCTTTC 840  
 |||  
 Sbjct 36842 CAAGAACTGTTTAAAGAGAGTCGGTGACCAATTTTCGGCCATGTTCAAAGAAAAGCTTTC 36901  
  
 Query 841 TTGCATTG 848  
 |||  
 Sbjct 36902 TTGCATTG 36909

**4. Alignment result of  $\beta$ -tubulin gene region of CN1 positive control to the top Blasting match**

***Saccharomyces uvarum* strain CBS7001 chromosome VI, complete sequence**

Sequence ID: [CP113769.1](#) Length: 546910 Number of Matches: 1

Score	Expect	Identities	Gaps	Strand
1572 bits(851)	0.0	853/854(99%)	0/854(0%)	Plus/Plus
Query 3	GACAGCGTCATGGACGTCATCAGACGGGAGGCCGAAGGGTGCATTCCCTGCAAGGTTTC	62		
Sbjct 36059	GACAGCGTCATGGACGTCATCAGACGGGAGGCCGAAGGGTGCATTCCCTGCAAGGTTTC	36118		
Query 63	CAGATCACGCATTCTCTTGGTGGTGGTACTGGTTCCGGTATGGGTACACTGTTAATCTCG	122		
Sbjct 36119	CAGATCACGCATTCTCTTGGTGGTGGTACTGGTTCCGGTATGGGTACACTGTTAATCTCG	36178		
Query 123	AAGATCAGAGAGGAGTTCCCGACCGTATGATGGCTACTTTCTCCGTCCTGCCCTCTCCA	182		
Sbjct 36179	AAGATCAGAGAGGAGTTCCCGACCGTATGATGGCTACTTTCTCCGTCCTGCCCTCTCCA	36238		
Query 183	AAGACCTCCGACACAGTCGTGGAGCCCTACAACGCCACGTTGTCCGTGCACCAACTGGTA	242		
Sbjct 36239	AAGACCTCCGACACAGTCGTGGAGCCCTACAACGCCACGTTGTCCGTGCACCAACTGGTA	36298		
Query 243	GAACACTCCGATGAAACCTTCTGTATCGATAACGAAGCGCTATATGACATCTGCCAAAGA	302		
Sbjct 36299	GAACACTCCGATGAAACCTTCTGTATCGATAACGAAGCGCTATATGACATCTGCCAAAGA	36358		
Query 303	ACCCTGAAGTTGAACCAGCCTTCGTACGGGGACTTGAACAACCTGGTCTCGAGCGTCATG	362		
Sbjct 36359	ACCCTGAAGTTGAACCAGCCTTCGTACGGGGACTTGAACAACCTGGTCTCGAGCGTCATG	36418		
Query 363	TCCGGTGTCAACCACTTCGTTGCGTTACCCCGGTCAATTGAACTCCGATTTGAGAAAATTG	422		
Sbjct 36419	TCCGGTGTCAACCACTTCGTTGCGTTACCCCGGTCAATTGAACTCCGATTTGAGAAAATTG	36478		
Query 423	GCAGTCAACCTGGTGCCATTTCCACGTTTGCATTTCTTCATGGTTGGATATGCGCCATTG	482		
Sbjct 36479	GCAGTCAACCTGGTGCCATTTCCACGTTTGCATTTCTTCATGGTTGGATATGCGCCATTG	36538		
Query 483	ACTGCGATTGGTTCTCAATCGTTTCAGATCGTTGACCGTTCCTGAATTGACCCAGCAAATG	542		

Sbjct 36539 ACTGCGATTGGTTCTCAATCGTTCAGATCGTTGACCGTTCCTGAATTGACCCAGCAAATG 36598  
  
 Query 543 TTCGACTCCAAGAATATGATGGCCGCTGCTGACCCAAGAAACGGTAGATACTTGACCGTT 602  
 |||  
 Sbjct 36599 TTCGACTCCAAGAATATGATGGCCGCTGCTGACCCAAGAAACGGTAGATACTTGACCGTT 36658  
  
 Query 603 GCGGCATTCTTTAGAGGTAAAGTTTCCGTAAAGGAAGTAGAAGACGAAATGCACAAAGTC 662  
 |||  
 Sbjct 36659 GCGGCATTCTTCAGAGGTAAAGTTTCCGTAAAGGAAGTAGAAGACGAAATGCACAAAGTC 36718  
  
 Query 663 CAATCCAAGAACTCAGACTACTTTGTTCGAATGGATTCCCTAACACGTGCAAACCGCCGTG 722  
 |||  
 Sbjct 36719 CAATCCAAGAACTCAGACTACTTTGTTCGAATGGATTCCCTAACACGTGCAAACCGCCGTG 36778  
  
 Query 723 TGTTCGTGCTGCCACAAGGCTTGGACATGGCTGCTACTTTCATTGCTAATTCTACATCC 782  
 |||  
 Sbjct 36779 TGTTCGTGCTGCCACAAGGCTTGGACATGGCTGCTACTTTCATTGCTAATTCTACATCC 36838  
  
 Query 783 ATCCAAGAACTGTTTAAGAGAGTCGGTGACCAATTTTCGGCCATGTTCAAAGAAAAGCT 842  
 |||  
 Sbjct 36839 ATCCAAGAACTGTTTAAGAGAGTCGGTGACCAATTTTCGGCCATGTTCAAAGAAAAGCT 36898  
  
 Query 843 TTCTTGCATTGGTA 856  
 |||  
 Sbjct 36899 TTCTTGCATTGGTA 36912



Sbjct 74867 GTCGGCTACGCTCCATTGACGGCAATTGGCTCTCAATCATTAGATCTTTGACTGTCCCT 74926

Query 540 GAATTAACACAGCAAATGTTTGATGCCAAGAACATGATGGCTGCTGCCGATCCAAGAAAC 599  
 |||

Sbjct 74927 GAATTAACACAGCAAATGTTTGATGCCAAGAACATGATGGCTGCTGCCGATCCAAGAAAC 74986

Query 600 GGTAGATACCTTACCGTTGCAGCCTTCTTTAGAGGTAAAGTTCCGTTAAGGAGGTGGAA 659  
 |||

Sbjct 74987 GGTAGATACCTTACCGTTGCAGCCTTCTTTAGAGGTAAAGTTCCGTTAAGGAGGTGGAA 75046

Query 660 GATGAAATGCATAAAGTGCAATCTAAAACTCAGACTATTTTCGTGGAATGGATCCCCAAC 719  
 |||

Sbjct 75047 GATGAAATGCATAAAGTGCAATCTAAAACTCAGACTATTTTCGTGGAATGGATCCCCAAC 75106

Query 720 AATGTGCAAAC TGCTGTGTGTTCTGTGCTCCTCAAGGTTTGGACATGGCTGCTACTTTC 779  
 |||

Sbjct 75107 AATGTGCAAAC TGCTGTGTGTTCTGTGCTCCTCAAGGTTTGGACATGGCTGCTACTTTC 75166

Query 780 ATTGCTAACTCCACATCTATTCAAGAGCTATTCAAGAGAGTTGGTGACCAATTTTCCGCT 839  
 |||

Sbjct 75167 ATTGCTAACTCCACATCTATTCAAGAGCTATTCAAGAGAGTTGGTGACCAATTTTCCGCT 75226

Query 840 ATGTTCAAAGAAAAGCTTTCTTGAC 866  
 |||

Sbjct 75227 ATGTTCAAAGAAAAGCTTTCTTGAC 75253

**6. Alignment result of  $\beta$ -tubulin gene region of EC1118, 20% rot to the top Blasting match**

***Saccharomyces cerevisiae* YJM270 chromosome VI sequence**  
 Sequence ID: [CP004895.2](#) Length: 244497 Number of Matches: 1

Score	Expect	Identities	Gaps	Strand
1520 bits(823)	0.0	868/889(98%)	7/889(0%)	Plus/Plus
Query 1		GGTGCGGAACCTGCAGACCATGCGTCATAGATGTCATTAGACGAGAGGCCGAAGGATGCG		60
Sbjct 37757		GGTGCTGAGCTGTAGAC-A-GCGTCATGGATGTTATTAGACGAGAGGCCGAAGGATGCG		37814
Query 61		ACTCCCTTCAAGGCTTCCTACATCACACATTCTCTTGGTGGTGATACCGTTCCNGGTAT		120
Sbjct 37815		ACTCCCTTCAAGGTTTCC-AGATCACACATTCTCTTGGTGGTGGTACCGTTCC-GGTAT		37872
Query 121		GGGTACNGCTTTTGATCTCGANNAGATTAGAGAAGAGTTGCCTGATCGAATGATGGCCAC		180
Sbjct 37873		GGGTAC-GCTTTTGATCTCGA--AGATTAGGAAGAGTTTCTGATCGTATGATGGCCAC		37929
Query 181		CTTCTCCGTCTTGCCCTCTCCAAAGACTTCTGACACCGTTGTCGAACCATAACAATGCCAC		240
Sbjct 37930		CTTCTCCGTCTTGCCCTCTCCAAAGACTTCTGACACCGTTGTCGAACCATAACAATGCCAC		37989
Query 241		GTTGTCTGTGCACCAATTGGTAGAACACTCTGATGAAACATTCTGTATCGATAACGAAGC		300
Sbjct 37990		GTTGTCTGTGCACCAATTGGTAGAACACTCTGATGAAACATTCTGTATCGATAACGAAGC		38049
Query 301		ACTTTATGACATCTGTCAAAGGACCTTGAAGTTGAATCAACCTTCTTATGGAGATTTGAA		360
Sbjct 38050		ACTTTATGACATCTGTCAAAGGACCTTGAAGTTGAATCAACCTTCTTATGGAGATTTGAA		38109
Query 361		CAACTTGGTCTCGAGCGTCATGTCTGGTGTGACAACTTCATTGCGTTATCCCGCCAATT		420
Sbjct 38110		CAACTTGGTCTCGAGCGTCATGTCTGGTGTGACAACTTCATTGCGTTATCCCGCCAATT		38169
Query 421		GAACTCTGATTTGAGAAAGTTGGCTGTAACTTGTGCCATTCCCACGTTTACATTTCTT		480
Sbjct 38170		GAACTCTGATTTGAGAAAGTTGGCTGTAACTTGTGCCATTCCCACGTTTACATTTCTT		38229
Query 481		CATGGTCGGCTACGCTCCATTGACGGCAATTGGCTCTCAATCATTTAGATCTTTGACTGT		540
Sbjct 38230		CATGGTCGGCTACGCTCCATTGACGGCAATTGGCTCTCAATCATTTAGATCTTTGACTGT		38289

Query 541 CCCTGAATTAACACAGCAAATGTTTGATGCCAAGAACATGATGGCTGCTGCCGATCCAAG 600  
 |||  
 Sbjct 38290 CCCTGAATTAACACAGCAAATGTTTGATGCCAAGAACATGATGGCTGCTGCCGATCCAAG 38349

Query 601 AAACGGTAGATACCTTACCGTTGCAGCCTTCTTTAGAGGTAAAGTTCCGTTAAGGAGGT 660  
 |||  
 Sbjct 38350 AAACGGTAGATACCTTACCGTTGCAGCCTTCTTTAGAGGTAAAGTTCCGTTAAGGAGGT 38409

Query 661 GGAAGATGAAATGCATAAAGTGCAATCTAAAACTCAGACTATTTTCGTGGAATGGATCCC 720  
 |||  
 Sbjct 38410 GGAAGATGAAATGCATAAAGTGCAATCTAAAACTCAGACTATTTTCGTGGAATGGATCCC 38469

Query 721 CAACAATGTGCAAACCTGCTGTGTGTTCTGTCGCTCCTCAAGGTTTGGACATGGCTGCTAC 780  
 |||  
 Sbjct 38470 CAACAATGTGCAAACCTGCTGTGTGTTCTGTCGCTCCTCAAGGTTTGGACATGGCTGCTAC 38529

Query 781 TTTCATTGCTAACTCCACATCTATTCAAGAGCTATTCAAGAGAGTTGGTGACCAATTTTC 840  
 |||  
 Sbjct 38530 TTTCATTGCTAACTCCACATCTATTCAAGAGCTATTCAAGAGAGTTGGTGACCAATTTTC 38589

Query 841 CGCTATGTTCAAAGAAAAGCTTGCTTGCACTGTNATACTAGTGAAGGT 889  
 |||  
 Sbjct 38590 CGCTATGTTCAAAGAAAAGCTTTCTTGCACTGGTATACTAGTGAAGGT 38638

**7. Alignment result of  $\beta$ -tubulin gene region of EC1118, 40% rot to the top Blasting match**

***Saccharomyces cerevisiae* strain KSD-Yc chromosome 6**

Sequence ID: [CP024000.1](#) Length: 287260 Number of Matches: 1

Score	Expect	Identities	Gaps	Strand
1568 bits(849)	0.0	868/876(99%)	7/876(0%)	Plus/Plus
Query 1	GTGCTGAGC-TGTAGACAGCGTCATGGATGTTATTAGACGAGAGGCCGAAGGATGCGACT	59		
Sbjct 74391	GTGCTGAGCTTGTAGACAGCGTCATGGATGTTATTAGACGAGAGGCCGAAGGATGCGACT	74450		
Query 60	CCCTTCAAGGTTTCCAGATCACACATTCTCTGGTGGTGGTACCGGTTCCGGTATGGGTA	119		
Sbjct 74451	CCCTTCAAGGTTTCCAGATCACACATTCTCTGGTGGTGGTACCGGTTCCGGTATGGGTA	74510		
Query 120	CGCTTTTGATCTCGAAGATTAGGGAAGAGTTTCTTGATCGTATGATGGCCACCTTCTCCG	179		
Sbjct 74511	CGCTTTTGATCTCGAAGATTAGGGAAGAGTTTCTTGATCGTATGATGGCCACCTTCTCCG	74570		
Query 180	TCTTGCCCTCTCCAAAGACTTCTGACACCGTTGTCGAACCATAACAATGCCACGTTGTCTG	239		
Sbjct 74571	TCTTGCCCTCTCCAAAGACTTCTGACACCGTTGTCGAACCATAACAATGCCACGTTGTCTG	74630		
Query 240	TGCACCAATTGGTAGAACACTCTGATGAAACATTCTGTATCGATAACGAAGCACTTTATG	299		
Sbjct 74631	TGCACCAATTGGTAGAACACTCTGATGAAACATTCTGTATCGATAACGAAGCACTTTATG	74690		
Query 300	ACATCTGTCAAAGGACCTTNAAGTTGAATCAACCTTCTTATGGAGATTGAACAACCTGG	359		
Sbjct 74691	ACATCTGTCAAAGGACCTTAAAGTTGAATCAACCTTCTTATGGAGATTGAACAACCTGG	74750		
Query 360	TCTCGAGCGTCATGTCTGGTGTGACAACTTCATTGCGTTATCCCGCCAATTGAACTCTG	419		
Sbjct 74751	TCTCGAGCGTCATGTCTGGTGTGACAACTTCATTGCGTTATCCCGCCAATTGAACTCTG	74810		
Query 420	ATTTGAGAAAGTTGGCTGTTAATCTTGTCACATCCACGTTTACATTTCTTCATGGTCTG	479		
Sbjct 74811	ATTTGAGAAAGTTGGCTGTTAATCTTGTCACATCCACGTTTACATTTCTTCATGGTCTG	74870		
Query 480	GCTACGCTCCATTGACGGCAATTGGCTCTCAATCATTTAGATCTTTGACTGTCCCTGAAT	539		

Sbjct 74871 GCTACGCTCCATTGACGGCAATTGGCTCTCAATCATTTAGATCTTTGACTGTCCCTGAAT 74930

Query 540 TAACACAGCAAATGTTTGATGCCAAGAACATGATGGCTGCTGCCGATCCAAGAAACGGTA 599  
 |||

Sbjct 74931 TAACACAGCAAATGTTTGATGCCAAGAACATGATGGCTGCTGCCGATCCAAGAAACGGTA 74990

Query 600 GATACCTTACCGTTGCAGCCTTCTTTAGAGGTAAAGTTTCCGTTAAGGAGGTGGAAGATG 659  
 |||

Sbjct 74991 GATACCTTACCGTTGCAGCCTTCTTTAGAGGTAAAGTTTCCGTTAAGGAGGTGGAAGATG 75050

Query 660 AAATGCATAAAGTGCAATCTAAAACTCAGACTATTTTCGTGGAATGGATCCCCAACAATG 719  
 |||

Sbjct 75051 AAATGCATAAAGTGCAATCTAAAACTCAGACTATTTTCGTGGAATGGATCCCCAACAATG 75110

Query 720 TGCAAACCTGCTGTGTGTTCTGTCGCTCCTCAAGGTTTGGACATGGCTGCTACTTTCATTG 779  
 |||

Sbjct 75111 TGCAAACCTGCTGTGTGTTCTGTCGCTCCTCAAGGTTTGGACATGGCTGCTACTTTCATTG 75170

Query 780 CTAACCTCCACATCTATTCAAGAGCTATTCAAGAGAGTTGGTGACCAATTTTCCGCTATGT 839  
 |||

Sbjct 75171 CTAACCTCCACATCTATTCAAGAGCTATTCAAGAGAGTTGGTGACCAATTTTCCGCTATGT 75230

Query 840 TCAAAAGAAAAGCATNTGTACTTGCTAGCTGGTATA 875  
 |||

Sbjct 75231 TCAAAAGAAAAGC-T-T-T-CTTGC-A-CTGGTATA 75260

**8. Alignment result of  $\beta$ -tubulin gene region of EC1118 positive control to the top Blasting match**

***Saccharomyces cerevisiae* strain KSD-Yc chromosome 6**

Sequence ID: [CP024000.1](#) Length: 287260 Number of Matches: 1

Score	Expect	Identities	Gaps	Strand
1576 bits(853)	0.0	856/858(99%)	0/858(0%)	Plus/Plus
Query 11	TGTAGACAGCGTCATGGATGTTATTAGACGAGAGGCCGAAGGATGCGACTCCCTTCAAGG	70		
Sbjct 74401	TGTAGACAGCGTCATGGATGTTATTAGACGAGAGGCCGAAGGATGCGACTCCCTTCAAGG	74460		
Query 71	TTTCAGATCACACATTCTCTTGGTGGTGGTACCGTTCCGGTATGGGTACGCTTTTGAT	130		
Sbjct 74461	TTTCAGATCACACATTCTCTTGGTGGTGGTACCGTTCCGGTATGGGTACGCTTTTGAT	74520		
Query 131	CTCGAAGATTAGGGAAGAGTTTCTTGATCGTATGATGGCCACCTTCTCCGTCTTGCCCTC	190		
Sbjct 74521	CTCGAAGATTAGGGAAGAGTTTCTTGATCGTATGATGGCCACCTTCTCCGTCTTGCCCTC	74580		
Query 191	TCCAAAGACTTCTGACACCGTTGTGCGAACCATACAATGCCACGTTGTCTGTGCACCAATT	250		
Sbjct 74581	TCCAAAGACTTCTGACACCGTTGTGCGAACCATACAATGCCACGTTGTCTGTGCACCAATT	74640		
Query 251	GGTAGAACACTCTGATGAAACATTCTGTATCGATAACGAAGCACTTTATGACATCTGTCA	310		
Sbjct 74641	GGTAGAACACTCTGATGAAACATTCTGTATCGATAACGAAGCACTTTATGACATCTGTCA	74700		
Query 311	AAGGACCTTNAAGTTGAATCAACCTTCTTATGGAGATTTGAACAACCTGGTCTCGAGCGT	370		
Sbjct 74701	AAGGACCTTAAAGTTGAATCAACCTTCTTATGGAGATTTGAACAACCTGGTCTCGAGCGT	74760		
Query 371	CATGTCTGGTGTGACAACCTTCATTGCGTTATCCCGCCAATTGAACTCTGATTTGAGAAA	430		
Sbjct 74761	CATGTCTGGTGTGACAACCTTCATTGCGTTATCCCGCCAATTGAACTCTGATTTGAGAAA	74820		
Query 431	GTTGGCTGTTAATCTTGTCCATTCCACGTTTACATTTCTTCATGGTCGGCTACGCTCC	490		
Sbjct 74821	GTTGGCTGTTAATCTTGTCCATTCCACGTTTACATTTCTTCATGGTCGGCTACGCTCC	74880		
Query 491	ATTGACGGCAATTGGCTCTCAATCATTTAGATCTTTGACTGTCCCTGAATTAACACAGCA	550		

Sbjct 74881 ATTGACGGCAATTGGCTCTCAATCATTAGATCTTTGACTGTCCCTGAATTAACACAGCA 74940

Query 551 AATGTTTGATGCCAAGAACATGATGGCTGCTGCCGATCCAAGAAACGGTAGATACCTTAC 610  
 |||

Sbjct 74941 AATGTTTGATGCCAAGAACATGATGGCTGCTGCCGATCCAAGAAACGGTAGATACCTTAC 75000

Query 611 CGTTGCAGCCTTCTTTAGAGGTAAAGTTCCGTTAAGGAGGTGGAAGATGAAATGCATAA 670  
 |||

Sbjct 75001 CGTTGCAGCCTTCTTTAGAGGTAAAGTTCCGTTAAGGAGGTGGAAGATGAAATGCATAA 75060

Query 671 AGTGCAATCTAAAACTCAGACTATTTTCGTGGAATGGATCCCCAACAATGTGCAAACTGC 730  
 |||

Sbjct 75061 AGTGCAATCTAAAACTCAGACTATTTTCGTGGAATGGATCCCCAACAATGTGCAAACTGC 75120

Query 731 TGTGTGTTCTGTCGCTCCTCAAGGTTTGGACATGGCTGCTACTTTCATTGCTAACTCCAC 790  
 |||

Sbjct 75121 TGTGTGTTCTGTCGCTCCTCAAGGTTTGGACATGGCTGCTACTTTCATTGCTAACTCCAC 75180

Query 791 ATCTATTCAAGAGCTATTCAAGAGAGTTGGTGACCAATTTCCGCTATGTTCAAAAGAAA 850  
 |||

Sbjct 75181 ATCTATTCAAGAGCTATTCAAGAGAGTTGGTGACCAATTTCCGCTATGTTCAAAAGAAA 75240

Query 851 AGCATTCTTGCACTGGTA 868  
 |||

Sbjct 75241 AGCTTTCTTGCACTGGTA 75258

9. Alignment result of *GDH1* igs region of CN1, 0% rot to the top Blasting match

***Saccharomyces uvarum* strain CBS7001 chromosome VIII, complete sequence**

Sequence ID: [CP113771.1](#) Length: 838652 Number of Matches: 1

Score	Expect	Identities	Gaps	Strand
721 bits(390)	0.0	393/396(99%)	0/396(0%)	Plus/Minus
Query 3		TTGCCNTCCTTAGTCNAGGGTGCTAACATTGCCAGTTTCATTAAGGTCTCTGATGCTATG		62
Sbjct 780623		TTGCCATCCTTAGTCAAGGGTGCTAACATTGCCAGTTTCATTAAGGTCTCTGATGCTATG		780564
Query 63		TTCGACCAAGGTGATGTATTTTAAATAGTCTAAAGAAAAGAGAAAAGACAGCATAATTGT		122
Sbjct 780563		TTCGACCAAGGTGATGTATTTTAAATAGTCTAAAGAAAAGAGAAAAGACAGCATAATTGT		780504
Query 123		TCTTTTTAAATAGTTTAGATAGATAATGAGATAAAAGAAGCaaaaaaaaatcgtgtaata		182
Sbjct 780503		TCTTTTTAAATAGTTTAGATAGATAATGAGATAAAAGAAGCAAAAAAAAAATCGTGTAAATA		780444
Query 183		taaaaaaaaaatcatacttttgatagagaaaggcaaaaaaagggaaaaaaaaaGATTTT		242
Sbjct 780443		TAAAAAAAAAATCATACTTTTGATAGAGAAAGGCAAAAAAAGGAAAAAAAAAAGATTTT		780384
Query 243		TAAAGTACATTTATTTGAATCATGACATGGCATGGCCGGGATATAACAAAGAGACAAAAT		302
Sbjct 780383		TAAAGTACATTTATTTGAATCATGACATGGCATGGCCGGGATATAACAAAGAGACAAAAT		780324
Query 303		ATTTATTTATTTATGTATGAAGGAGTGAATGGAAACAATGGATAACTAACCAGCTCGACT		362
Sbjct 780323		ATTTATTTATTTATGTATGAAGGAGTGAATGGAAACAATGGATAACTAACCAGCTCGACT		780264
Query 363		GGAATTAGTCTTCTAACTNGGCACGAACGGCCTTAA 398		
Sbjct 780263		GGAATTAGTCTTCTAACTTGGCACGAACGGCCTTAA 780228		



**11. Alignment result of *GDH1* igs region of CN1, 40% rot to the top Blasting match  
*Saccharomyces uvarum* strain CBS7001 chromosome VIII, complete sequence**  
 Sequence ID: [CP113771.1](#) Length: 838652 Number of Matches: 1

Score	Expect	Identities	Gaps	Strand
712 bits(385)	0.0	386/387(99%)	0/387(0%)	Plus/Minus
Query 1		TCCTTAGTCAAGGGTGCTAACATTGCCAGTTTCATTAAGGTCTCTGATGCTATGTTTCGAC		60
Sbjct 780617		TCCTTAGTCAAGGGTGCTAACATTGCCAGTTTCATTAAGGTCTCTGATGCTATGTTTCGAC		780558
Query 61		CAAGGTGATGTATTTTAAATAGTCTAAAGAAAAGAGAAAAGACAGCATAATTGTTCTTTT		120
Sbjct 780557		CAAGGTGATGTATTTTAAATAGTCTAAAGAAAAGAGAAAAGACAGCATAATTGTTCTTTT		780498
Query 121		TAAATAGTTTAGATAGATAATGAGATAAAAAGAAGCaaaaaaaaatcgtgtaataataaaaa		180
Sbjct 780497		TAAATAGTTTAGATAGATAATGAGATAAAAAGAAGCAAAAAAAAAATCGTGTAAATATAAAAA		780438
Query 181		aaaaatcataacttttgatagagaaaggcaaaaaaagggaaaaaaaaaaGATTTTTAAAGT		240
Sbjct 780437		AAAAATCATACTTTTGATAGAGAAAGGCAAAAAAAGGGAIAAAAAAAAAAGATTTTTAAAGT		780378
Query 241		ACATTTATTTGAATCATGACATGGCATGGCCGGGATATAACAAAGAGACAAAATATTTAT		300
Sbjct 780377		ACATTTATTTGAATCATGACATGGCATGGCCGGGATATAACAAAGAGACAAAATATTTAT		780318
Query 301		TTATTTATGTATGAAGGAGTGAATGGAAACAATGGATAACTAACCAGCTCGACTGGAATT		360
Sbjct 780317		TTATTTATGTATGAAGGAGTGAATGGAAACAATGGATAACTAACCAGCTCGACTGGAATT		780258
Query 361		AGTCTTCTAACTNGGCACGAACGGCCT 387		
Sbjct 780257		AGTCTTCTAACTTGGCACGAACGGCCT 780231		

**12. Alignment result of *GDH1* igs region of CN1 positive control to the top Blasting match  
*Saccharomyces uvarum* strain CBS7001 chromosome VIII, complete sequence**

Sequence ID: [CP113771.1](#) Length: 838652 Number of Matches: 1

Score	Expect	Identities	Gaps	Strand
717 bits(388)	0.0	389/390(99%)	0/390(0%)	Plus/Minus
Query 1	TCCTTAGTCAAGGGTGCTAACATTGCCAGTTTCATTAAGGTCTCTGATGCTATGTTTCGAC	60		
Sbjct 780617	TCCTTAGTCAAGGGTGCTAACATTGCCAGTTTCATTAAGGTCTCTGATGCTATGTTTCGAC	780558		
Query 61	CAAGGTGATGTATTTTAAATAGTCTAAAGAAAAGAGAAAAGACAGCATAATTGTTCTTTT	120		
Sbjct 780557	CAAGGTGATGTATTTTAAATAGTCTAAAGAAAAGAGAAAAGACAGCATAATTGTTCTTTT	780498		
Query 121	TAAATAGTTTAGATAGATAATGAGATAAAAAGAAGCaaaaaaaaatcgtgtaataataaaaa	180		
Sbjct 780497	TAAATAGTTTAGATAGATAATGAGATAAAAAGAAGCAAAAAAAAAATCGTGTAAATATAAAAA	780438		
Query 181	aaaaatcatacttttgatagagaaaggcaaaaaagggaaaaaaaaaGATTTTTAAAGT	240		
Sbjct 780437	AAAAATCATACTTTTGATAGAGAAAGGCAAAAAAGGGAAAAAAAAAAGATTTTTAAAGT	780378		
Query 241	ACATTTATTTGAATCATGACATGGCATGGCCGGGATATAACAAAGAGACAAAATATTTAT	300		
Sbjct 780377	ACATTTATTTGAATCATGACATGGCATGGCCGGGATATAACAAAGAGACAAAATATTTAT	780318		
Query 301	TTATTTATGTATGAAGGAGTGAATGGAAACAATGGATAACTAACCAGCTCGACTGGAATT	360		
Sbjct 780317	TTATTTATGTATGAAGGAGTGAATGGAAACAATGGATAACTAACCAGCTCGACTGGAATT	780258		
Query 361	AGTCTTCTAACTNGGCACGAACGGCCTTAA	390		
Sbjct 780257	AGTCTTCTAACTTGGCACGAACGGCCTTAA	780228		

**13. Alignment result of *GDH1* igs region of EC1118, 0% rot to the top Blasting match  
*Saccharomyces cerevisiae* strain CEN.PK113-7D chromosome XV  
Sequence ID: [CP046095.1](#) Length: 1085503 Number of Matches: 1**

Score	Expect	Identities	Gaps	Strand
754 bits(408)	0.0	417/421(99%)	1/421(0%)	Plus/Minus
Query 9	CATCTTTGGTC-AAGGTGCTAATATCGCAAGTTTCATCAAGGTCTCTGATGCTATGTTTG	67		
Sbjct 1036002	CATCTTTGGTCAAAGGTGCTAATATCGCAAGTTTCATCAAGGTCTCTGATGCTATGTTTG	1035943		
Query 68	ACCAAGGTGATGTATTTTAAATAGTCTAAAAGAAAGAAAAGAGGAAAGTTCATAAAAAGT	127		
Sbjct 1035942	ACCAAGGTGATGTATTTTAAATAGTCTAAAAGAAAGAAAAGAGGAAAGTTCATAAAAAGT	1035883		
Query 128	TCTTTCtttttttAAATAACTTAGATAGATAATGAGATAAAAAGAAGTaaaaaaCGGAA	187		
Sbjct 1035882	TCTTTCTTTTTTTAAATAACTTAGATAGATAATGAGATAAAAAGAAGTAAAAAACGGAA	1035823		
Query 188	TCGTAACGCAATTAATTAATTAAGAAAATTGATTATCGGGAGaaaaaaattttatttttt	247		
Sbjct 1035822	TCGTAACGCAATTAATTAATTAAGAAAATTGATTATCGGGAGAAAAAATTTTATTTTTT	1035763		
Query 248	attttattttCTTTAAAGTACATATATTTGAAATGATGACATGTGGAAATATAACAGAGA	307		
Sbjct 1035762	ATTTTATTTCTTTAAAGTACATATATTTGAAATGATGACATGTGGAAATATAACAGAGA	1035703		
Query 308	CAGAATATTTAATTTTATGTATGTAAGCATCGATTGGACACCAGGCTTATTGATGACCTT	367		
Sbjct 1035702	CAGAATATTTAATTTTATGTATGTAAGCATCGATTGGACACCAGGCTTATTGATGACCTT	1035643		
Query 368	ACTCGTCCAATTTGGCACGGACCGCTTTAACTTGCAAGTAGTTTTGTAAGCCATCGACAG	427		
Sbjct 1035642	ACTCGTCCAATTTGGCACGGACCGCTTTAACTTGCAAGTAGTTTTGTAAGCATCAACAG	1035583		
Query 428	A 428			
Sbjct 1035582	A 1035582			

**14. Alignment result of *GDH1* igs region of EC1118, 20% rot to the top Blasting match**  
***Saccharomyces cerevisiae* strain CEN.PK113-7D chromosome XV**  
Sequence ID: [CP046095.1](#) Length: 1085503 Number of Matches: 1

Score	Expect	Identities	Gaps	Strand
732 bits(396)	0.0	396/396(100%)	0/396(0%)	Plus/Minus
Query 1	CTTGCCATCTTTGGTCAAAGGTGCTAATATCGCAAGTTTCATCAAGGTCTCTGATGCTAT	60		
Sbjct 1036007	CTTGCCATCTTTGGTCAAAGGTGCTAATATCGCAAGTTTCATCAAGGTCTCTGATGCTAT	1035948		
Query 61	GTTTGACCAAGGTGATGTATTTTAAATAGTCTAAAAGAAAGAAAAGAGGAAAGTTCATAA	120		
Sbjct 1035947	GTTTGACCAAGGTGATGTATTTTAAATAGTCTAAAAGAAAGAAAAGAGGAAAGTTCATAA	1035888		
Query 121	AAAGTTCCTTTCcttttttttAAATAACTTAGATAGATAATGAGATAAAAAGAAGTaaaaaaa	180		
Sbjct 1035887	AAAGTTCCTTTCCTTTTTTTAAATAACTTAGATAGATAATGAGATAAAAAGAAGTAAAAAAA	1035828		
Query 181	CGGAATCGTAACGCAATTAATTAATTAAGAAAATTGATTATCGGGAGaaaaaaattttat	240		
Sbjct 1035827	CGGAATCGTAACGCAATTAATTAATTAAGAAAATTGATTATCGGGAGAAAAAATTTTAT	1035768		
Query 241	tttttattttattttCTTTAAAGTACATATATTTGAAATGATGACATGTGGAAATATAAC	300		
Sbjct 1035767	TTTTTATTTTATTTTCTTTAAAGTACATATATTTGAAATGATGACATGTGGAAATATAAC	1035708		
Query 301	AGAGACAGAATATTTAATTTTATGTATGTAAGCATCGATTGGACACCAGGCTTATTGATG	360		
Sbjct 1035707	AGAGACAGAATATTTAATTTTATGTATGTAAGCATCGATTGGACACCAGGCTTATTGATG	1035648		
Query 361	ACCTTACTCGTCCAATTTGGCACGGACCGCTTTAAC	396		
Sbjct 1035647	ACCTTACTCGTCCAATTTGGCACGGACCGCTTTAAC	1035612		

**15. Alignment result of *GDH1* igs region of EC1118, 40% rot to the top Blasting match  
*Saccharomyces cerevisiae* strain CEN.PK113-7D chromosome XV  
Sequence ID: [CP046095.1](#) Length: 1085503 Number of Matches: 1**

Score	Expect	Identities	Gaps	Strand
734 bits(397)	0.0	397/397(100%)	0/397(0%)	Plus/Minus
Query 3		CTTGCCATCTTTGGTCAAAGGTGCTAATATCGCAAGTTTCATCAAGGTCTCTGATGCTAT		62
Sbjct 1036007		CTTGCCATCTTTGGTCAAAGGTGCTAATATCGCAAGTTTCATCAAGGTCTCTGATGCTAT		1035948
Query 63		GTTTGACCAAGGTGATGTATTTTAAATAGTCTAAAAGAAAGAAAAGAGGAAAGTTCATAA		122
Sbjct 1035947		GTTTGACCAAGGTGATGTATTTTAAATAGTCTAAAAGAAAGAAAAGAGGAAAGTTCATAA		1035888
Query 123		AAAGTTCCTTTCttttttttAAATAACTTAGATAGATAATGAGATAAAAGAAGTaaaaaaaa		182
Sbjct 1035887		AAAGTTCCTTCTTTTTTTTAAATAACTTAGATAGATAATGAGATAAAAGAAGTAAAAAAAA		1035828
Query 183		CGGAATCGTAACGCAATTAATTAATTAAGAAAATTGATTATCGGGAGaaaaaaaaattttat		242
Sbjct 1035827		CGGAATCGTAACGCAATTAATTAATTAAGAAAATTGATTATCGGGAGAAAAAAAAATTTTAT		1035768
Query 243		tttttattttattttCTTTAAAGTACATATATTTGAAATGATGACATGTGGAAATATAAC		302
Sbjct 1035767		TTTTTATTTTATTTTCTTTAAAGTACATATATTTGAAATGATGACATGTGGAAATATAAC		1035708
Query 303		AGAGACAGAATATTTAATTTTATGTATGTAAGCATCGATTGGACACCAGGCTTATTGATG		362
Sbjct 1035707		AGAGACAGAATATTTAATTTTATGTATGTAAGCATCGATTGGACACCAGGCTTATTGATG		1035648
Query 363		ACCTTACTCGTCCAATTTGGCACGGACCGCTTAACT	399	
Sbjct 1035647		ACCTTACTCGTCCAATTTGGCACGGACCGCTTAACT	1035611	

**16. Alignment result of *GDH1* igs region of EC1118, 40% rot to the top Blasting match  
*Saccharomyces cerevisiae* strain CEN.PK113-7D chromosome XV  
Sequence ID: [CP046095.1](#) Length: 1085503 Number of Matches: 1**

Score	Expect	Identities	Gaps	Strand
745 bits(403)	0.0	403/403(100%)	0/403(0%)	Plus/Minus
Query 1		GTAAGGTCTTGCCATCTTTGGTCAAAGGTGCTAATATCGCAAGTTTCATCAAGGTCTCTG		60
Sbjct 1036014		GTAAGGTCTTGCCATCTTTGGTCAAAGGTGCTAATATCGCAAGTTTCATCAAGGTCTCTG		1035955
Query 61		ATGCTATGTTTGACCAAGGTGATGTATTTTAAATAGTCTAAAAGAAAGAAAAGAGGAAAG		120
Sbjct 1035954		ATGCTATGTTTGACCAAGGTGATGTATTTTAAATAGTCTAAAAGAAAGAAAAGAGGAAAG		1035895
Query 121		TTCATAAAAAGTTCTTTCtttttttAAATAACTTAGATAGATAATGAGATAAAAAGAAGT		180
Sbjct 1035894		TTCATAAAAAGTTCTTTCtttttttAAATAACTTAGATAGATAATGAGATAAAAAGAAGT		1035835
Query 181		aaaaaaaaCGGAATCGTAACGCAATTAATTAATTAAGAAAATTGATTATCGGGAGaaaaaa		240
Sbjct 1035834		AAAAAACCGGAATCGTAACGCAATTAATTAATTAAGAAAATTGATTATCGGGAGAAAAAA		1035775
Query 241		attdttattdtttdattdttattdttCTTTAAAGTACATATATTTGAAATGATGACATGTGGAA		300
Sbjct 1035774		ATTTTATTTTTATTTTTATTTCTTTAAAGTACATATATTTGAAATGATGACATGTGGAA		1035715
Query 301		ATATAACAGAGACAGAATATTTAATTTTATGTATGTAAGCATCGATTGGACACCAGGCTT		360
Sbjct 1035714		ATATAACAGAGACAGAATATTTAATTTTATGTATGTAAGCATCGATTGGACACCAGGCTT		1035655
Query 361		ATTGATGACCTTACTCGTCCAATTTGGCACGGACCGCTTTAAC	403	
Sbjct 1035654		ATTGATGACCTTACTCGTCCAATTTGGCACGGACCGCTTTAAC	1035612	

Table A1.2: Volatile aroma compounds, retention times, target and confirming ions, standard curves, % recovery, calibration ranges, and % coefficient of variation (CV).

Compound	Retention Time (min)	Target Ion (m/z)	Confirming Ions (m/z)	Standard Curve (R <sup>2</sup> )	% Recovery	Calibration Range Lowest to Highest (µg/L)	%CV
Ethyl acetate	6.929	43	45, 61	0.9919	108	793-7940	0-6, Average: 2.64
2-methyl-1-propanol	8.757	31	43, 59	0.9956	91	1087-8700	1-5, Average: 2.26
Ethyl isobutyrate	15.549	71	88, 116	0.9910	104	62-625	1-5, Average: 3.37
Ethyl butyrate	17.143	88	101, 60	0.9869	107	10-180	0-5, Average: 2.22
Ethyl 2-methylbutyrate	20.073	102	57, 85	0.9967	88	6-500	0-2, Average: 0.23
Ethyl isovalerate	20.308	88	85, 57	0.9982	93	1-8	0-6, Average: 3.24
Isoamyl acetate	21.886	43	87, 73	0.9935	84	42-680	0-6, Average: 2.57
Hexanol	22.764	56	55, 84	0.9922	80	62-500	0-8, Average: 2.94
Ethyl hexanoate	28.891	88	115, 60	0.9979	105	42-340	0-6, Average: 1.66
Hexyl acetate	29.804	43	56, 70, 83	0.9902	83	12.5-100	0-5, Average: 2.29
2-phenylethyl alcohol	34.831	91	92, 122	0.9947	112	1250-10000	0-5, Average: 2.03
Ethyl octanoate	39.358	88	101, 129	0.9901	120	12-380	1-10, Average: 4.60
Ethyl decanoate	48.597	88	101, 143	0.9900	124	5-210	0-10, Average: 4.63
Hexanoic acid	31.827	60	73, 87	0.9914	93	39-781	2-12, Average: 7.54
Octanoic acid	41.052	60	73, 101	0.9900	80	122-976	2-12, Average: 7.54
Decanoic acid	49.874	60	73, 129	0.9897	81	250-2000	1-12, Average: 8.54

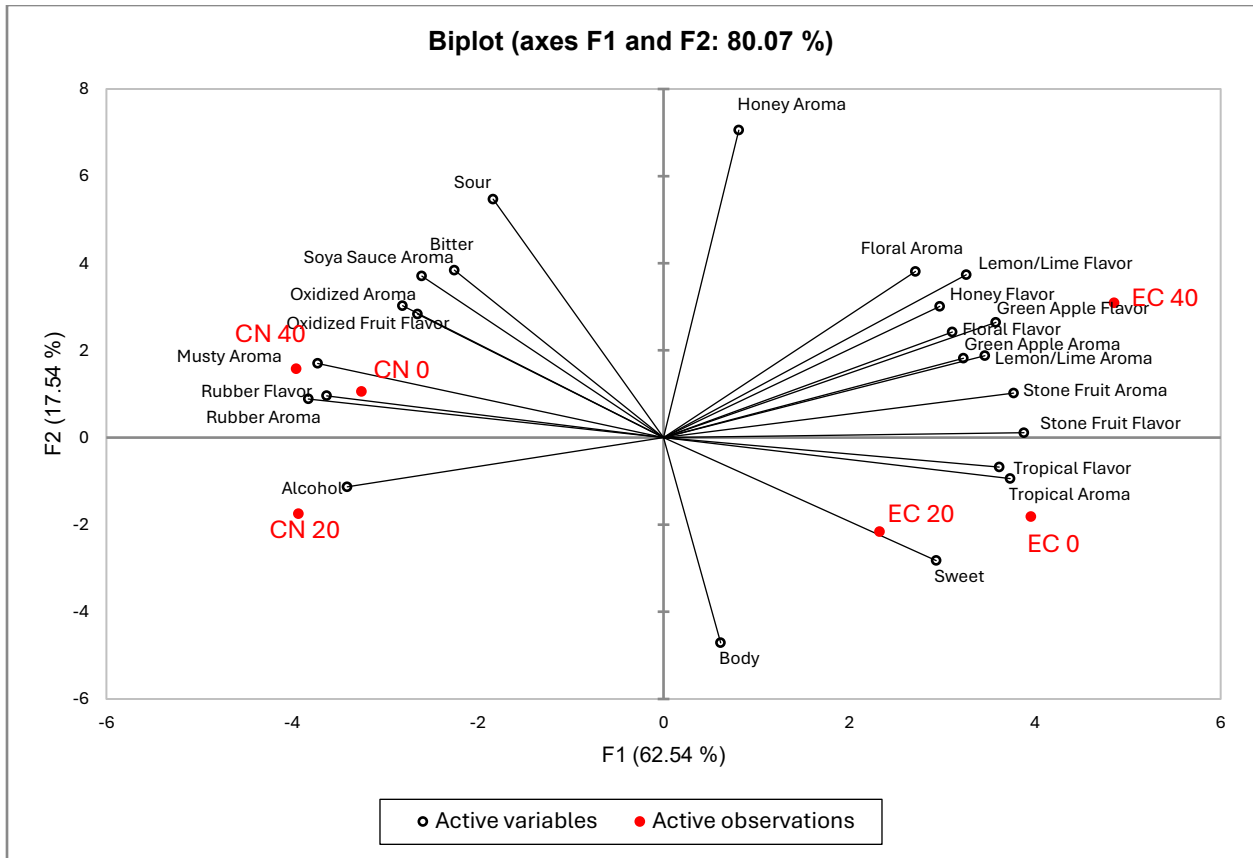


Figure A1.3: Sensory map of Riesling wines fermented with *S. cerevisiae* EC1118 and *S. uvarum* CN1 made using an increasing percentage of rot-infection by weight (control (0% rot), 20% rot, and 40% rot) via PCA on Factors 1 and 2.

Table A1.3: Mean concentrations ( $\mu\text{g/L} \pm$  standard error) of higher alcohols, acetate esters, ethyl esters, and fatty acids in Riesling wines fermented with *Saccharomyces cerevisiae* EC1118 or *Saccharomyces uvarum* CN1 at three levels of rot inclusion (0%, 20%, 40% by weight). Within each compound, different letters indicate significant differences between treatments as determined by Fisher's LSD test ( $p < 0.05$ ).

	0% Rot		20% Rot		40% Rot	
	<i>S. cerevisiae</i> EC1118	<i>S. uvarum</i> CN1	<i>S. cerevisiae</i> EC1118	<i>S. uvarum</i> CN1	<i>S. cerevisiae</i> EC1118	<i>S. uvarum</i> CN1
<b>Higher Alcohols</b>						
2-phenylethanol	15847 $\pm$ 2612 d	211971 $\pm$ 38838	17821 $\pm$ 2220 d	217916 $\pm$ 63102 a	16838 $\pm$ 1488 d	172838 $\pm$ 15341 c
Hexanol	1078 $\pm$ 121 e	1642 $\pm$ 88 a	1226 $\pm$ 100 d	1508 $\pm$ 231 b	1098 $\pm$ 175 e	1325 $\pm$ 52 c
2-methyl-1-propanol	14832 $\pm$ 1258 e	54936 $\pm$ 8671 a	14940 $\pm$ 1003 de	43459 $\pm$ 6218 b	16073 $\pm$ 1320 d	39069 $\pm$ 1488 c
<b>Acetate Esters</b>						
Ethyl acetate	49463 $\pm$ 4229 b	21856 $\pm$ 3346 e	42406 $\pm$ 2682 c	25546 $\pm$ 4064 d	52528 $\pm$ 4206 a	24604 $\pm$ 208 d
Hexyl acetate	500 $\pm$ 39 a	216 $\pm$ 24 d	377 $\pm$ 34 b	226 $\pm$ 21 d	366 $\pm$ 49 c	189 $\pm$ 31 e
Isoamyl acetate	3688 $\pm$ 382 a	2682 $\pm$ 86 c	2944 $\pm$ 300 b	2048 $\pm$ 331 d	3648 $\pm$ 349 a	1627 $\pm$ 87 e
<b>Ethyl Esters</b>						
Ethyl isobutyrate	92 $\pm$ 1 e	113 $\pm$ 3 b	98 $\pm$ 1 d	110 $\pm$ 4 bc	110 $\pm$ 2 c	117 $\pm$ 6 a
Ethyl butyrate	495 $\pm$ 72 a	105 $\pm$ 3 f	427 $\pm$ 54 c	177 $\pm$ 23 d	483 $\pm$ 47 b	163 $\pm$ 8 e
Ethyl 2-methylbutyrate	83 $\pm$ 0 d	86 $\pm$ 0 a	83 $\pm$ 0 d	86 $\pm$ 1 a	83 $\pm$ 0 c	85 $\pm$ 1 b
Ethyl isovalerate	3 $\pm$ 0 e	8 $\pm$ 1 a	3 $\pm$ 0 d	7 $\pm$ 1 b	5 $\pm$ 0 c	7 $\pm$ 0 b
Ethyl hexanoate	1772 $\pm$ 208 a	130 $\pm$ 4 c	1273 $\pm$ 120 b	151 $\pm$ 11 c	1252 $\pm$ 40 b	140 $\pm$ 4 c
Ethyl octanoate	638 $\pm$ 113 ab	174 $\pm$ 18 c	653 $\pm$ 73 a	200 $\pm$ 22 c	607 $\pm$ 193 b	186 $\pm$ 29 c
Ethyl decanoate	131 $\pm$ 13 bc	110 $\pm$ 6 d	172 $\pm$ 25a	141 $\pm$ 31 b	162 $\pm$ 47 a	128 $\pm$ 32 c
<b>Fatty Acids</b>						
Hexanoic acid	868 $\pm$ 89 a	57 $\pm$ 4 c	584 $\pm$ 42 b	59 $\pm$ 5 c	590 $\pm$ 45 b	62 $\pm$ 5 c
Octanoic acid	1046 $\pm$ 116 a	227 $\pm$ 24 d	858 $\pm$ 62 b	260 $\pm$ 14 d	794 $\pm$ 44 c	277 $\pm$ 24 d
Decanoic Acid	463 $\pm$ 90 a	250 $\pm$ 34 d	387 $\pm$ 78 b	345 $\pm$ 52 c	313 $\pm$ 27 c	344 $\pm$ 37 c